

AD-A164 213

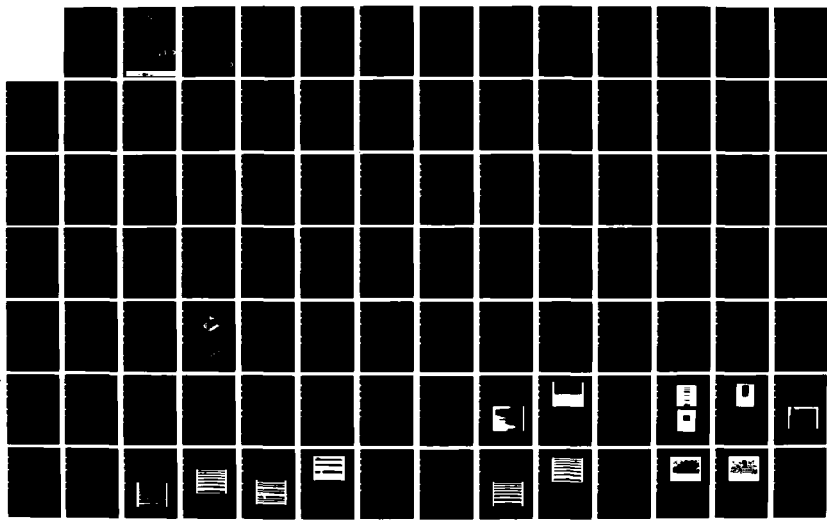
PSEUDO-COLOR DISPLAY OF LASER RADAR IMAGERY(U) AIR  
FORCE INST OF TECH WRIGHT-PATTERSON AFB OH SCHOOL OF  
ENGINEERING N BARSALOU 02 DEC 85 AFIT/GE/ENG/85D-3

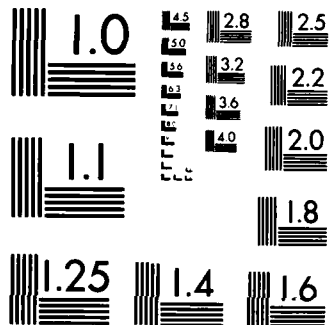
1/3

UNCLASSIFIED

F/G 14/5

ML





MICROCOPY RESOLUTION TEST CHART  
NATIONAL BUREAU OF STANDARDS - 1963-A

OTTC FILE COPY

AD-A164 213



## PSEUDO-COLOR DISPLAY OF

## LASER RADAR IMAGERY

## THESIS

AFIT/GE/ENG/85D-3

Norman Barsalou  
Captain, USAF

DISTRIBUTION STATEMENT A

Approved for public release  
Distribution Unlimited

**DEPARTMENT OF THE AIR FORCE  
AIR UNIVERSITY  
AIR FORCE INSTITUTE OF TECHNOLOGY**

## **Wright-Patterson Air Force Base, Ohio**

86 2 12 041

AFIT/GE/ENG/85D-3

(6)

PSEUDO-COLOR DISPLAY OF  
LASER RADAR IMAGERY  
THESIS

AFIT/GE/ENG/85D-3

Norman Barsalou  
Captain, USAF

Approved for public release; distribution unlimited

"Original contains color plates: All DTIC reproductions will be in black and white"

DTIC  
ELECTED  
S FEB 13 1986 D  
B

AFIT/GE/ENG/85D-3

PSEUDO-COLOR DISPLAY OF LASER RADAR IMAGERY

THESIS

Presented to the Faculty of the School of Engineering  
of the Air Force Institute of Technology  
Air University  
In Partial Fulfillment of the  
Requirements for the Degree of  
Master of Science in Electrical Engineering

Norman Barsalou, B.S., B.S.E.E.

Captain, USAF

December 1985

Approved for public release; distribution unlimited

## Preface

The purpose of this study was to investigate the use of pseudo-color to enhance laser radar data for display to humans. Additional points of concern were the relevancy of synthetic laser radar data with respect to real data, and the benefits of designing a laser radar display format based on synthetic data alone.

My previous assignment at the Air Force Armament Laboratory was my introduction to active IR systems. I would like to thank Mr. Mack Gay, and Lt Col Larry Ankeney for all their help and assistance in "showing me the ropes".

During this thesis effort, I received great support from the Avionics Laboratory AAAT-3 Branch, and a special thanks to them, especially Lt Paul Blase. I also owe Capt Jim Riggins and Lt Mike Lankford a word of thanks for getting the laser radar data on time, and Mr. Dennis Garbo for being my "Vax expert on the phone".

Back here at AFIT, I would like to thank my thesis committee - Dr Kabrisky, Capt King, and Dr Lamont for all their help and assistance. Finally, I want to thank my wife Patricia for all her patience, and her help with the photographic work on this project. Keep the aspidistra flying.

Norman Barsalou

## T A B L E   O F   C O N T E N T S

Preface.....	ii
List of Figures.....	vii
Abstract.....	ix
<b>1. Chapter 1.....</b>	<b>1</b>
1.1. General.....	1
1.2. Background.....	1
1.3. Objectives.....	2
1.4. Scope.....	2
1.5. Summary.....	3
<b>2. Chapter 2.....</b>	<b>3</b>
Human Visual System	
2.1. Eye as Camera Model.....	3
2.2. Retina.....	5
2.3. Spatial Sampling.....	7
2.4. Spectral Response.....	8
2.5. Helmholtz Theory of Color Vision.....	9
2.6. Dimensions of the HVS.....	11
2.7. Colorimetry.....	12
2.8. Color Measurement Principles.....	13
2.8.1. Subtractive Systems.....	13
2.8.2. Additive Systems.....	14
2.9. Standard Observer.....	16
2.10. CIE Color Standard.....	17
<b>3. Chapter 3.....</b>	<b>20</b>
Active Infra-Red Systems	
3.1. Applications of Imaging Sensors.....	20
3.2. Types of Sensors.....	21
3.3. Disadvantages of Passive Infra-Red.....	22
3.4. Active Infra-Red Sensor Development.....	23
3.5. Laser Radar Function.....	25
3.6. Modulation Formats of Ladar Systems.....	30
3.7. Three Dimensional Nature of Ladar Data.....	32
3.8. Ladar Data and Modelling Simplicity.....	33
<b>4. Chapter 4.....</b>	<b>36</b>
Laser Radar Simulation	
4.1. Synthetic Scene Simulation Routine.....	36
4.2. Verification of Synthetic Range Data.....	38
4.3. Synthetic Plywood Model Generation.....	41
4.4. Comparison of Synthetic and Real Data.....	44

<b>5. Chapter 5.....</b>	<b>49</b>
Display of Range Imagery to Humans	
5.1. Display Preparation.....	51
5.2. Image Format Specification.....	54
5.3. Color Display Design Methodology.....	55
5.4. Description of Color Routine.....	56
5.5. Display Color Scheme Generation.....	57
5.6. Conclusion to Display Generation.....	58
5.7. Preparation of Look-Up-Tables.....	58
5.8. Practical Limitations in Range Coloring.....	59
<b>6. Chapter 6.....</b>	<b>62</b>
Analysis of Laser Radar Imagery	
6.1. Pseudo 16 Bit Display.....	63
6.2. Full Dynamic Range Display Technique.....	64
6.3. Laser Radar Range Display Format .....	67
6.4. Comparison of 5 Bit Data.....	72
6.5. Synthetic Data Creation Parameters.....	72
6.6. Range Ambiguity Function.....	73
6.7. Difficulty with Gray Scale Display .....	79
6.8. Color Differencing and Contrast Limits.....	81
<b>7. Chapter 7.....</b>	<b>92</b>
Recommendations and Conclusions	
7.1. Dynamic Range Presentations.....	93
7.2. Possible Plans for Further Studies .....	95
7.2.1 Low Level Studies.....	96
7.2.2 High Level Process Enhancement.....	96
7.3. Limit of Human Visual Capacity.....	98
<b>8. BIBLIOGRAPHY.....</b>	<b>99</b>

## Appendices

<b>A. Listings for Target Files .....</b>	<b>100</b>
A.1. Listing for Stair Step Model Target File.....	100
A.2. Listing of Target File for Cone.....	102
<b>B. Target Signature Verification.....</b>	<b>106</b>
B.1. 500 Meter Range.....	106
B.1.1. Target Aspect 0 Degrees.....	106
B.1.2. Target Aspect 45 Degrees.....	107
B.2. Target Aspect 90 Degrees.....	108
B.3. Range 800 Meters.....	109
B.3.1. Aspect 0 Degrees.....	109
B.3.2. Target Aspect 45 Degrees.....	110
B.3.3. Target Aspect 90 Degrees.....	111
B.4. Range 500 Meters.....	112
B.4.1. Target Aspect 0 Degrees.....	112
B.4.1.1. <u>Scene Scaled by .0625</u> .....	113

B.4.1.2. <u>Synthetic Scenes</u> .....	114
B.4.2. Aspect Angle 45 Degrees .....	115
B.4.2.1. <u>Original Scene</u> .....	115
B.4.2.2. <u>Scene Scaled by .0625</u> .....	116
B.4.2.3. <u>Synthetic Scenes</u> .....	117
B.4.3. Aspect 90 Degrees.....	118
B.4.3.1. <u>Synthetic Data Scaled by .5</u> .....	120
B.4.3.2. <u>Synthetic Data Scaled by .25</u> .....	121
B.4.3.3. <u>Synthetic Data Scaled by .125</u> .....	122
B.5. 800 Meter Range.....	123
B.5.1. Aspect 0 Degrees.....	123
B.5.1.1. <u>Original Scene</u> .....	123
B.5.1.2. <u>Scene Scaled by .0625</u> .....	124
B.5.1.3. <u>Synthetic Scene</u> .....	125
B.5.2. Aspect 45 Degrees.....	126
B.5.2.1. <u>Original Scene</u> .....	126
B.5.2.2. <u>Scene Scaled by .0625</u> .....	127
B.5.2.3. <u>Synthetic Scene</u> .....	128
B.5.3. Aspect 90 Degrees.....	129
B.5.3.1. <u>Original Scene</u> .....	129
B.5.3.2. <u>Scene Scaled by .0625</u> .....	130
B.5.3.3. <u>Synthetic Scene</u> .....	131
C. Source Listing for Synthetic Scene Generator.....	133
C.1. Main Program Listing.....	133
C.2. Source for Subroutine TRANSF.....	135
C.3. Source for Subroutine SCANNER.....	137
C.4. Source for Subroutine FACET.....	138
C.5. Source for Subroutine NOISE.....	141
C.6. Source for Subroutine ROTATE.....	142
C.7. Source for Subroutine SHOW.....	143
C.8. Source for Subroutine BOX.....	144
C.9. Source for Subroutine HITBOX.....	145
C.10. Source for Subroutine HEADER.....	147
C.11. Source for Subroutine PUSH2.....	149
C.12. Source for Subroutine FIXED2.....	151
C.13. Source for Subroutine INPUT.....	153
C.14. Source for Subroutine SETUP.....	154
C.15. Source for Subroutine TEXTUR.....	155
D. RGB Listing for 255 Spec Color Look-Up-Table.....	161
E. RGB Listing for 32Spec Color Look-Up-Table .....	172
F. RGB Listing for 32Gray Look-Up-Table.....	174
G. RGB Listing for 255Gray Look-Up-Table.....	176
H. RGB Listing for 32Ran Color Look-Up-Table.....	187
I. System Specifications for CO <sub>2</sub> Ladar.....	189

Vita ..... 190

Accession For	
NTIS GRA&I	<input checked="" type="checkbox"/>
DTIC TAB	<input type="checkbox"/>
Unannounced	<input type="checkbox"/>
Justification _____	
By _____	
Distribution/ _____	
Availability Codes	
Dist	Specified
A-1	

## L I S T   O F   F I G U R E S

2-1: Anatomy of the Human Eye(8:24).....	4
2-2: Retinal Distribution of Rods and Cones(6:168).....	6
2-3: Spectral Response of Photoreceptors(10:82).....	9
2-4: Radiometric and Photometric Units(8:13).....	16
2-5: Derivation of CIE Chromaticity Chart.....	18
3-1: Transmission of 8-12 micron band.....	24
3-2: Conceptual Heterodyne CO <sub>2</sub> Laser Radar(9).....	25
3-3: Comparison of Ladar and MMW Spatial Resolution.....	28
3-4: Raster and Line Scanning Geometries.....	29
4-1: Plywood Stair Step Model.....	39
4-2: Computer Drawings of Plywood StairStep Model....	41
4-3: Range Geometry for Ladar Collection.....	42
4-4: Flow Diagram for Ladar Signal Processing.....	46
4-5: Plywood Target Masks.....	48
5-1: Image Processing System Configuration.....	53
5-2: Channel Assignments and Video Output Controllers....	53
6-1: 255Spec Color Look-Up-Table.....	66
6-2: 255Gray Look-Up-Table.....	67
6-3: 32Ran Color Scheme.....	69
6-4: 32Spec Color Scheme .....	69
6-5: 32Gray Display Scheme.....	70
6-6: Pseudo 16 Bit Display of Cone at 971 meters.....	71
6-7: Scene 1 Viewed through 32Ran Scheme.....	74
6-8: Scene 1 Viewed through 32Spec Scheme .....	75
6-9: Scene 2 Viewed through 32Ran Scheme.....	76
6-10: Scene 2 Viewed through 32Spec Scheme.....	77
6-11: Scene 3 Viewed through 32Gray Scheme.....	80
6-12: Scene 3 Viewed through 32Spec Scheme.....	81
6-13: Plywood Model at 500m, 90 degree aze - 255Spec....	83
6-14: Plywood Model at 500m, 90 degree aze - 255Gray....	84
6-15: Scene Scaled by .25 - 255Spec.....	86
6-16: Scene Scaled by .25 Displayed through 255Gray.....	86
6-17: Scene Scaled by .125 Displayed through 255Spec....	87
6-18: Scene Scaled by .125 Displayed through 255Gray....	88
6-19: Scene Scaled by .0625 Displayed through 255Spec....	89
6-20: Scene scaled by .0625 Displayed through 255Gray....	89
B-1: Real Signature.....	106
B-2: Synthetic Signature.....	106
B-3: Real Signature.....	107
B-4: Synthetic Signature.....	107
B-5: Real Signature.....	108
B-6: Synthetic Signature.....	108
B-7: Real Signature.....	109
B-8: Synthetic Signature.....	109

B-9:	Real Signature.....	110
B-10:	Synthetic Signature.....	110
B-11:	Real Signature.....	111
B-12:	Synthetic Signature.....	111
B-13:	Original Scene - 255Gray Look-Up-Table.....	112
B-14:	Original Scene -255Spec Look-Up-Table.....	112
B-15:	255Gray Look-Up-Table.....	113
B-16:	255Spec Look-Up-Table.....	113
B-17:	255Gray Look-Up-Table.....	114
B-18:	255Spec Look-Up-Table.....	114
B-19:	Original Scene - 255Gray.....	115
B-20:	Original Scene - 255Spec.....	115
B-21:	255Gray.....	116
B-22:	255Spec.....	116
B-23:	255Gray.....	117
B-24:	255Spec.....	117
B-25:	Full Resolution Data - 255Gray.....	118
B-26:	Full Resolution - 255Spec.....	119
B-27:	255Gray.....	120
B-28:	255Spec.....	120
B-29:	255Gray.....	121
B-30:	255Spec.....	121
B-31:	255Gray.....	122
B-32:	255Spec.....	122
B-33:	255Gray.....	123
B-34:	255Spec.....	123
B-35:	255Gray.....	124
B-36:	255Spec.....	124
B-37:	255Gray.....	125
B-38:	255Spec.....	125
B-39:	255Gray.....	126
B-40:	255Spec.....	126
B-41:	255Gray.....	127
B-42:	255Spec.....	127
B-43:	255Gray.....	128
B-44:	255Spec.....	128
B-45:	255Gray.....	129
B-46:	255Spec.....	129
B-47:	255Gray.....	130
B-48:	255Spec.....	130
B-49:	255Gray.....	131
B-50:	255Spec.....	131

### **Abstract**

A pseudo-color representation of CO<sub>2</sub> laser radar data is developed. The pseudo-color scheme is based on the dilution of a set of baseline hues by white. The synthetic generation of laser radar scenes is used for display creation, and the results of analysis on synthetic scenes is applied to data collected by a CO<sub>2</sub> pulsed ladar system.

## Chapter 1

### 1.1. General

The display of information to humans is a difficult task in the sense that few of the human processes that are involved are well understood. Modern combat aircraft systems present a large volume of information to the pilot. This is because of a number of reasons, not the least of which is the complexity of the weapon systems such aircraft are carrying, and are planned to carry. It is a cycle of increased cost, increased performance and increased complexity necessary to accomplish increasingly complex missions. Current technology is headed towards autonomous weapons which engage the enemy after launch from manned aircraft systems.

### 1.2. Background

In the interim before the arrival of totally autonomous systems, there will be the continued extension of the pilot's senses to the battlefield. Man-in-the-loop systems such as the GBU-15 and the laser guided bomb enable the weapon system operator to guide the weapon to the target while remaining in less hostile airspace. Until the arrival of totally autonomous systems, it is likely that such systems will continue to proliferate. Recent advances in sensor technology have resulted in the development of infrared laser radar(ladar) systems capable of producing high resolution range and angle measurements. The added dimension

of range may provide many capabilities to weapon systems carrying such sensors. Problems arise, however, when these data are displayed to humans. This thesis attempts to deal with a number of these problems.

### 1.3. Objectives

This thesis has three objectives:

- 1) Verification of synthetic infra-red radar data for use in training humans and algorithms.
- 2) Design of a display format for representing the full dynamic range of 16 bit range imagery.
- 3) Investigate the advantages or possible benefit of color coding infra-red radar data.

Two common items in each of the objectives are the infra-red radar data, and the human visual system. The approach taken is the evaluation of real ladar data as compared to synthetic data created to mimic the real data in target signature only. By comparing the real data with the synthetic data, the data verification can be done before various target aspects and range parameters can be created synthetically in order to understand the problems involved with color coding range data. Any expected results can then be tested by color coding the real data.

### 1.4. Scope

This investigation contains:

- 1) An introduction of the human visual system in order to show the complexity of displaying information to humans.
- 2) A description of CO<sub>2</sub> ladar systems that illustrates the creation of data by such sensors. This will be

contrasted with the data that the human visual system usually collects.

3) The description of a simulation that creates ladar data, and a comparison between synthetic target signatures, and real ladar target signatures.

4) Analysis of geometry changes in data collection, and the effects that such changes have on various display schemes investigated.

5) Color coding of real data based on the analysis and color scheme developed by manipulating the synthetic data on an image processing system.

#### 1.5. Summary

The basic conclusion of this thesis is that synthetic data may be used in place of real target signature data for training purposes, and color coding of the real or synthetic can be at least as acceptable as gray scale, and will be improved with further investigations.

## Chapter 2

### Human Visual System

The human visual system (**HVS**) is the pathway for an estimated 75% of the information that humans receive about the environment. Among the complexities of human vision is the overlap of various subsystems, which are not usually noticed by the individual. Vision in humans is actually a product of two visual fields. One field measures changes in brightness, while the other measures the average brightness. The effects of these two separate fields are rarely noticed by individuals because of the scanning behavior of the visual system. This chapter will present a brief description of the human visual system, and the rationale behind the utility of encoding sensor range data as color. It will be seen that color is a multi-dimensioned space that the HVS can quickly and randomly sample with sensitivity.

#### 2.1. Eye as Camera Model

The eye as camera model is useful in understanding the optics of the eye; the parts of the eye have camera equivalents. The eye has all the essential components of any camera, a body, a lens, an aperture, and a recording or light sensitive system. The lens is made primarily of water and protein. The interface between the environment and the eye is the cornea. The cornea might be viewed as a lens cover of sorts, but it actually provides most of the

refractive power of the eye.

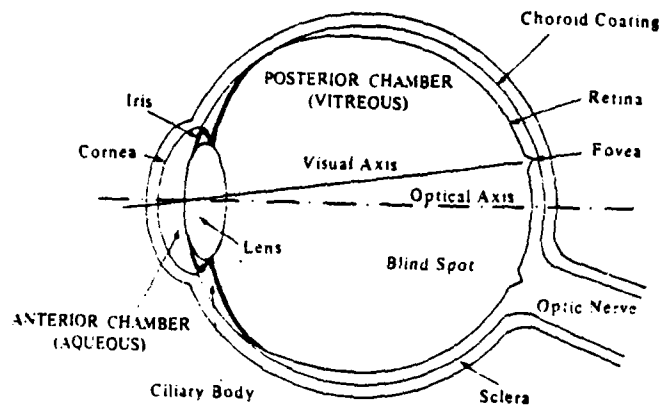


Fig. 2-1: Anatomy of the Human Eye(8:24)

The lens is a variable focus device. It can be flattened or curved to enable focusing of the image on the retina, or "film" of the eye. Between the lens and the cornea is the ciliary body. The ciliary body is where the cornea, and the sclera ,which is the outermost opaque layer of the eye, meet. In front of the ciliary body is the variable aperture or iris of the eye. The iris, by varying in diameter, can adjust light intensity on the retina. The iris can typically vary in diameter from 2 to 8 mm, this increases the dynamic range of the visual system by 24 dB. This is possible by the ability of the iris to constrict or relax according to the ambient light intensity. This adjustment is accomplished by a neural reflex.

## 2.2. Retina

The film of the eye is the retina, and it has the highest metabolic rate of any tissue in the human body. The

high metabolic rate is necessary to sustain many complex photochemical and biochemical processes that occur on the retina itself. This activity occurs in photoreceptors. The photoreceptors are commonly separated into two classes, rods and cones. The rods are 2 to 5 microns at the peripheral areas of the retina, while the cones are anywhere from 5 to 8 microns in diameter. In the fovea, or center of the retina, the cones are smaller than they are at the periphery and are about 1.5 microns in diameter.

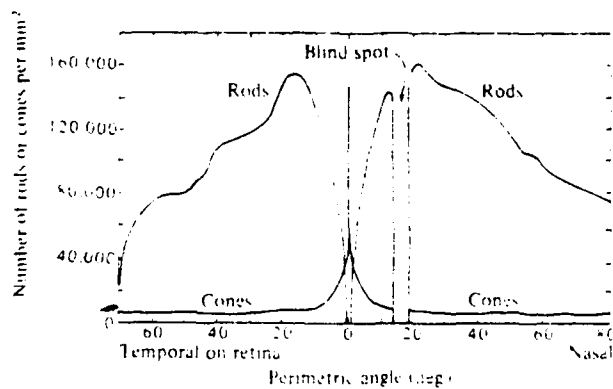


**Fig. 2-2: Retinal Distribution of Rods and Cones (6:168)**

Rods have the photochemical rhodopsin as their primary light sensitive material. Cones use a similar substance with a different protein structure that enables the cones to be sensitive to various frequencies of light in the visible band. The distribution of rods and cones in various regions of the retina is not uniform. The distribution varies drastically from the fovea, where the concentration of cones is high, and rods is extremely low, to the periphery where

the rods are more concentrated than cones. This non-uniformity in distribution of the respective photoreceptors should lead to a non-uniform response to color, depending on the area of the retina that the colored image falls upon. This is the case as colors are perceived as being somewhat different when placed in areas that cause the focus to vary over the retina(3:63). In everyday situations, this is rarely noticed by individuals, as they can simply orient their eyes and head in such a manner to insure that the image is centered on the foveal region of the retina. As the chart indicates, the field of regard of high resolution vision, as well as high resolution color, is quite small.

### 2.3. Spatial Sampling

Humans are able to compensate for the rather limited high resolution field of regard by scanning the high resolution region of the retina over the field of regard. Such movements of the eye are called saccadic movements. Saccadic movements are the result of several sophisticated reflex mechanisms that control the eye as it is scanned across the visual field of regard. One such reflex that is principally unnoticed is the suppression of information during scanning or movement of the eyes during a saccadic trajectory. This helps to stabilize the perceived image; it is done at a level in the HVS above the retinal level. The brain thus insures that the perceptual outside world is stabilized in matching its reality, and does not appear as a

blur, despite the movement of the retinal image.

#### 2.4. Spectral Response

The visible band of light is named primarily due to the response of the photochemicals in the human visual system. The band is considered to lie between wavelengths of 350 nm and 780 nm. As mentioned earlier, the response of the rods and cones are different. The rods are responsible for scotopic vision. This is essentially, monochromatic or gray scale vision. Lower levels of ambient light are necessary to trigger signals from the rods, as compared to the response of the cones. This is the reason that low light, or night vision in humans is monochromatic. Night vision occurs when the light intensity for color or photopic vision is below the noise level for the photochemical processes that produce the sensations of color. The sensitivity to light of the rods is greater than that of the cones. The retina itself is capable of adjusting the sensitivity of the photochemical processes that occur on it. This adjustment has a longer time constant than the reflex which opens or closes the iris. The photochemical adjustment to light intensity has a dynamic range of  $10^{100}$  (6:26). The primary means that enables the retina to set its overall sensitivity to light, or the gain of photochemical process is regulation of the concentration of rhodopsin, and the other photochemicals. High luminance in the environment will result in lower photochemical concentration, while low luminance levels

results in higher concentrations of these photochemicals.

Although the various chemical participants in human color vision have been isolated as various forms of rhodopsin in the cones, there are several models of human color vision. The differences in the absorption characteristics of these opsins, as they are called, are presumably the basis for color vision. Figure 2-3 shows the sensitivity of the various "color" receptive photochemicals found in the retina.

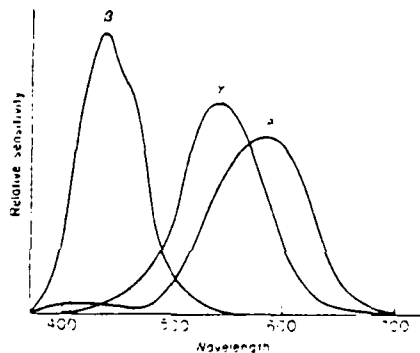


**Fig. 2-3: Spectral Response of Photoreceptors (10:82)**

It must be reiterated that these responses are not consistent across the retina. Even the sensitivities to various wavelengths of light varies as the light is focused on various parts of the retina.

#### 2.5. Helmholtz Theory of Color Vision

The first theory of color vision in humans was proposed by Young and later expanded by Helmholtz. The Helmholtz-Young theory of color vision states that there are three

types of cones. Each cone is sensitive to light corresponding to the colors of red, green, and blue. The integration of these signals then results in a perceived color. The spectral responsivities of the three different types of cones have been measured(6:350). Models of color vision differ in the area of retinal-brain fusion of the various signals produced by the "color sensitive" photochemicals. The basis of the most workable theory of color vision is the three color theory. This is based on the fact that individuals with normal color vision can match any color presented to them with at least three colors. The three colors, or primaries used, have to differ in spectral characteristics, but the characteristics do not necessarily have to be separation of frequency content between the three colors used as primaries. The spectral distributions of the primaries have to vary. The primaries do not have to be pure tones, in fact the spectral content of the primaries can even overlap(12:327). Using appropriately different primaries, individuals can match any color by additively varying the amount of each primary added to the color patch in such a way as to produce a viewable copy of the target color. The net response of such a color matching scheme can be tested over a wide range of different target colors, and sizes of target colors. Difficulties arise when using color matching instruments that cover more than 4% of the visual field(3:61-64). In this circumstance, the three color theory

of color vision does have some problems. The problems may have basis in the differences in distributions of rods and cones in individuals. Von Kries has proposed that the tri-color theory is valid at the photoreceptor level only(7:32).

Several experiments have revealed that at least some fusion of the information must occur. If a red filter is placed over one eye, and a green filter over the other, most objects in the visual field will appear yellow. Clearly, the retinal sensations alone cannot explain the effect. Color models vary greatly with regard to how much fusion occurs between the retina and brain. Retinal level processes can be viewed as low level, and brain level processes can be regarded as high level.

## 2.6. Dimensions of the HVS

The HVS is capable of resolving the world in four dimensions:

- 1) Motion (Time varying intensity)
- 2) Background Intensity (Average intensity)
- 3) Color (Photopic vision)
- 4) Luminance (Scotopic vision)

Presentation of information to humans may involve one or any number of these dimensions. Practical limitations occur in displaying information only as motion (such as a blinking light or alpha-numeric display), background intensity, and luminance or gray scale. The HVS is limited in the number of

simultaneous gray shades it can differentiate. This is due largely to the mechanisms that increase the dynamic range of the amount of luminance intensity that the eye responds to. If the dark-light adaptation mechanism of the retina is viewed as an automatic gain control circuit, the available dynamic range at any time is limited unless the gain control is reset. This mechanism drastically limits the number of gray scales that the HVS can discriminate at any particular AGC setting. The HVS performs as a contrast limited system with respect to gray scale detection and discrimination. The color domain, however, is much more flexible as long as there exists enough ambient light to enable the HVS to view the world photopically.

## 2.7. Colorimetry

Colorimetry is the science of measuring color, and defining colors scientifically. Truly color blind, or monochromat, individuals make up less than .0033% of the population(12:335). For a true monochromat, the world is a series of darkness and brightness, and nothing which could even be construed as variation among objects of the same brightness. For trichromats, the world presents a different set of data entirely. Light is able to acquire particular qualities other than merely brightness, or darkness, and varying degrees between. These qualities, to be measured and explained, have been enumerated through color science. The

essential problem is that measurable physical differences such as luminance and frequency of the light, do not often lead to complete characterizations of the psycho-physical effect that the viewed light has on humans. There exist a number of measurements in color science that are purely physical and there are also such measurements that are purely psycho-physical. Confusion often arises when the essential physical and psycho-physical definitions of terms and measurements are confused. An additional complication is the simple fact that humans tend to believe all what their eyes present to them.

The Committee on Colorimetry of the Optical Society of America has defined color: "Color consists of the characteristics of light other than spatial and temporal inhomogeneities." (4)

## 2.8. Color Measurement Principles

### 2.8.1. Subtractive Systems

Confusion usually occurs when describing color systems because there are several ways of characterizing a color. The approaches are those of additive and subtractive systems. Those who are painters are probably at least familiar with the problem of mixing paints to arrive at new colors on the palette; this is a subtractive color system. Simply stated, the white piece of paper that the painter is working with reflects all (or most) of the white light

source in the room, from the paper to the eyes of the painter. Now, the purpose of the paint pigment is to remove some section of the white light source, and reflect the rest of the white-filtered light. Yellow paint removes blue from the white light and leaves green and red parts of the spectrum unaffected. The net appearance to the painter is "yellow". It is clear from the onset that the original source of the "white light", in this case probably some form of incandescent light if the painter was indoors, has significant effect on the color balance of the painted scene. The HVS has the ability to normalize the color content towards an acceptable white. This is quite noticeable during the day when lamps in the house appear more yellow or green with respect to the sunlight outdoors. The brain accommodates such shifts in white in an attempt to make objects appear the same color when viewed under different sources of white light.

#### 2.8.2. Additive Systems

Television displays use the principle of additive color. This differs from subtractive color in one essential way. The electron beam of the CRT on the television cannot deposit the equivalent of a paint-like substance which then subtracts a selected portion of the spectrum from the ambient white light source in the room. This is not physically possible. It is possible, however, for the

electron beam to deposit energy in such a manner as to excite a phosphor which emits light energy of a particular spectral distribution. Then, if three differing phosphors can be found, the tri-color theory can be applied and the three spectral distributions can be combined to form colors. Red, green, and blue are the usual primary colors for additive colorimetry. The addition of red and green light fluxes in suitable proportions to produce a new color—"yellow".

Since the coloring schemes investigated in this thesis are concerned with television display of information which is color coded, it is worthwhile to expand on the additive system as well as some standard color representation systems, and nomenclatures for describing colors if physical, and not psycho-physical terms.

Light can be measured as electromagnetic radiation, for that is the exact nature of the phenomenon. The chart on the following page illustrates the differences between radiometric or physical attributes of light and photometric or psycho-physical attributes of light that is viewed by a standard human observer.

Radiometric and photometric units*					
Radiometry (Physical units)			Photometry (Psychophysical units)		
Symbol	Definition	SI unit	Symbol	Definition	SI unit
$Q$	Radiant energy	joule	$Q$	Luminous energy	lumen second (lalbers)
$w$	Radiant density	joules per cubic meter	$w$	Luminous density	lumen seconds per cubic meter (lalbers/m <sup>3</sup> )
$P$	Radiant flux or power	watt	$P$	Luminous flux or power	lumen
$M$	Radiant emittance	watts per square meter	$M$	Luminous emittance	lumens per square meter (lux)
$E$	Irradiance	watts per square meter	$E$	Illuminance	lumens per square meter (lux)
$I$	Radiant intensity	watts per steradian	$I$	Luminous intensity	candela (lumens per steradian)
$N$	Radiance	watts per steradian and square meter	$B$	Luminance	lumens per steradian and square meter (nits)
$r(\lambda)$	Spectral reflectance		$r(\lambda)$	Luminous reflectance	
$t(\lambda)$	Spectral transmittance		$t(\lambda)$	Luminous transmittance	
$\alpha(\lambda)$	Spectral absorptance		$\alpha(\lambda)$	Luminous absorptance	

\*Ratio of photometric quantity to corresponding radiometric quantity (standard units) is luminosity or luminous efficiency  $K$  ( $1/W$ ) or spectral luminous efficacy  $K(\lambda)$  ( $1/W$ ). Luminous efficiency is the ratio of the spectral luminous efficacy to its maximum value and thus is a numerical quantity.

Fig. 2-4: Radiometric and Photometric Units (8:13)

## 2.9. Standard Observer

The standard observer is an international standard under the CIE or Commission Internationale de l'Eclairage (International Commission on Illumination). The original basis for all photometric measurements was the candle, since it was the only form of illumination at the time that photometric standards were originated. After the establishment of psycho-physically based photometric standards, the metric system established several measurements concerning electromagnetic energy. These standards comprise the physical or radiometric units of the charts. The comparisons and conversions between the two systems can be quite easily done, as the processes , such as energy from a candle (radiant energy) has been measured and the conversion between the two systems is thus possible. It

is necessary to understand the distinction and use of both the radiometric and photometric systems, as color standards are usually expressed in photometric units.

#### 2.10. CIE Color Standard

The CIE sought to establish a two-dimensional color standard that was accurate enough to specify any color with particular accuracies. This was essentially done by establishing a chromaticity diagram, on which any set of primaries could be plotted and then aligned to any reference white. The addition of the flexibility of aligning to any reference white was necessary if the viewing conditions of the particular color was to be properly considered. Chromaticity is defined as being the color quality of the stimulus. The main difficulty in establishing such a chromaticity diagram is the definition of saturated colors. The difficulty is inherent in the nature of the relationship between primaries and their complements. The complement of every primary color is a combination of the other two remaining primaries, by definition. Then all three primary colors are actually half complements of each other. Any additive mixture of the primaries will then have an unsaturated effect. Here unsaturated is related to the amount of energy that corresponds to a single frequency in the electromagnetic spectrum. If pure laser light is used to produce the psycho-physical color, cross-talk between the cones causes the laser generated primary to appear

unsaturated. The problem is due to the response of the photo-receptors themselves. The CIE then extrapolated the existence of all saturated colors to lie on the locus as shown in figure 2-5 around three primaries, say red, green and blue. In order to contain all possible colors, the existence of super primaries was postulated, and X, Y, and Z were placed around the locus of saturated colors.

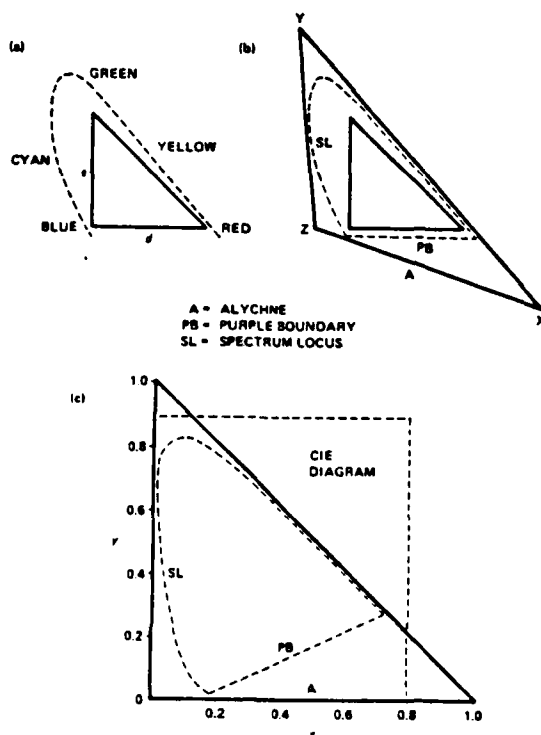


**Fig. 2-5: Derivation of CIE Chromaticity Chart**

This postulation was based on data collected by various groups concerning the color matching by human subjects on test colors that were made of large amounts of primaries in various combinations. It was found that all colors tested could be diluted by adding one or more primaries to the test

sample and that the test sample could then be compared with great accuracy to the standard colors they tested against. Hence the hypothesis of super-saturated colors would enable any color to be described. The triangle of the super-saturated colors would then encompass all physically realizable colors. In the final preparation of the chromaticity diagram, it was decided that the spectral energy distribution of the Y component primary should match the luminosity function curve. The luminosity function curve is essentially the response of the HVS to green light. It was then decided to place the X and Z primaries lie on a hypothetical line called the alychne. The alychne is a line of theoretical limits. It is the line where the subtractive color-matching process is exhausted, the line where the colors have zero luminance. The combined effect of all this manipulation was a diagram that not only tabulates the total chromaticity of a color, but also its luminance.

The use of CIE system is useful in explaining color content. For this thesis it is easier to specify the color content by specification of red, green and blue components. This, by itself cannot specify the total effect unless the monitor characteristics are aligned, and the brightness control adjusted or somehow calibrated. CIE specification can be found given RGB values, and assumed constant luminance.

## Chapter 3

### Active Infra-Red Systems

Much current work in the Department of Defense (DOD) concerns the computer generation of imagery. Computer generation of imagery is quite often less expensive than collection by a real sensor. In many instances the actual imagery of the sensor or candidate sensor is simulated by computer program before the actual sensor is operational. The flexibility of such computer generated imagery is often a major factor contributing to the development of a "sensor simulation" capable of producing two dimensional data that have the proper characteristics with respect to the sensor being simulated.

Very often, sensor simulations begin with "first principles" models, or, the basic physics or mathematical model which dictates sensor function. In short, if the sensor is acquiring visible light data, then a first principles model would somehow involve an illumination model as well as a reflectivity model. The sensor model would then proceed to more refined physical models of the interaction of the received light energy with the receiving transducer.

#### 3.1. Applications of Imaging Sensors

Imaging sensors in the DOD have a wide range of applications. Data collected by imaging sensors are used in reconnaissance, strike planning, and even terminal guidance

applications to name just a few applications. Any particular mission usually requires digital processing of the information after collection by the sensor, and the ability to predict the content of the signal collected by the sensor with respect to the anticipated sensor performance is crucial in the development of algorithms that further process the information after collection. Thus a sensor simulation of some sort is usually necessary in order to develop applications software that enable the sensor system (sensor plus associated digital hardware) to perform its desired function.

### 3.2. Types of Sensors

Many DOD imaging systems collect infra-red imagery. The bulk of the infra-red imaging systems in the inventory or in development within the DOD are passive sensors. Passive sensors measure the irradiance of the source, as well as reflectivity of other infra-red sources that may be illuminating objects that are in the field of regard of the sensor. Autonomous target recognition systems using current technology are usually passive infra-red systems. The only exceptions are those involving MMW(millimeter-wave), which is not infra-red, and active laser ranging systems (ladar). There are several inherent difficulties in using information provided by a passive infra-red sensor for automatic target recognition. By a first principles account, the environmental factors that

affect the signal stationarity are complex and variable according to seasonal, diurnal and target initial conditions. Target initial conditions refers to the state of the vehicle previous to collection of passive infra-red imagery on the target. These variables have to be normalized if target recognition of that vehicle is to be done. For these reasons alone, it is exceedingly difficult to predict the signature of a vehicle in the passive infra-red bands. Several DOD programs have attempted to model the physics of infra-red scene generation, as well as a sensors performance based on the mathematical prediction of the simulation.

### 3.3. Disadvantages of Passive Infra-Red

Part of the difficulty in locating targets with a passive IR sensor autonomously is the complexity of the data set provided by such sensors. An actual infra-red sensor image of a non-moving target is constantly changing with such variables as sun angle between target and sensor, cloud cover between sun and target and atmospheric conditions between target and sensor. Consequently, any algorithm dedicated to finding targets in any realistic scenario has to compensate for the intrinsic variability of the sensor data. This is typically done by training the algorithm against any number of expected situations that may be encountered by the sensor-algorithm system. Due the extreme variability of passive IR scenes, the number of circumstances that an algorithm may have to be trained

against is enormous. In order to increase performance more sensor data must be collected , and the algorithms must be re-trained against the newly acquired data. By the time the process is complete, the performance of the sensor can be viewed as a mere characterization of the data-set generated by the sensor. This makes accurate predictions of the actual target signature generated by the vehicle difficult.

### 3.4. Active Infra-Red Sensor Development

The difficulties involved with working with passive IR data and more restrictive guidance requirements have caused several DOD agencies to investigate alternative sensor technologies. One such technology is active infra-red imaging. An active infra-red sensor is a sensor with a carrier frequency in the infra-red band. In short, an active IR sensor can be a radar or a radiometer. Early active laser systems merely measured the intensity of the reflected laser light returned to the sensor. More recent systems provide very high resolution range data spatially ordered in two angles, azimuth and elevation, on the sensed scene. Current ladar sensors have the angular resolution of passive infrared sensors with range accuracies less than a meter. Such a sensor might have provide a data set capable of supporting many of the requirements of future autonomous attack vehicles.

Specifically, one such sensor under consideration for

future applications is the CO<sub>2</sub> laser radar. With advances in wave-guide lasers, it is possible to package compact high power, efficient sources at wavelengths of 10.6 microns. The wavelength corresponding to the P0 line of CO<sub>2</sub> is 10.6 microns, and this corresponds to an atmospheric window. Figure(3-1) shows the transmissivity through the atmosphere in the 8 to 12 micron band.

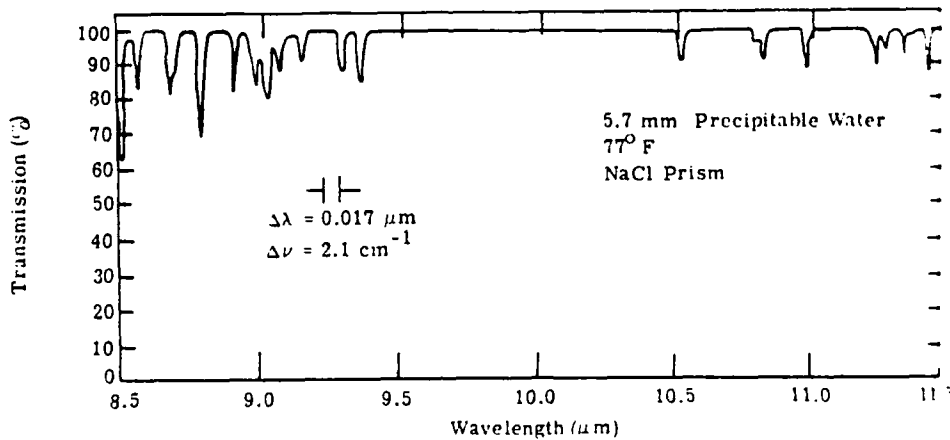


Fig. 3-1: Transmission of 8-12 micron band(16:5-90)

A CO<sub>2</sub> system will have adequate weather capability, and due to the fact that it will be a narrowbeam sensor, it will be a low probability of intercept system. Figure 3-2 (next page) illustrates a conceptual heterodyne CO<sub>2</sub> ladar system. The heterodyne system may be modulated in time or frequency. The principal difference between the continuous wave modulation format and the pulsed modulation format is the necessity of the pulsed system to have a separate local oscillator.

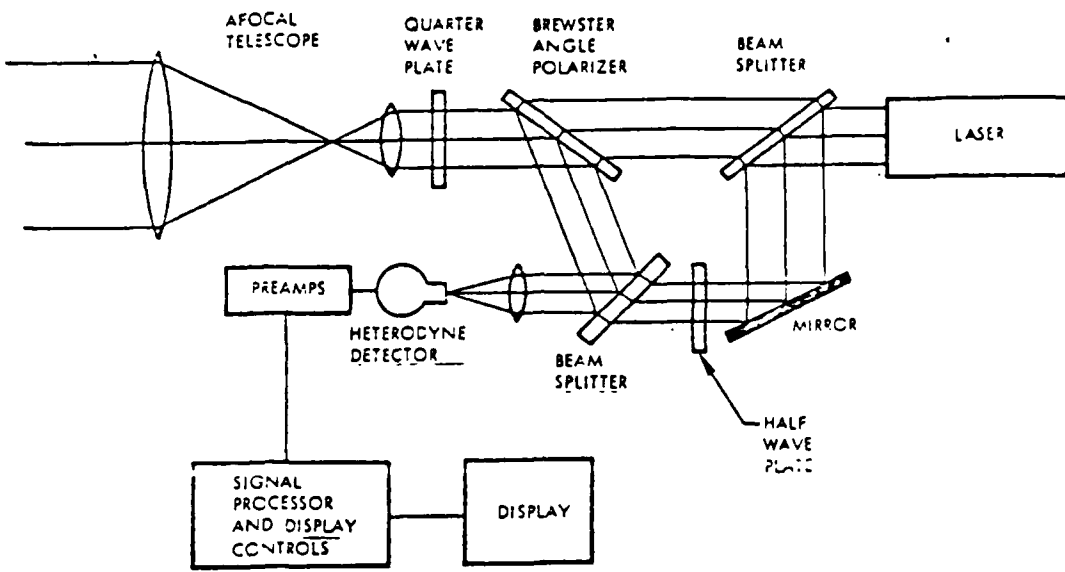


Fig. 3-2: Conceptual Heterodyne CO<sub>2</sub> Laser Radar(9)

### 3.5. Laser Radar Function

The laser energy is generated in the CO<sub>2</sub> waveguide laser. In a CW system the beam then leaves the laser cavity and proceeds through an optical beam splitter where the beam is split to form the local oscillator and the transmitted signal. The local oscillator beam then proceeds through a half wave plate. The half wave plate polarizes the light in such a manner to properly combine with the signal reflected

from the target. After the beam splitter, the transmitter beam proceeds through a quarter wave plate, and out the lens system to the far field . After reflection from the target, the returned signal is collected by the telescope, and due to the polarization change of reflection, is deflected by the Brewster angle polarizer, and sent to optically mix with the local oscillator on the detector. In current CO<sub>2</sub> systems, the detector used is a high bandwidth mercury-cadmium-telluride (HgCdTe) detector. Typical electrical bandwidth at the detector is on the order of 3-4 Ghz. It must be pointed out that the heterodyning of the returned signal and the local oscillator occurs physically at the detector. This improves the performance, and allows operation of the sensor to perform in a shot-noise limited capacity. The background noise of the environment at 10.6 microns does not limit sensor performance as the energy in band will not be in phase with the signal transmitted from the sensor. The heterodyne implementation also allows the usage of a lower powered transmitter for a particular probability of false alarm versus an incoherent system. (Similar to an RF radar system.) For pulse systems the path through the optics is identical with the exception of the beamsplitter that is placed at the exit of the laser cavity. Because the laser is not transmitting continuously during the time of flight of the pulse of laser light, it is necessary for a pulse system to have a separate local

oscillator in order to operate as a heterodyne system. Pulse systems also operate at the shot noise limit of the photo-voltaic detector. Currently in the DOD, pulsed and CW ladar systems are being developed; each modulation format has its separate advantages depending on the particular application. Clearly, such an optical system as the conceptual design in Figure 3-2, will have significantly better spatial resolution than any RF system. Figure 3-3 illustrates the advantages of an active IR ranging system with 10 cm optics versus a MMW RF sensor with a 30 cm antenna at a range of 1500 meters. This high fidelity data will provide a geometric data set to the processors, as opposed to radiometric data that a passive IR system collects. Because the data collected by a ladar is geometric, target features can be based on the physical attributes of the target with respect to target geometry, and not on irradiance and emissivity of the target. No thermal model is necessary to properly model a target for an active ranging system simulation. A ladar produces data by calculating the time of flight of a pulse of laser energy, or by measuring a frequency offset between the returned signal and the local oscillator. This function is not unique to a ladar system. The resolution of the data as Figure 3-3 illustrated is finer than any RF system other than, perhaps, a synthetic aperture radar (SAR).

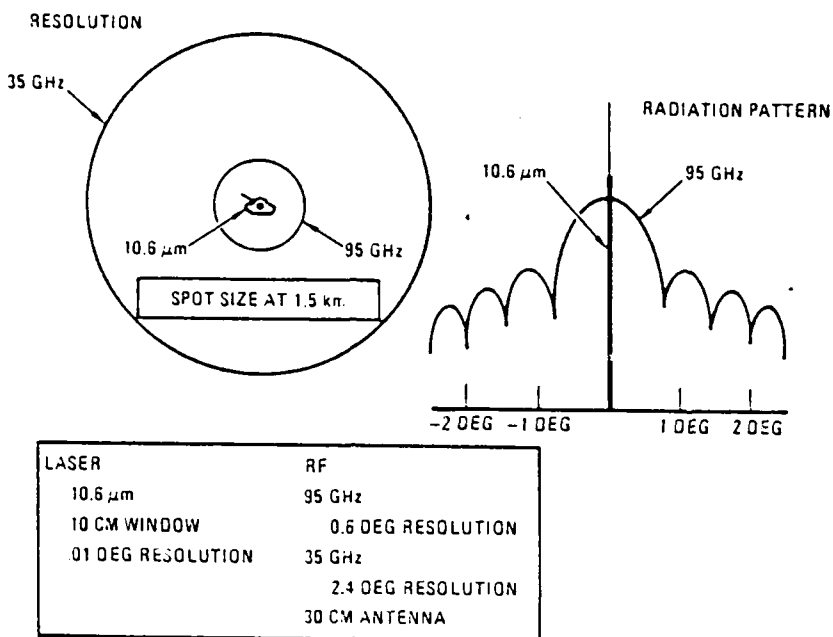
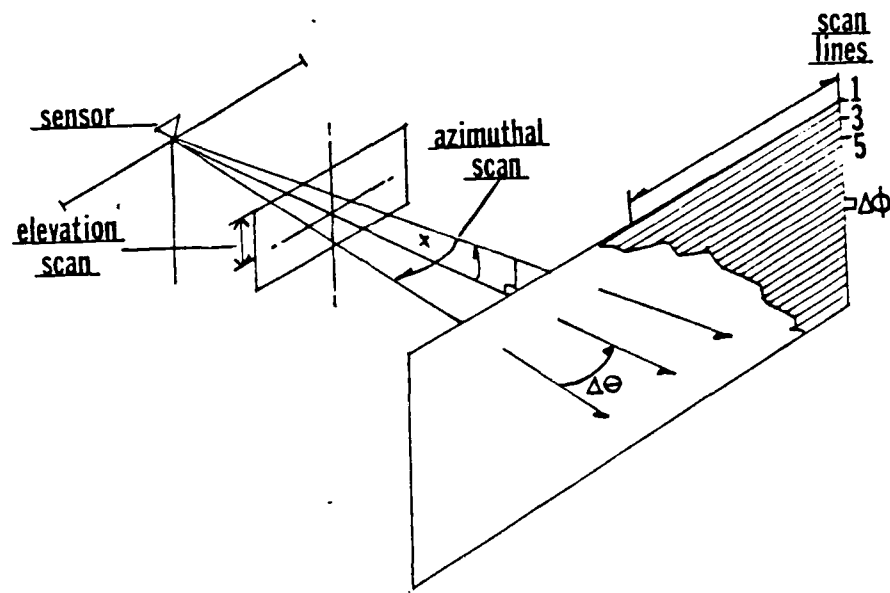


**Fig. 3-3: Comparison of Ladar and MMW Spatial Resolution**

The information provided by a ladar sensor is spatially arranged with respect to the environment . The sensor may scan the field of regard in any pattern that other optical sensors are capable of scanning. The two most common types of scanning are raster and line scanning. A raster scan covers two angles, azimuth and elevation, whereas a line scanner only scans in azimuth. The diagram on the following page illustrates both raster and line scanning patterns.

### Raster Framing Scanning Geometry



### Push Broom Scanning Geometry

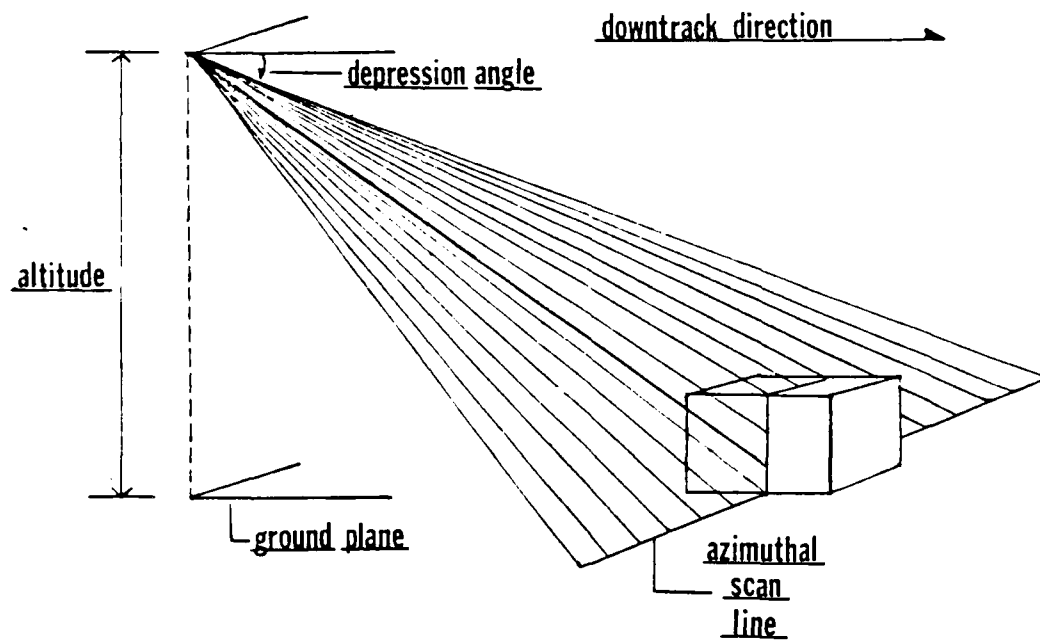


Fig. 3-4: Raster and Line Scanning Geometries

The line scanning sensor would usually rely on the down track motion of the vehicle it is on to provide data as the vehicle moves. The line scanner then sweeps across the field of regard like someone pushing a broom, and hence the term "push-broom" line scanner is also used. Line scanners have an advantage over a raster framing sensor with respect to moving parts. Since the vehicular down track motion enables sampling down track, no motors or galvanometers are needed to scan the sensor in the downtrack direction. The following diagram illustrates the differences in the two scans.

As the sensor scans the field of regard, it is collecting data. Usually, in the case of electro-optic sensors, the position of the scan within the field of regard is time synchronized with information on the sensed instantaneous field of view. This information allows for the proper placement of the data. In an imaging system, this means that the spatial arrangement of the data is possible. In an active laser system the laser is modulated in time or frequency as the field of regard is being scanned.

### 3.6. Modulation Formats of Ladar Systems

Modulation formats of an active laser ranging system are as versatile and diverse as any RF radar. In fact, ladar systems under development employ many standard radar waveforms, as well as standard radar electronic circuitry and techniques to decode the waveform after heterodyning. The traditional radar parameters of interest, such as

antenna size, wavelength of the transmitter, bandwidth of the receiver transmitter, as well as power are all applicable to ladar systems. The high spatial resolution of ladar systems allows for meaningful geometric interpretation of the laser range data. This is not always the case for range data gathered by RF radars.

Even though an RF system is collecting range information, it is usually coarse in either range or angle. In fact, most RF radars trade off range resolution for angular resolution. The trade-off between angular resolution and range resolution occurs in RF systems because the target is usually smaller than the beamwidth. As long as the target is inside the beamwidth of the radar, range resolution and angular resolution can be traded off with one another. In narrowbeam sensors such as a CO<sub>2</sub> laser radar, the spot size of the sensor is small enough to insure that several resolution elements or samples of the target will be scanned. In this circumstance, the target is larger than several beamwidths of the sensor, and angular resolution, and range resolution are separate parameters. Applications that require several pixels across the minimum dimension of the target can be achieved as in any radar system. The issue in most ladar designs is the determination of exactly how many pixels are required to do the task. Target recognition requires finer spatial resolution than target detection does, and system requirements ultimately trace back to such

basic sensor parameters as the size of the optics, scan rates, and pointing accuracies to name a few. A laser radar system does not have to make the same system trades as it is a narrowbeam sensor and sidelobes are considerably narrower than on RF systems. The physics of the collection process of the antenna or optics of a laser radar system enables the data to be represented as a 2 dimensional surface mapping of the range to each point sampled in the scene. with the exception of a SAR system, RF radar data cannot easily and accurately be modeled this way.

### 3.7. Three Dimensional Nature of Ladar Data

Because of the nature of the two-dimensional surface mapping of the environment that a ladar is capable of producing, the ladar data is said to have a 3-D quality: often it is spoken as "3-D ladar". The fact that an image collected by a ladar can be presented to a human viewer via a CRT, and the data appears as a low resolution television scene contributes to the usage of the term "3-D" with the term ladar. By properly interpreting the intensity of the two dimensional array as an encoded value of the range from the sensor to the particular ordered two dimensional point, the data may be viewed as having a three dimensional effect. Much can be learned of the sensed scene by looking at the laser data collected on the particular scene. Objects at the same range will appear as the same intensity, while those at other ranges will appear as different intensities, hues,

or whatever else is allowed to vary according to the viewing scheme, which is implemented.

### 3.8. Ladar Data and Modelling Simplicity

The important aspect of ladar imagery is that the first principles model dictating a target signature can be easily, and quite accurately extrapolated before any data are ever collected on that particular target. All that has to be known is the shape of the target, and its size. Since the ladar data are essentially two dimensional surface maps of the scene, it is relatively easy to construct the mapping of a known target.

In actuality, the first principles model of the ladar simulation is simpler than any similar model for a thermal imager. Noise models for a ladar receiver are more difficult than the purely geometric aspects of the sensor function.

Current work in robotics has a particular emphasis in the use of range data by robots to manipulate parts, inspect parts, or to simply identify parts. Many studies in this area have considered the problem of stereoscopically derived range images. In addition, work in this area has contributed to the computer representation of 3-d objects. Most of this work has dealt with the problem of simulating a particular scene as it would appear to a machine that viewed it with two separated cameras that operate passively in the

infra-red or visible bands.

There are many schemes that represent the data as a collection of surfaces in three space. Depending on the nomenclature, some schemes represent complete surfaces, while others merely represent the boundaries of surfaces, and assume a standard or set of surfaces that are between each of the boundaries or edges. All schemes usually require a large amount of data depending on the complexity of the solid object represented.

Synthetic laser radar images can be easily simulated with any set of data that represents a solid object or a two dimensional surface of some sort. For robotics applications, the generation of a synthetic television scene is a difficult task with respect to generating a synthetic laser radar scene. It is more complicated to calculate the illuminance of an object with respect to a source (or simulated source of light energy) than it is to calculate the intersection of a line with a surface of the object.

The benefit of using synthetic data for algorithm training as opposed to real data collected by a sensor is a complex issue. Arguments over the benefit of synthetic training data are numerous. There is no argument with regard to the simplicity of using computer generated imagery provided the imagery generated is somewhat similar to data that the real sensor would collect in the field. In any

final application the most meaningful test of a sensor with hardware for making decisions on the data is obtained with the sensor system operating on real data collected in an environment as similar as possible to the operational environment of the system.

Current work in the development of CO<sub>2</sub> ladar and the applications of that technology has relied primarily on the assumption that simulated ladar imagery is simple to create and that data produced by any of the numerous simulations are somewhat similar to the data that an active IR system would collect. The significant tests of the sensors that measure the angular and range separation of two dimensional objects such as flame sprayed aluminum plates have been conducted. For this investigation seeking the proper display format of ladar data for human viewing, most of the representation schemes investigated will use computer generated range , azimuth, elevation data. The next chapter will provide a verification that the usage of the synthetic data and the technique used to develop the imagery is valid for the first principles model of laser radar theory and function.

## Chapter 4

### Laser Radar Simulation

For the purposes of evaluating ladar display schemes for the display to humans the use of a synthetically generated range, angle, angle for display scheme was decided upon. The most important consideration for using synthetic data is simplicity of creation as well as cost. In addition the target and sampling parameters sought in the investigation of the various display formats, were readily obtainable by simulation.

The simulation used was developed at Eglin AFB in support of the Backbreaker/Optionbreaker Program. Full details of the simulation and proper documentation are available (15). For this effort, the simulation had to be rehosted on a Vax 11-780 computer. Access to a machine identical to the original host (CDC-Cyber) was limited. After rehosting, the simulation created several test scenes in order to verify that the software was performing properly. The test scenes were kept until they could be inspected on an image display system.

#### 4.1. Synthetic Scene Simulation Routine

The scene generator creates synthetic laser radar imagery based on solution of a line-plane intersection. The target files were derived from an Army-Air Force munitions targets modelling standard. This enabled the creation of

metric range, angle, angle information on real targets. The target set includes many terrestrial and airborne Soviet and Warsaw Pact vehicles, as well as some vehicles from NATO countries. The targets are described by a set of triangular facets that cover the surface of the target vehicle. The data on particular vehicles( e.g. T-72 tank) are derived by stereoscopic photographs of an actual vehicle. Facets are then laid out on the vehicle surface by a semi-automated process. Target file preparation is a labor intensive operation, so the compatibility of the simulation with a rich data base was the deciding factor in using the triangular facet format in the simulation.

The simulation is capable of generating any resolution spatially and any range and apparent target aspect. This is done primarily by treating the coordinate system of the target in a relative manner with respect to the "scanner geometry". The "scanner geometry" is actually the reference image plane. All perspective transformations are done with respect to what a sensor would collect given a set of sampling parameters in two angles(azimuth, and elevation) and an along boresight or line-of sight to the target. This is a spherical coordinate system. The target facet information is then oriented with respect to the required viewing angles and ranges to the target with respect to the sensor's spherical coordinate system.

Such a simulation is rather straight forward. The

complexities arise when the extent of the target files is considered. A typical number of triangular facets on a Shotgen target file is on the order of 20,000. This makes the creation of a synthetic image on that large a number of facets more difficult. Calculations must be performed in order to limit the number of candidate facets. Not all facets can be viewable at one time, and this simple fact eliminates a large number of candidate facets. The simulation calculates such items before any attempt is made to find the intersection of any line drawn from the sensor to the ground plane.

After the target facets have been oriented and screened with respect to the desired collection parameters, the sensor scans the extent of the target file in its entirety by placing a box around the extent of the target file as projected on the image plane or sensor location. The format of the sampling of the image plane projected target file can be controlled to the extent of scanning the target file as if it had been scanned and sampled by a raster framing scanner, or a linescanner. Both scanning techniques differ from each other in complexity. It requires an equal amount of time to collect data from either format.

#### 4.2. Verification of Synthetic Range Data

The synthetic data used in the investigation of various coloring and display schemes for presenting ladar data to humans was contrasted in several areas with real data

collected from a ladar sensor. Real data were collected on a target fabricated from plywood sheets specifically for the validation of the synthetic scene generator. Plywood was assembled to form four boxes of various dimensions, the boxes were stacked to form a series of 4 steps. The following diagram and schematic illustrates target dimensions.

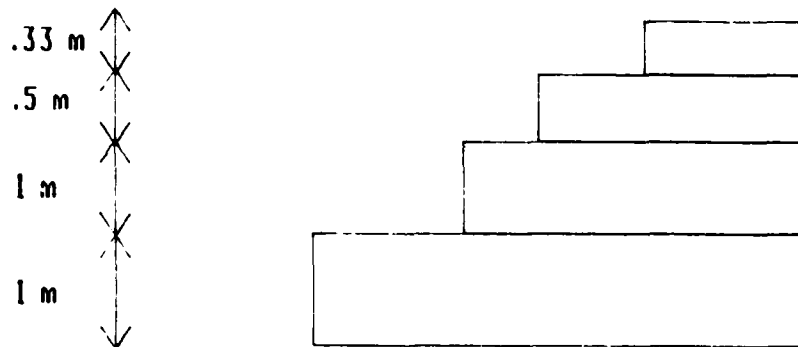


Fig. 4-1: Plywood Stair Step Model

Previous analyses of the signals returned from imaging ladars have dealt with the single measurement of sensor resolution and accuracy figures of merit. This is usually accomplished by placing plates of relative high reflectivity at 10.6 microns at varying distances along the

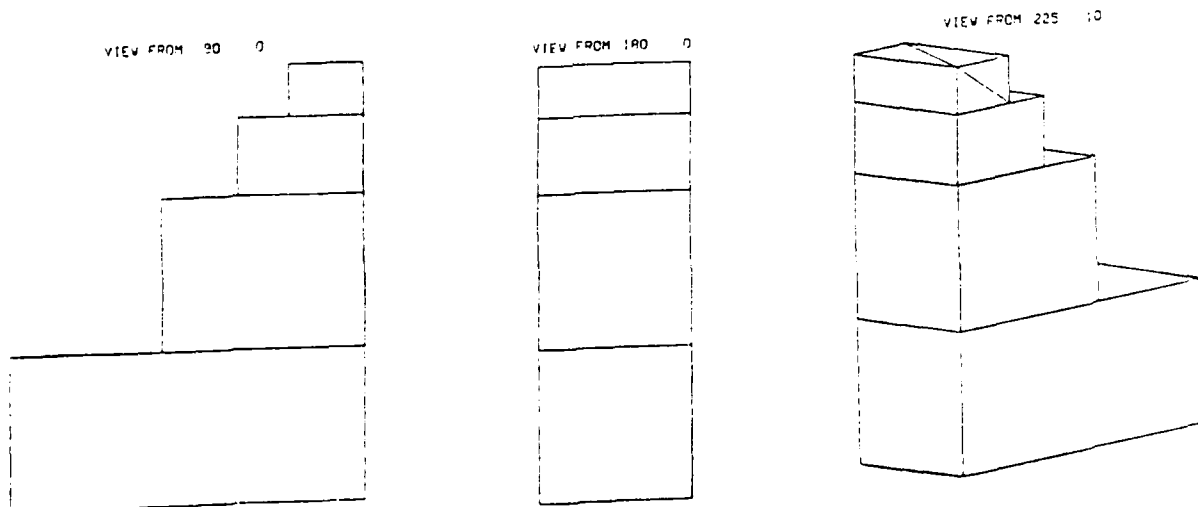
Z-axis of the sensor. (the term Z-axis here refers to the distance along the line of sight at the particular angular orientation) Analogously, the spatial resolution of the sensor is measured by placing two calibration plates side by side at the same range and separating them in angle. By using combinations of these two techniques, it is possible to determine all critical performance parameters of the sensor. These parameters include spatial resolution, range resolution, range accuracy, and angular accuracy. What was done for the validation of the simulation, was to compare directly, the data collected by a CO<sub>2</sub> ladar on the stair step target with the data produced by the simulation. The critical issue in determining the relevance of modelling laser radar data as range and two angles was the ground truth of the data collected. The data were collected on the stair step target at various ranges and depression angles as well as target orientations.

For the data validation of this project several modifications of the simulation were required. One involved the creation of a synthetic target model identical in metric proportions to the original plywood model, and the other modifications involved rewriting parts of the simulation to accommodate the collection parameters that were specific to the test set up at Eglin Air Force Base.

#### 4.3. Synthetic Plywood Model Generation

Once the drawings of the stair step model and the dimensions of the stair step model were received, this information was coded into the appropriate triangular facet representation. After the model was generated, several test runs were performed on the simulation to insure that the format of the stair step target data was correct. The data created on the target file were subsequently validated at Eglin by a program which plots the projected outlines of the triangular faceted target file at various orientations.

Below is the output of the target verification.



"View from X,Y" means X = azimuth, Y = elevation  
**Fig. 4-2: Computer Drawings of Plywood Stair Step Model**

After the synthetic model of the stair step model was created and verified for accuracy, the simulation itself had to be modified in order to accommodate the geometry of the test range at Eglin AFB. The driving reason behind modifying the simulation was the tower height at the test range. The tower is 11 meters high. The plywood model was to be placed at distances of 500 meters and 800 meters from the base of the tower. At the 500 meter range the slant range to the target is 500.12 meters and, more importantly, the depression angle along the line of sight to the target is 1.26 degrees. The depression angle from the horizontal is .78 degrees shallower at the 800 meter range. Figure 4-3 shows the collection geometry of the plywood stair step range data.

#### RANGE GEOMETRY

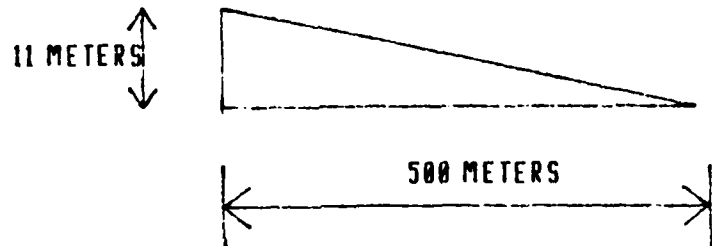


Fig. 4-3: Range Geometry for Ladar Collection

The depression angles of the collected imagery were closer to the horizontal than the simulation was

originally written to support. The main problem occurred in the generating and scanning of the scene so that the depression angle did not approach the horizontal. As initially written, the software driver for the raster framer would, by default, place the center of the raster frame directly the target origin. In this configuration, the sampling of the synthetic scene is then done by specifying the number of scan lines and pixels desired. Since the dimension of the line which emanates from the simulated sensor is a purely one dimensional entity, the exact location of where the line intersects the target is controlled only by specifying the angular constraints on the particular sample. The line is dithered randomly inside the prescribed cone . This simplifies the calculation of range, and also allows for using relatively simple target files. The random dither within specified constraints of angle allows the usage of large triangles with long edges . The synthetic stair step model has edges between facets that account for , in some instances, 50% of the distance in that dimension of the target file. If a uniform approach to sampling at every angle as determined by the accuracy of the host computer were employed, several pixel dropouts would occur as a result of the projected ray from the simulated sensor striking an edge of two facets. Because the sensor calculates the intersection of a plane with a line, the line which forms the intersection of two planes is treated as a

line, which it is. The simulation cannot recognize the edge as belonging to either one of its facets. This becomes further complicated as several facets could, and many often do, intersect in a common point. Due to the random nature of creating the line target facet intercept , it was necessary to insure that no drop out occur on the synthetic data. Special code was written to insure that no pixel dropout occurred on a target pixel. The most accurate data possible was generated for the purposes of comparison with actual CO<sub>2</sub> laser radar data.

The simulation currently models no noise processes specific to a CO<sub>2</sub> system. The only noise that can be added to the collected pixels is random range noise. The simulation can provide Gaussian distributed or Rayleigh distributed noise globally across a simulated frame of data. Severe angular perturbations in the scanning process can be implemented on a pixel by pixel basis. This function was used to correct any "dropout" pixels if they occurred on the target.

#### 4.4. Comparison of Synthetic and Real Data

Evaluating the applicability of using synthetic data in place of real ladar data, was done by directly comparing target signatures generated by the simulation and the real target signatures generated by a CO<sub>2</sub> ladar. Initially, target masks were created by the simulation of the plywood stair step target at the identical geometric parameters that

the real data was collected. The synthetic range data were generated as masks. Mask refers to the fact that only pixels that would occur on the stair step target were created. Normally, the simulation creates data on a flat earth ground plane if a pixel is not found to lie on a target facet. For this evaluation, only target masks were created. These masks are basically a matrix arranged with zeroes in locations that do not correspond to a target pixel location. The target signature, is then placed against a zero background.

For evaluation purposes, the target signature of the plywood stair step model was then extracted from the real scenes collected by a CO<sub>2</sub> ladar system as described in appendix J. The target signature information from the real data was not extracted by use of an image processing system. Instead, it was extracted primarily by range gating the original data. The data as it arrived from the sponsor at Eglin AFB, was not in a form that could immediately be used as range,angle,angle data. The data, as received, came directly from the MULTI-BUS system which controls the laser radar. Figure 4-4 portrays the flow of data from the sponsor to a usable form as range angle, angle data, that can be manipulated as imagery. After an evaluation of a few scenes of real ladar data on an image processing system, it was determined that the data were being properly formatted as range image data.

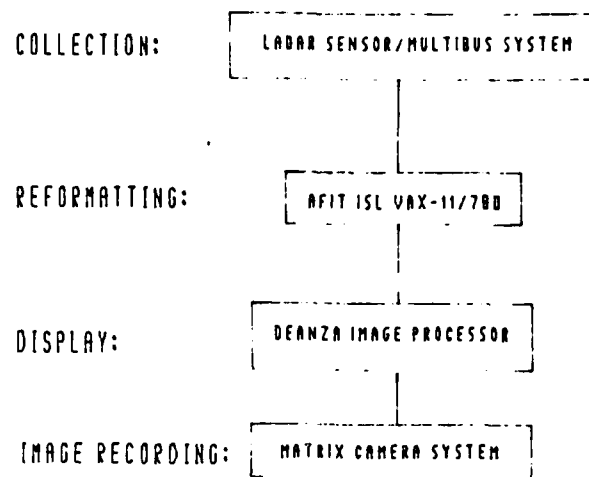


**Fig. 4-4: Flow Diagram for Ladar Signal Processing**

Target data of the plywood stair step at various locations were range gated and displayed as a three dimensional plot on a graphics terminal. These signatures appear on the next page.

Compare these target signatures: notice the clear target mask signature created by the simulation. It can be seen that the data as modelled by the simulation produce an accurate simulation of the actual target data as collected by an actual sensor. The image frames produced by Eglin AFB are 128 lines by 256 pixels. For the initial comparison of the data and the mask signatures, the data from the real sensor were down sampled to produce an evenly sampled image in elevation and azimuth. Masks were created accordingly: this was easily implemented as two separate parameters, namely the azimuthal quantization, and the elevation quantization in angle of the created masks. On visual inspection of the three dimensional plots of the two types

of data, it is apparent that similarities between the real data and the synthetic data do exist.

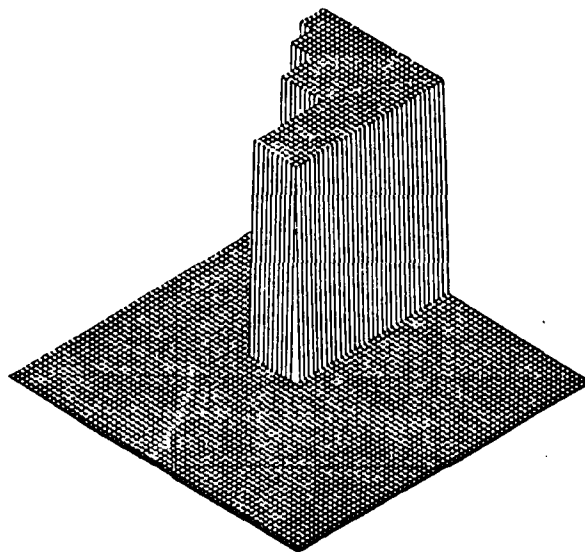
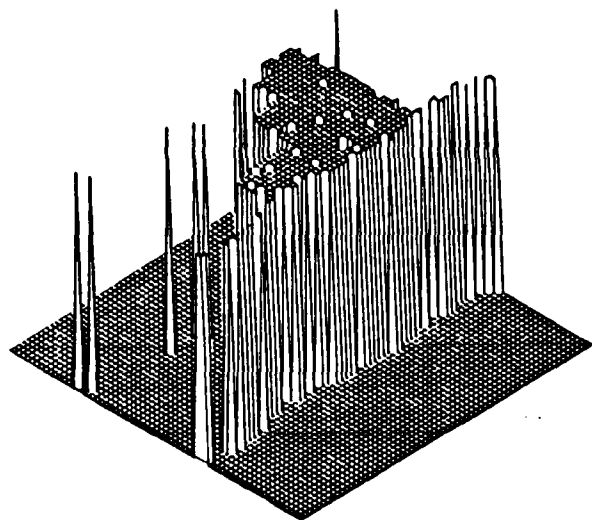


**Fig. 4-5: Plywood Target Masks**  
Range 500m, aspect angle 90 deg  
Real Data (top) Synthetic Data (bottom)

Note that no noise filtering or any processing of the real data collected by the sensor was attempted. The line of range pixels that extend in the azimuthal direction on the three dimensional plots is the ground plane upon which the plywood model is resting. This is easy to understand since the bottom of the target is at the same range as the ground upon which it rests. The remaining pixels to the left and right of the target on the ground plane are merely values of the ground plane that fall in to the selected range gate. Additional spikes that appear in the real data plots can be attributed to noise. The single spikes of range noise would be effectively removed with median filtering of the data. For the purposes of comparing the data generated by the simulation and real sensor data, it was more appropriate to use the data as they were collected with noise and any other distortion that might be present.

## Chapter 5

### Display of Range Imagery to Humans

The ability of humans to ascertain range to an object or area within their visual field is a complex learned task. The estimation of range is a complex computation on the environment. Because this information is valuable in everyday life the human brain computes it. Humans are capable of judging distances based on the information provided to them by the visual system and previous knowledge. Because the eyes are not capable of providing range information directly, the HVS must calculate it. This calculation is based on several pieces of information that the brain relates with range in the environment. One such item is scale. A large object has more spatial extent than a smaller object: the optical system of the HVS properly reports this. A large object farther away than a small object may not have the same spatial extent on the retina as the smaller. If the brain knows, *a priori*, the relative sizes of the two viewed objects, the information presented to the brain is scaled accordingly. Scale is one of the constant calculations that the HVS makes. It is a useful calculation to perform on the environment considering the sensors of the human visual system. Shading and texture are also other properties that the brain calculates on the environment. The lateral geniculate body fuses images from the two eyes. These measures on the environment extract information

pertaining to range, or information useful in the calculation of range. Calculating range is an important and innate ability, much of the everyday usage and calculation of range information by the human brain is done at an unconscious level. This may make the possibility of deriving a "natural" representation of laser radar information to humans a difficult task. Any representation of range data to the HVS will , at some level, be unnatural.

Displaying range as gray scale is more natural to the extent that bright things are closer than dark things if the two things happen to be of constant luminance and of different ranges. The color representation of range imagery is more complex, simply based on the fact that color space is multi-dimensional while gray scale space is not.

Much research has concerned the display of information to humans. Many of these studies have dealt with the display of alpha-numeric information to humans. These studies have investigated the optimum number of colors to use in the generation of alpha-numeric fonts, the size of the fonts, and the number of fonts that can be effectively used in a single display.

The use of the term alpha-numeric here also applies to symbols such as those found on stop signs and road-maps. Those symbols are alpha-numeric because they belong to the alphabet of "map language" or map symbology. Using the information and data collected by these previous studies, a

color code or set of symbols for range data were sought. The structure of the display is limited because the laser radar collects range. The spatial organization of the data is all that is in common with the data normally collected by the HVS. That part of the display scheme need not be derived. Difficulties arise when the presentation of the third dimension of the laser radar data is desired, namely that of metric range to the prescribed spatial location in an ordered two dimensional space. The HVS system is not acclimated to "viewing" range as a laser radar measures range.

It is quite possible that range information of the resolution and accuracy obtainable from a ladar may more benefit a man than a machine. This part of the thesis deals with the design of two color schemes, one scheme based on randomly selected colors, and another based on the concept of "warm" and "cool" colors as put forth by some artists. The utility of the warm and cool color display is based on the fact that a "favorite" color display would require a color display for every individual. If the display is to have some sort of intuitive meaning it should make sense; it seems natural for the display to represent the closer ranges as being "warmer" than the farther ranges. This is , at least, an apriori association of range with color.

### 5.1. Display Preparation

The system on which the color displays were created was

a Deanza IP-8500 Image Array Processor. The image array processor is hosted by a DEC Vax 11-780. Color image creation is possible by the use of three separate eight bit memory planes, each plane can be connected to an individual video output controller (VOC).

For pseudo-color images, it is possible to connect three image memory planes to a single VOC. Pseudo-color is possible by varying the transformation applied to the gray value resident in the image plane as the data flows through a look-up-table (LUT) for each of the three color guns. The color guns are driven by the VOC, which can be programmed in several ways.

The test scenes produced for this effort were true color images. A particular red, green, and blue value was calculated for every pixel. The look-up tables for the red, green, and blue channels were merely used as an intensity transformation table. The host computer would transform an image into the appropriate red, green, and blue values for the display scheme implemented. An additional set of programs would then load the image data and the look-up table values into the image array processor for display to the operator. Figure 5-1, on the next page, shows the system configuration for the creation of the scenes used in the evaluation.

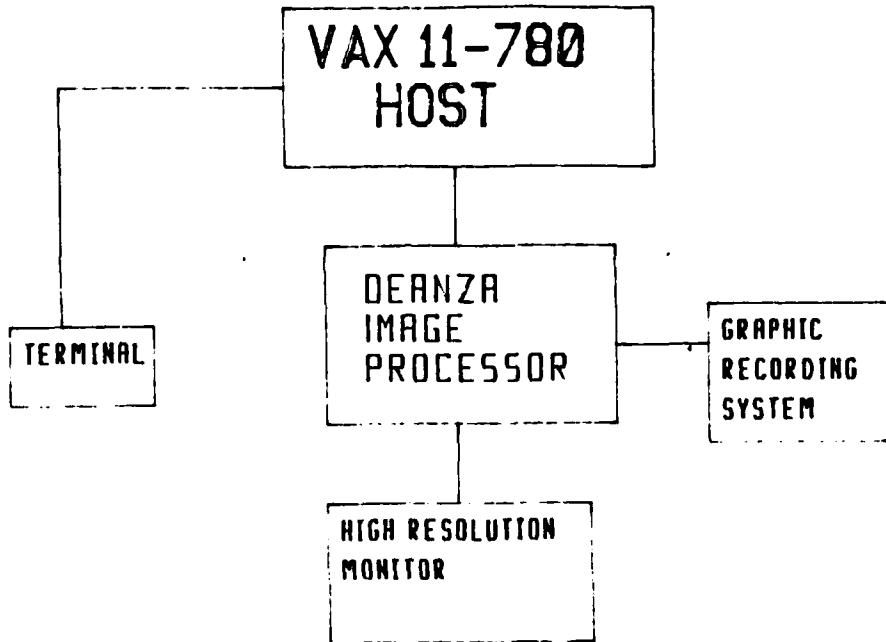


**Fig. 5-1: Image Processing System Configuration**

The following figure shows the flexibility in assigning channels through the video output controllers.

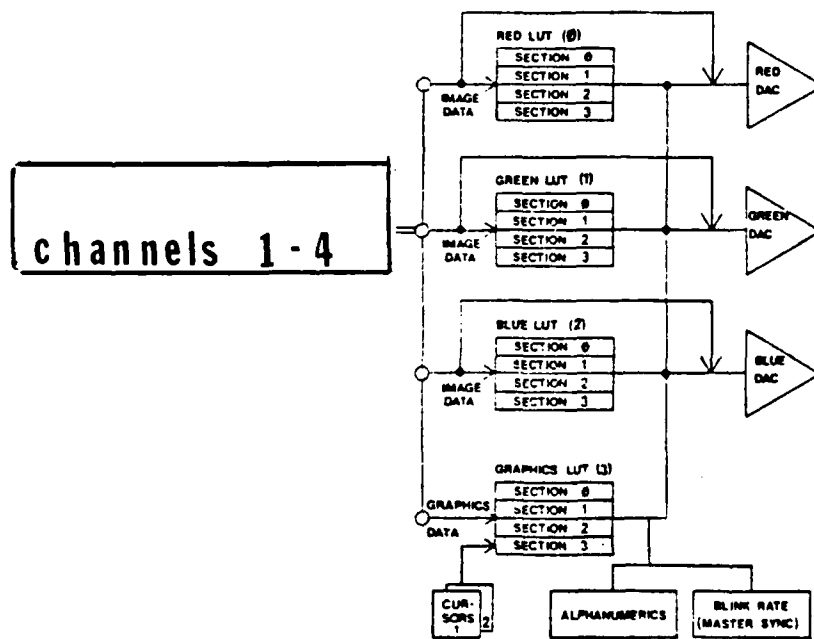


**Fig. 5-2: Channel Assignments and Video Output Controllers**

The image planes associated with the three channels portrayed in the diagram can be thought of as "red, green, and blue". This is not always the case, as reprogramming of the VOC can allow an assignment possibility:

```
Red=3  
Green=2  
Blue=1
```

But for the discussion here, it is assumed that channel one is associated with red, channel two with green and channel three with blue.

### 5.2. Image Format Specification

Each of the individual memory planes is 512 pixels by 512 lines, with each pixel represented by 8 bits, or a byte of memory. Since each byte has 256 possible values in three planes, and each gray level assignment may be mapped to one of an additional 256 values the number of possible color combinations with such a system is  $256^{**}3$  or over 16 million combinations. Unique color representation is possible for range pixels of twenty four bits, but not all of the color representations possible are discernible to a normal (non-color blind) individual. In color systems, much effort has been placed in the determination of color discrimination of humans. This is of particular interest in the textile industry . Some particular color which is expensive to reproduce may give the same psychophysical effect as another color which is less expensive. Fortunately

a large amount of this data has been collected, and often this phenomenon has been discussed as minimal perceptual difference. Due to the fact that the image display system can produce a large number colors, it was essential that color schemes developed for the test at least allow for minimal perceptual differences in color perception by humans.

### 5.3. Color Display Design Methodology

Due to the wealth of possible colors which can be generated, the display schemes developed could not have found potential color mappings of gray scale values completely randomly as this would have taken an inordinate amount of time. Additionally, there is no certainty that any two possible colors will be recognized due to minimal perceptual constraints. The only way to ascertain whether two color are differentiable is to view them side by side on the same background(3:62), The background against which a color is viewed does change the psychophysical effect of the individual color.

For these reasons, it was necessary to design an interface between operator and the color display system which could essentially, allow the operator to create colors on various background without regard to the spectral content or even the RGB (red,green,blue) values of the created colors. The interface was essentially a paint routine. This routine enabled the operator to interactively place a

particular color on a selected background, and view the color with respect to other colors.

#### 5.4. Description of Color Routine

The coloring routine placed a selected gray value in channel one of the display. The look up tables for the red green, and blue channel were loaded with values used in normal color image display. A set of intensity squares were written into channel three of the display system. When a particular color was searched for, the squares resident in channel three were enabled by setting the appropriate registers for the VOC and squares of various hue, intensity and saturation would appear on the output monitor. The operator could then choose a particular color from the screen by manipulating the cursor. After the color was selected the operator could select the color as a foreground or background color. If the color was selected was placed in the foreground, it could be manipulated from the keyboard terminal. The keyboard manipulation was limited to varying the saturation, and intensity of the color. Once a particular color was saturated, it would not change hue. This coloring routine proved useful in manipulating colors, and viewing colors against various backgrounds. After a particular candidate color is selected to correspond to a particular gray scale value or number, the contents of that color with respect to red, green, and blue is written to a buffer, and after the "coloring" session, the buffer is

written to a file. Later, the operator may re-edit the file, and display the colors that correspond to gray values. If desired, any color previously created may be placed in the foreground or background of the display. With this option, it is possible to create color look-up tables based on the assumption that minimal perceptual differences are satisfied. A selection of a color "X" for gray level "Y" should not look like color "A" for gray level "Y+1". The interactive nature of this utility precluded the selection of indifferentiable colors for different numbers to be represented.

#### 5.5. Display Color Scheme Generation

Using the coloring routine discussed in the previous section, the operator would select a color for the background. The background color would then fill the entire background. Next, a single color would be selected as a test color. The color would then be placed in the foreground as a single square. The operator could then color the background with the foreground color by moving the cursor or trackball. While the foreground was coloring the background, the intensity of the foreground could be varied by pressing keys on the keyboard. The red ,green and blue values of the chosen color were manipulated as long as the color would not become saturated. Once a color was saturated, pressing on the keys did not change its value unless the key for "less" intensity was being pressed. After the selected foreground

color had been displayed from less saturated to most saturated, the operator could, if desired, selected any location on the color line and assign a gray level number to it. After this was done, control was established to the extent that if color "x" was assigned to number "y", then the proper RGB components necessary to create "x" were known. This was the process used for coloring the gray value with pseudo-color.

#### 5.6. Conclusion to Display Generation

A user friendly interface was developed that allowed the manipulation of colors on a CRT monitor. Colors could, with constraints of saturation, be generated and manipulated. The RGB constants of the particular color scheme could then be loaded in the look-up tables of the red green and blue channels. The RGB values could then be stored, re-edited, or displayed at a later time.

#### 5.7. Preparation of Look-Up-Tables

The coloring utility served as the interface between the host computer, display system and the operator. Initially, the creation of the baseline hues was a time consuming and labor intensive effort. This was due to the design goal of presenting the colors as a spectrum which started at pure red and moved through orange, yellow, green, blue, and finally from dark blue to a neutral gray which

varied in luminance to dark. The design of the psycho-physical effect of the desired look up table was simple ,but manipulation of the color values was more difficult than expected. Difficulty often occurred in selecting an appropriate color which could be varied in intensity to a transition to another hue in a reasonable or "linear" fashion. Linear is not necessarily the correct term, orderly is more correct, but a seemingly orderly arrangement of the red green and blue values to be placed in the look up table often produces colors which are either indistinguishable, or seemingly unrelated to the color assignment of the previous gray number. Gray number here refers to the value of the one byte value that is to be placed on an image memory plane. Recall that the laser radar simulated imagery is in the Fortran Integer\*2 format, which means that the value of the particular range pixel is represented by two bytes. In keeping with the limits of the display, any representation of the particular Integer\*2 number will be a combination of three single bytes, each byte residing in an image memory plane of the display system. The warm-cool color scheme developed for the laser radar imagery proceeded along certain limitations in the ability to assign colors to range values.

#### 5.8. Practical Limitations in Range Coloring

The wealth of possible color assignments to any of the possible  $2^{**}16$  or 65636 possible values that can be

represented by a 16 bit pixel is rich. In principle, it is theoretically possible to generate a particular color for any 16 bit pixel value. The utility of such a representation would be questionable. Also the time required to generate the color mappings would be great. This coupled with the fact that no data are available on the exact number of differentiable colors can be displayed on such a system led to the simple solution of coding the information according to some scheme other than just color.

If laser radar scenes, either real or synthetic, are viewed on a CRT monitor, it is apparent that the information content of the high bits is less than that of the lower bits. This assumes that the quantization level of the data is at the sensor noise level, or above it. Randomly fluctuating lower bits provide no information. This argument can be further stressed by considering the geometry of the sensor scan. If the sensor is scanning a rather flat benign background, the range values will vary smoothly in accordance with the quantization of the sensor output in range. The CO<sub>2</sub> laser radar developed at the Air Force Armament Laboratory at Eglin AFB is typical of most state of the art CO<sub>2</sub> systems, and it has a range quantization of about .33m. Much more quantization is often not necessary in tactical applications, nor affordable.

Because the high byte of the range data varies slowly with respect to the lower byte, it makes sense that

not every value should have its own particular color. In fact, color coding in conjunction with another display scheme other than a color for each representable 16 bit value makes sense with regard to any transmission scheme of such data. Clearly if any data link system would attempt to perform bandwidth compression on a transmitted laser radar signal, any visual display system should also attempt to "keep down the bandwidth".

## Chapter 6

### Analysis of Laser Radar Imagery

By interactively manipulating laser range data, several items could be discovered about the nature of an effective display of that information. Typical image processing techniques such as thresholding , cursor and trackball investigations of numerical values, and biasing and scaling of the data were found most useful in determining the visual effects of the particular operation on the range data. Thresholding, for instance, on range data is simply an act of "range gating" the data. Range gating is quite common in most radio-frequency radars, and applying a threshold operation on range data displayed as an image is analogous to presenting only the data that is present at a prescribed range from the sensor. The prescribed range is metric, and can varied by interacting with the display system. It is difficult to display the full resolution of a 16 bit pixel on the display simultaneously. This can only be accomplished by displaying two or more channels simultaneously if no 16 bit color mapping is present.

In preparing these displays the upper byte was loaded into one channel and the lower byte was loaded in another. Operations could be performed on the 16 bit pixel, but the channels had to be displayed simultaneously. This was accomplished by in one of two ways. The high byte was displayed through the red gun and the lower byte was

displayed through the green gun, or the two channels were split, that is , half of the red channel was displayed and half the green channel was displayed on the monitor. This was accomplished by manipulating the control register of the image array processor, and setting it so that the VOC would pass the particular channel (high or low byte) to the desired color gun for display on the CRT monitor. After performing several threshold comparisons of the data it became obvious that a viable display scheme for the range data could be accomplished by displaying both the high and low bytes simultaneously. The key was that the high byte and low byte for every pixel would not be displayed. This makes sense when the relative low frequency content of the high byte with respect to the lower byte is considered. The display scheme for the 16 bit range pixel evolved according to the a priori information known about the intrinsic nature of the data itself.

#### 6.1. Pseudo 16 Bit Display

Since an occasional display of the information in the high byte was decided upon, the display scheme design now focused on the issue of determining how to present the high byte in an effective manner. Since this work is considering only static display of the imagery in non-real time, the consideration of having the VOC alternate between the channel containing the high byte and the channel containing the low byte was dismissed. This technique could be quite

effective. The advantage the alternating high byte - low byte display would have over a split scheme is that every range pixel would have its full 16 bits displayed, but not simultaneously. This technique would, in effect, be time multiplexing the display monitor between the two bytes of range information. Again, it must be pointed out that this discussion is concerned with the problem of displaying the full dynamic range of a 16 bit pixel without uniquely coloring each range pixel.

### 6.2. Full Dynamic Range Display Technique

The technique decided upon for the presentation of the full 16 bit range imagery works under two assumptions:

- 1) The full dynamic range of every single pixel need not be presented to the human.
- 2) It is not desirable to color each range value of a 16 bit pixel uniquely.

The first point is justified based on the low information content of the high byte. In scenarios where the range to the target is varying quickly or the quantization level of the range data is extremely low, the information content of the high byte will be high. For the application under consideration here, namely the usage of laser range data for the terminal guidance of a missile or glide bomb, the high byte, from pixel to pixel, will not vary as quickly as the low byte, and hence, it should not be as well presented to the human. Based on psychological and man-machine interface studies, it is unlikely that a human would

perform favorably with a suite of 65636 different colors. In addition there is the problem of not knowing how many distinguishable colors are physically realizable on current RGB display systems. The additional problem of aligning and calibrating a display monitor for a possible 65636 colors may preclude the unique representation of a 16 bit range pixel based on maintainability. This can be borne out by the difficulties encountered on this project in selecting only 256 colors, or coloring uniquely, a single byte. The non-linearities with the display as it heated and cooled during the day oftentimes caused a noticeable color drift during the creation of the look up tables developed under this effort. Any number of colors beyond 256 would add to the difficulty of maintaining constant color balance of the monitor. This problem may result into a need for fewer than 256 colors. There is also the problem that the HVS shifts, at least, its neutral white value, and that it is probably not stable with a large palette of colors.

For the previously mentioned reasons, a display scheme of pseudo-coloring the range information in conjunction with spatially multiplexing the data was decided upon. Spatial multiplexing means that the information in the high byte and low byte are presented on the same display screen. Although the information contained in either bytes may physically reside in separate memory planes. The test scenes developed for this project did, in fact, reside in separate

planes. After the color code was developed in a final form, an algorithm was written that decomposed a 16 bit number into its appropriate high byte and low byte representation. A unique representation of 256 colors for 256 values, and the simultaneous display of black and white requires using three memory planes. The following figures are the look-up-tables corresponding to the full 255 color look-up-table called 255Spec and the full 255 gray scale look-up-table called 255Gray. The top left entry in the table corresponds to the color assigned to the value 0, and the bottom left entry of the look-up-table corresponds to the value 255.



**Fig. 6-1: 255Spec Color Look-Up-Table**  
Top Left Corresponds to Value 0  
Bottom Right Corresponds to Value 255



**Fig. 6-2: 255Gray Look-Up-Table**  
Top Left Corresponds to Value 0  
Bottom Right Corresponds to Value 255

### 6.3. Laser Radar Range Display Format

In addition to the creation of a full 255 color look-up table which traversed the visible spectrum from red to violet, through an additional 16 neutral grays, two 32 level color look-up tables were created. This enabled the comparison between a look up table which was arranged according to some rule to be compared with a color scheme which was completely random in color assignment of values. Colors for the random look up table were created in the same manner as the 32 color scheme which varied according to the visible spectrum. The random color scheme shall henceforth

be referred to as "32Ran"(for 32-random), while the scheme which varies according to the visible spectrum will be referred to as "32Spec"(for 32-spectrum). The 32Spec look up table was created to have 8 separate hues, and each hue was to be diluted by neutral white 3 times. This makes  $8 * 4$ , or 32 possible colors in this scheme. Since the baseline hue was diluted by white, in colorimetric terms this is corrupting the purity of that baseline hue. White light is a composite of all primaries in an additive system. The following two photographs of the monitor contrast the 32Ran and 32Spec color tables. A third table, that of a neutral gray look-up table is also included for comparison. The 32 gray scale scheme spans the entire dynamic range of gray from complete darkness, 0, to complete whiteness, 255. This is accomplished by a linear ramp of slope -8 which starts at 255 and proceeds to 0. A data entry of value zero would appear as white, and white is displayed by having the value of 255 loaded in the red, green, and blue channels simultaneously. Similarly, the three channels would be loaded with register values of 247 for a data entry of 2. This is the easiest way to visualize the coloring process. It must be pointed out that the luminance display or gray scale is not biased or adjusted to provide maximum contrast on a step-wise basis, it does, however, use the entire available contrast that the display is capable of producing.

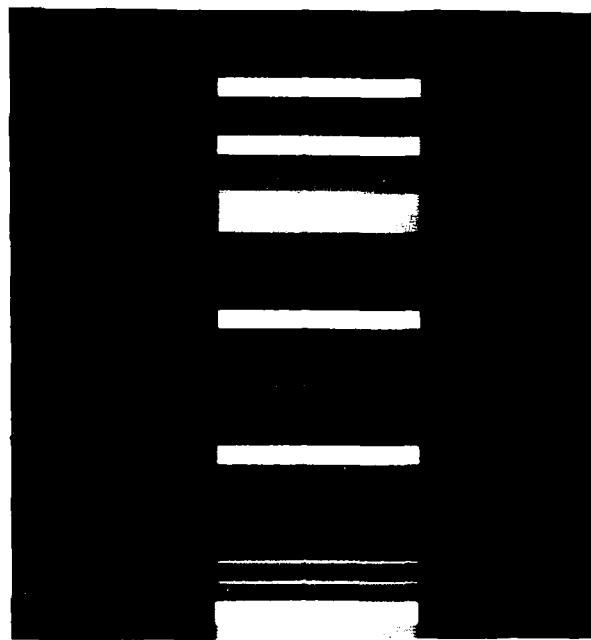


**Fig. 6-3: 32Ran Color Scheme**  
Top Value is 1, Bottom Value is 32

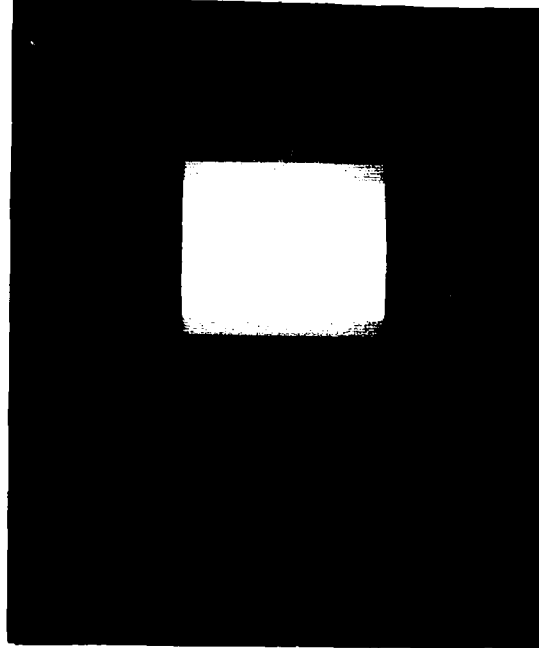


**Fig. 6-4: 32Spec Color Scheme**  
Top Value is 1, Bottom Value is 32

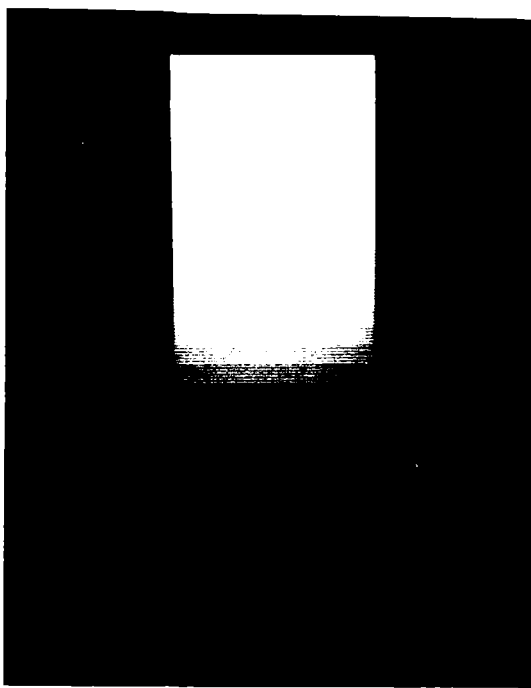


**Fig. 6-5: 32Gray Display Scheme**  
Top Value is 1, Bottom Value is 32

The following two scenes are illustrating the full dynamic range of a 16 bit pixel as displayed through the full dynamic range display scheme developed. The 32 pixel wide bar at the left of the scene denotes the value of the high byte for that particular scan line. If the value of the high byte changes along a scan line, the value of the high byte which is in the majority over the scan line is used to fill the color bar value. Notice the compression of the color bar as the scene is viewed from the bottom of the scene to the top of the scene. This is due to the geometry of the scene. As the depression angle of the sensor approaches the horizon, the range to the ground plane

becomes infinite. The  $\tan(90)$  is undefined, and the range value is resultingly large. The edge at the top of the scene is the horizon. This display provides much of the information present in an aircraft artificial horizon display. This is purely a function of the scene geometry. In an actual application, it would be possible to alpha-numerically list the range to the color bar at the left, and the additional range to the target or object of interest in the scene could be quickly calculated as an offset from the color bar range value. The target portrayed is a cone located at the 384th scan line and centered at the 128th pixel. The range to the cone along the bore-sight of the sensor is 971.2 meters. The cone itself is 18 meters high.

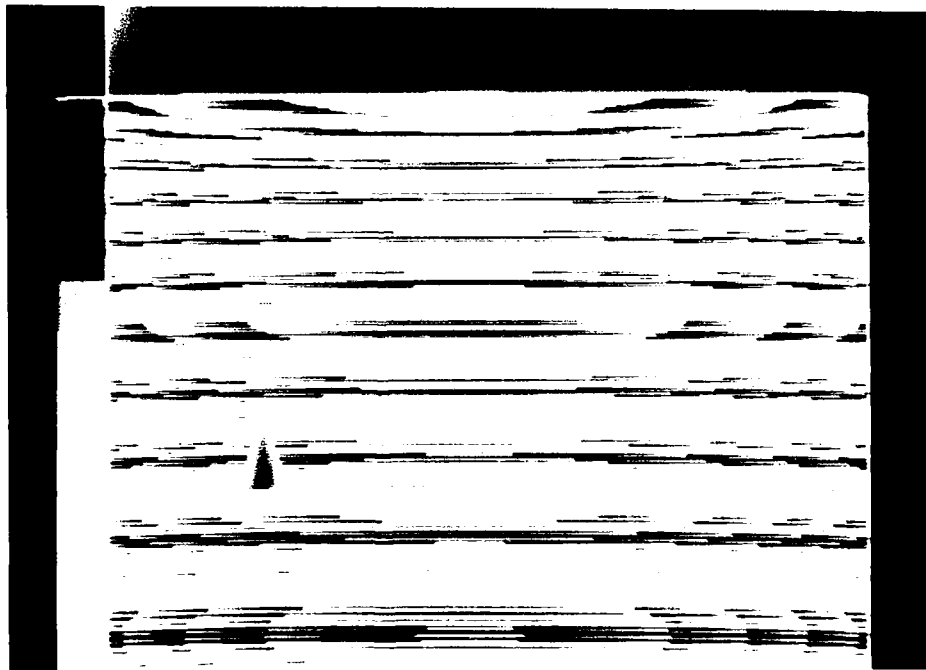


**Fig. 6-6: Pseudo 16 Bit Display of Cone at 971 meters**  
Color Bar at Left Denotes Value of High Byte-32Ran Scheme  
Lower Byte of Image Displayed Through 255Spec Color Table

#### 6.4. Comparison of 5 Bit Data

Since  $2^5=32$ , 5 bit imagery was used to compare the differences between images colored by 32Ran, 32Spec, and the 32 gray schemes. Two target models were used. The target was the stair step model used in the evaluation of real sensor data in Chapter 3. The second synthetic target was a cone. These two targets were selected because they are relatively simple, and image creation is quick. The cone is particularly useful in that it has curvature which often results in shading differences under the display schemes. The flat surfaces of the stair step do not always provide the appropriate geometry for such shading to occur. The cone has an altitude of 4.5 meters, and is 3 meters in diameter at the base. These dimensions insure enough curvature under the sample geometry used.

#### 6.5. Synthetic Data Creation Parameters

For the 5 bit evaluation, a sensor altitude of 60 meters above the ground plane, and the targets were placed at 160 meters downrange from the sensor. An additional downrange value of 320 meters was also used in order to create scenes of varying dynamic range along the sensor boresight. The two scene geometry produced data which were indicative of 8 and 9 bit scenes, with the quantization level of .33 meters(1 foot) in range. The scenes were produced at a greater dynamic range than 5 bits to insure that there would be several ambiguity intervals in the

image.

### 6.6. Range Ambiguity Function

The ambiguity function occurs as a result of the display scheme. Since there are 8 or 9 bits of dynamic range in the original image and only 5 bits in the display scheme, repetition will occur. Because the data was created with a quantization level of .33 meters, and the display is modulo 32, the ambiguity function is displaced every  $32 \times .33$  meters or 10.6 meters. This corresponds to 32 feet. Thus all points in the scene that are the same color are at the same range under modulo 32 arithmetic. It could be viewed that this data was created with a relative range sensor, say a radar that was amplitude modulated. The waveform has no ability to measure any phase delay over 360 degrees. Thus, any range value measured will be modulo 360 in phase. Any range scene encoded with less dynamic range in the coding scheme than the scene content will appear to have ambiguity intervals in it.

Compare the following scenes displayed in the various 32 entry look-up tables. The location of the target in Fig 6-7 is at the 128th pixel of the 128th scan line. The target is the stair step model at an apparent aspect of 135 degrees. Range to the target along the boresight is 178.64 meters. The 32Ran display scheme shows details across the target more clearly than the 32Spec scheme does. The target stands out more apparently in the 32Spec scheme however.

This is due to two factors. The first is the geometry of this particular scene, and the second is the display schemes. The rapidly changing colors of the 32Ran scheme provide more visible detail across the target as each different color corresponds to a difference in range along the boresight of .33 meters. The silhouette of the target stands out more clearly in the 32Spec scheme as there are the same number of colors present as in the 32Ran scheme, but the background changes more slowly because the 32Spec scheme changes from one hue to another through 3 dilutions of the baseline hue.



Fig. 6-7: Scene 1 Viewed through 32Ran Scheme

Hence the 32Ran scheme varies, at first appearance four times faster than the 32Spec scheme does. Upon close scrutiny, it can be seen that the 32Spec display does indicate the changes in range across the target. Several of this type were developed, and the problem of determining the proper of colors to display frequently arose.



**Fig. 6-8: Scene 1 Viewed through 32Spec Scheme**

Any display scheme should support the detection of the target from the background as well as the recognition of the target.

The next set of images will attempt to illustrate the inherent problem with providing too much discernible

difference across a common target. To further compare the differences between the 32Ran and 32Spec schemes, Scene 2 illustrates a situation where detection of the target in either the 32Ran or 32Spec schemes is of the same difficulty. These scenes were created with the proper geometry for this comparison in mind.



**Fig. 6-9: Scene 2 Viewed through 32Ran Scheme**

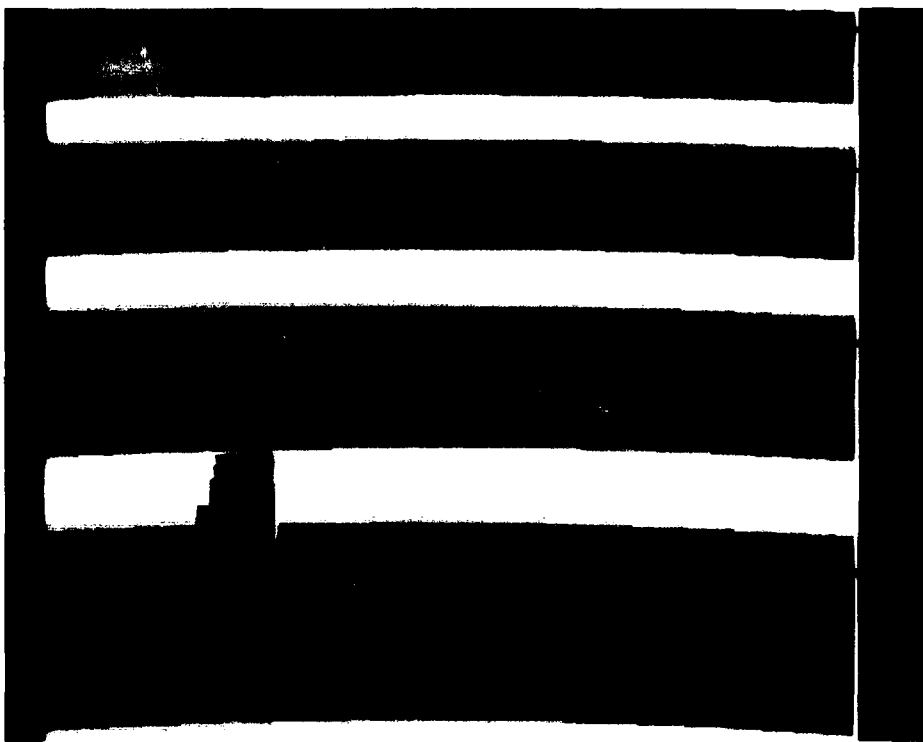


**Fig. 6-10: Scene 2 Viewed through 32Spec Scheme**

The segmentation of the target in the 32Ran scheme is a disadvantage. This scheme breaks up the target into too many sub-targets. The accuracy of the representation is not the issue; the recognizability of the object as opposed to its appearance in the 32Spec scheme is. For this scene, the target is located at about the 128th pixel of the 384th scan line. The target is 69.3 meters from the sensor. Apparent aspect to the target is 167 degrees. The 32Spec scheme keeps most of the pixels on the target in the same hue, namely blue, while the 32Ran scheme has colored several of the regions on the back part of the target. If such a scheme as

32Ran were used in a scene with range noise at an rms value of .33 meters, the color fluctuation across the target would be considerably more distracting to a human than display of the same noisy scene through the 32Spec scheme. For comparison, the 32Spec scheme could tolerate at least as much as 2 times the range noise as the 32Ran scheme and not have the pixels change hue. Thus the sensitivity to noise of a scheme like 32Ran would not be expected to be as robust as a scheme such as 32Spec.

In the first two sets of images, the differences between a totally random coloring scheme and one with an ordered progression of colors were investigated. Several color look up tables and test images were developed during the investigation, and these two selected compare the fundamental difference found with respect to locating targets in synthetic range imagery. For the investigation, target parameters were varied as well as sample geometries, the difficulty in finding targets with the 32Ran scheme compared to the 32Spec scheme quickly became apparent after several test scenes were displayed. The 32Ran scheme with a highly trained individual viewing the ladar data may have some advantages. The simple fact that each range difference is a totally different hue with respect to the previous hue may enable a trained individual to detect detail that may be imperceptible under the 32Spec scheme.

### 6.7. Difficulty with Gray Scale Display

Because the HVS can detect fewer number of gray scale changes than it can color changes, the limitation of a gray scale display is thus known. The relative effectiveness, of a gray scale display may not, however, detract from system performance. The exact nature of the particular scene displayed has a bearing on the effectiveness of any display scheme. For the most part, the limiting factor in a gray scale display is the uncertainty of where the target will be. This is significant when it is considered that a gray scale typically ranges from white to black. A black gray scale presentation of range data to humans will always result in a contrast limited situation. Contrast differences do not limit any color display of ladar data. Two colors may be of the same contrast level, but be viewably different. Recall from the discussion of the human visual system that contrast detection or perception is primarily a determination by the HVS of the luminance. Thus it is possible to have several different hues at the same luminance. This is an inherent benefit of encoding data in color. Figures 6-11 and 6-12 illustrate the difficulty in using any gray scale presentation scheme. Notice that the target might have easily occurred in a location that rendered its display largely in a dark region. The contrast between the target and the background in a gray scale display scheme will always be the limiting factor in the

display scheme. The fact is that humans cannot recognize more than about 50 levels of gray at any time. The possibility of a scenario that requires more than 50 different range numbers to be presented to the human is not unreasonable.

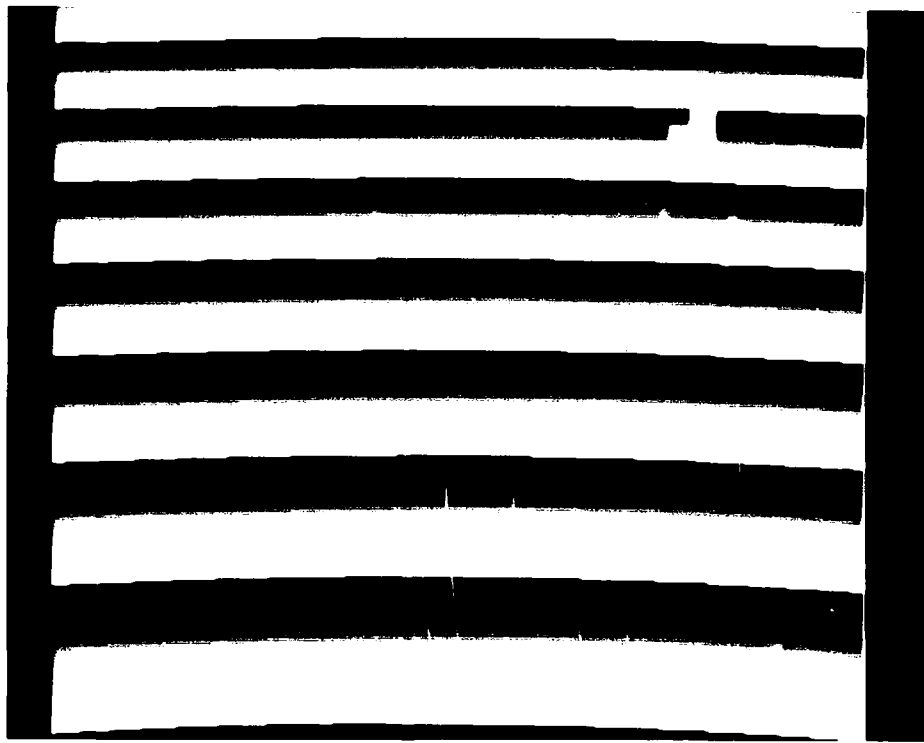


**Fig. 6-11: Scene 3 Viewed through 32Gray Scheme**



**Fig. 6-12: Scene 3 Viewed through 32Spec Scheme**

Clearly a total gray scale presentation of more than 50 levels of gray would not satisfy all display requirements. Color coding as opposed to gray scale coding of the data offers more flexibility in the presentation of range values to the human.

#### **6.8. Color Differencing and Contrast Limits**

The final comparison of the benefit of a color scheme that advances through the visible spectrum of colors is shown in this section. The primary limitation of any monochrome display is due to the limited dynamic range of gray scales that may be simultaneously displayed to the

human. Although gray scale presentation is useful in the presence of high noise, it is inherently limited in dynamic range.

The full 255 color look-up table designed for this thesis was based on the same idea as the 32Spec look-up-table discussed earlier. The primary concept was to group the colors in some order, namely warm colors to cool colors, and include a decrease in purity from a baseline hue. This would enable various effects on the ladar data to be produced by simple multiplication and division of the absolute range values. All effects are "non-linear" with respect to the HVS, as the processed image appears differently from the original image as displayed through the 255Spec, or 255 color look-up-table which traverses the visible spectrum. All images are displayed through the 255Spec color table, and all operations are a result of 16bit scaling operations on the data.

Division of the full 16 bit range values will result in a decrease in the quantization level of the original data. This will also result in a decrease in range resolution of the original scene. Compare the original image of the plywood stair step model at 500m range displayed through the 255Spec look-up-table. The plywood stair step target is in the center of the frame and is at an apparent aspect of 90 degrees to the sensor. Details are rather difficult to discern.



**Fig. 6-13: Plywood Model at 500m, 90 degree aze - 255Spec**

The next scene is the same data in the previous scene displayed through the 255 gray scale look-up-table. The target stands out distinctly in the gray scale display. The dynamic range of the original scene is 4200.(1400 meters original dynamic range of the scene, but quantized at .3 meters/bit). Displaying a unique color for every value of the lower byte is simply too much information for the human. The gray scale presentation of the data is limiting the number of viewable values to about 50. The gray values seen are falling into differentiable grays as a function of the HVS. The net effect is a more understandable scene.

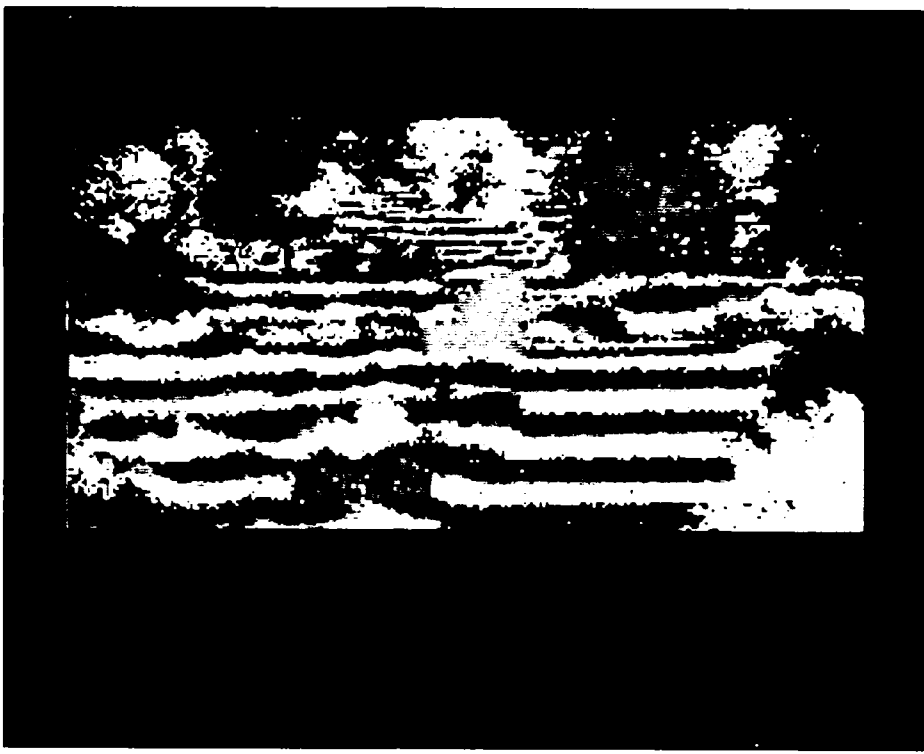


**Fig. 6-14: Plywood Model at 500m, 90 degree aze - 255Gray**

Panels at the low left of the scene are calibration panels for the ladar sensor. They are viewably more distinct in the gray scale presentation of the data. Due to the structure of the 255Spec look-up-table, it is possible to scale the data in such a manner as to vary the quantization level of the data and achieve the appearance of having stretched the colors over larger sections of the scene. This occurs because the 255Spec display scheme is a composite of various hues that are grouped together, and within each hue a trend from the pure baseline hue to a more impure rendition of that hue is accomplished.

The display of the data through the gray scale

presentation is best when there are rapid spatial variations of the contrast content of the scene. Recall that in every instance of traversing from white to black in the gray scale presentation, the data along the boresight of the sensor has moved 85 meters(255 feet). In the 255Spec display, this same 85 meters along the boresight of the sensor results in crossing the color spectrum from red to violet.

Because a color appears differently when viewed against different backgrounds, an improvement in the displayed scheme should result from varying the colors across the scene more slowly. This would serve to stretch the colors across a greater range variation, and hence a greater part of the scene. This is accomplished by simply multiplying the original 16 bit range data by a scaling factor. The result of scaling by a number less than one is to reduce the quantization of the original data. The dynamic range of the original scene is large enough to result in a full range of values from 0 to 255 in the low byte of the 16 bit range values. Note the effect of the reduced quantization on the gray scale presentation. The gray scale presentation may still be better than the 255Spec presentation. Transitions from one hue to the next can be more easily seen in the scaled data as opposed to the original data in the 255Spec presentation. The result of scaling the original data by .25 and displaying it through the 255Gray and 255Spec look-up-tables is shown in the next two photographs.

AD-R164 213

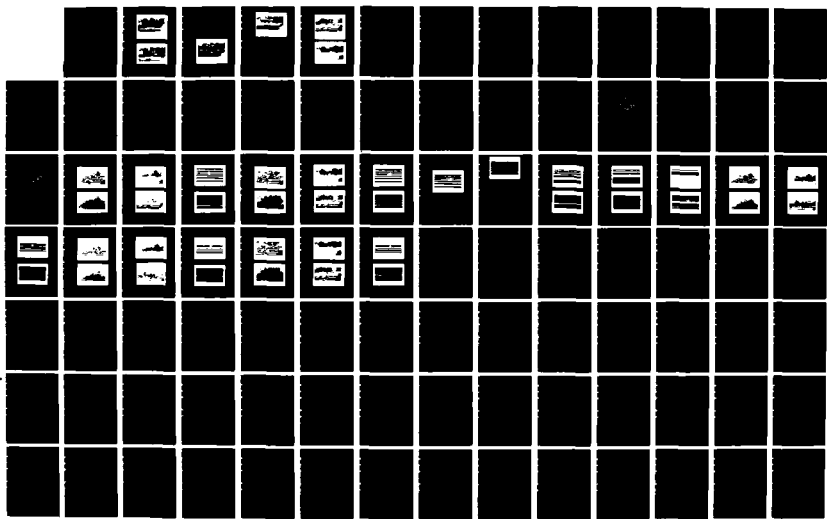
PSEUDO-COLOR DISPLAY OF LASER RADAR IMAGER(V) AIR  
FORCE INST OF TECH WRIGHT-PATTERSON AFB OH SCHOOL OF  
ENGINEERING N BARSALOU 02 DEC 85 AFIT/GE/ENG/85D-3

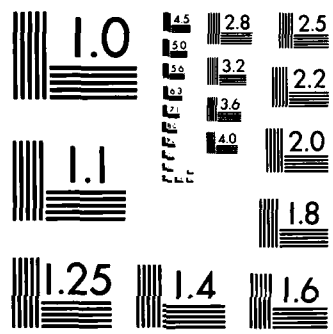
2/3

UNCLASSIFIED

F/G 14/5

NL





MICROCOPY RESOLUTION TEST CHART  
NATIONAL BUREAU OF STANDARDS-1963-A

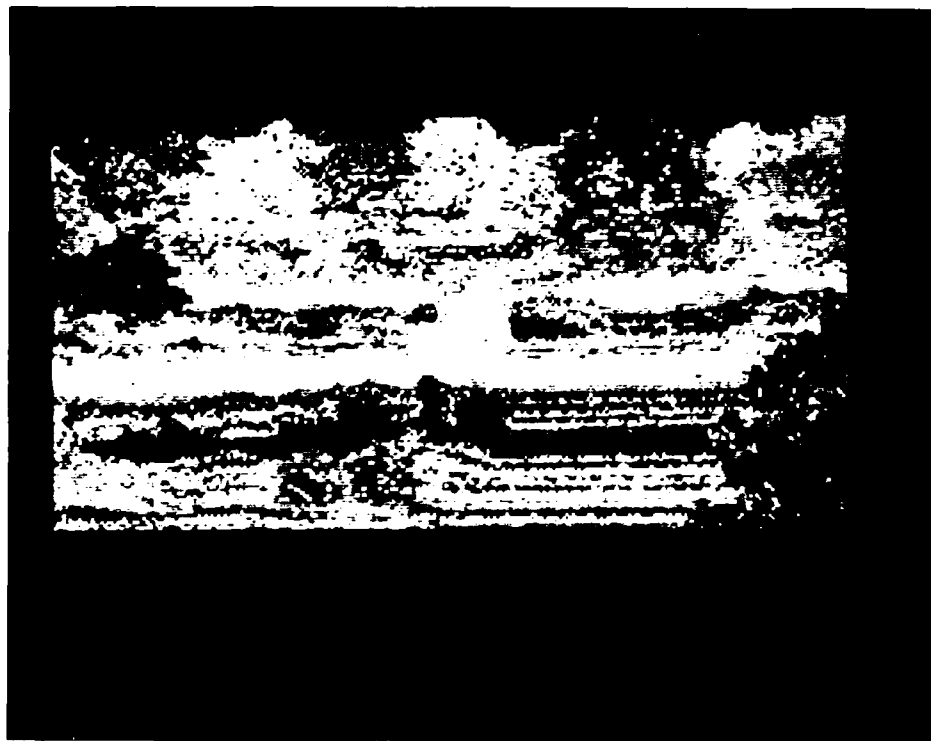


Fig. 6-15: Scene Scaled by .25 – 255Spec



Fig. 6-16: Scene Scaled by .25 Displayed through 255Gray

The next set of two images is the original data scaled by a factor of .125 . Notice how the gray scale presentation is losing information due to the stretching of the contrast function over a larger portion of the scene. The 255Spec presentation is able to present more detail to the human as a result of its not having the same contrast limit as the gray scale look-up-table. Again, the low byte has a dynamic range of a full 8 bits.

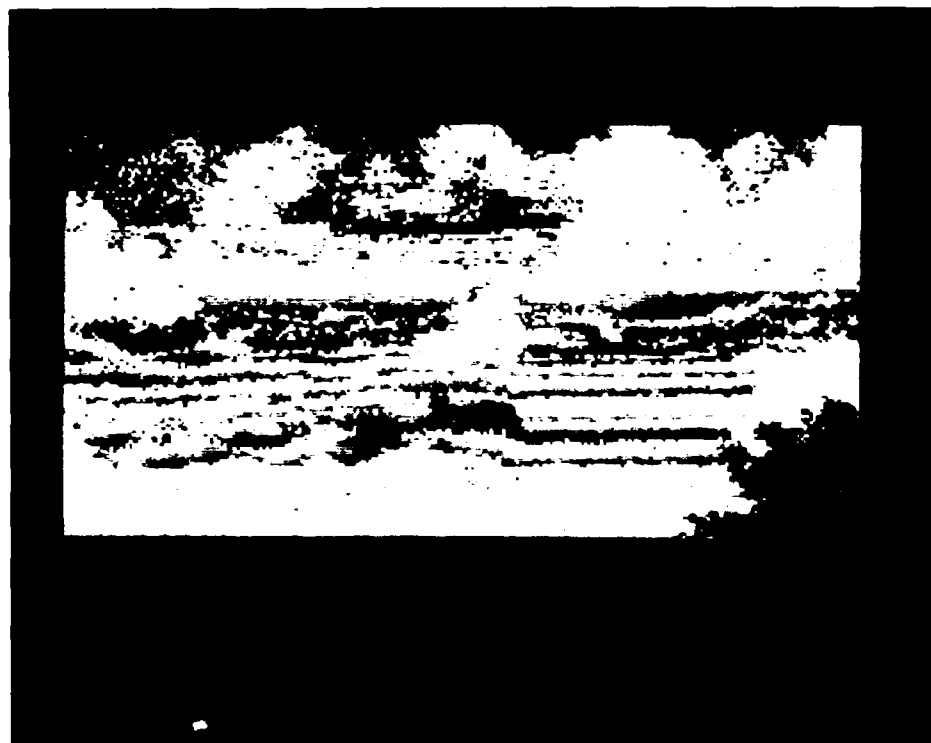


Fig. 6-17: Original Scene Scaled by .125 Displayed through 255Spec



**Fig. 6-18: Original Scene Scaled by .125 Displayed through 255Gray**

The final set of images illustrates the advantage of a color display over any gray scale display scheme. For this scene, the original 16 bit range data was scaled by .0625. Again, the dynamic range of the low byte was still a full 8 bits. The main point in comparing these images that have been scaled by various factors is the progression of the display from scaling factor to scaling factor. The color bands in the 255Spec displayed scenes varied from having color transitions that occurred at relatively short intervals in the original data, to bands that occurred at longer intervals. This rendered the data more intelligible, but not at the expense of reduced contrast. This particular scene geometry was more advantageous to the 255Gray display

scheme with the original data.

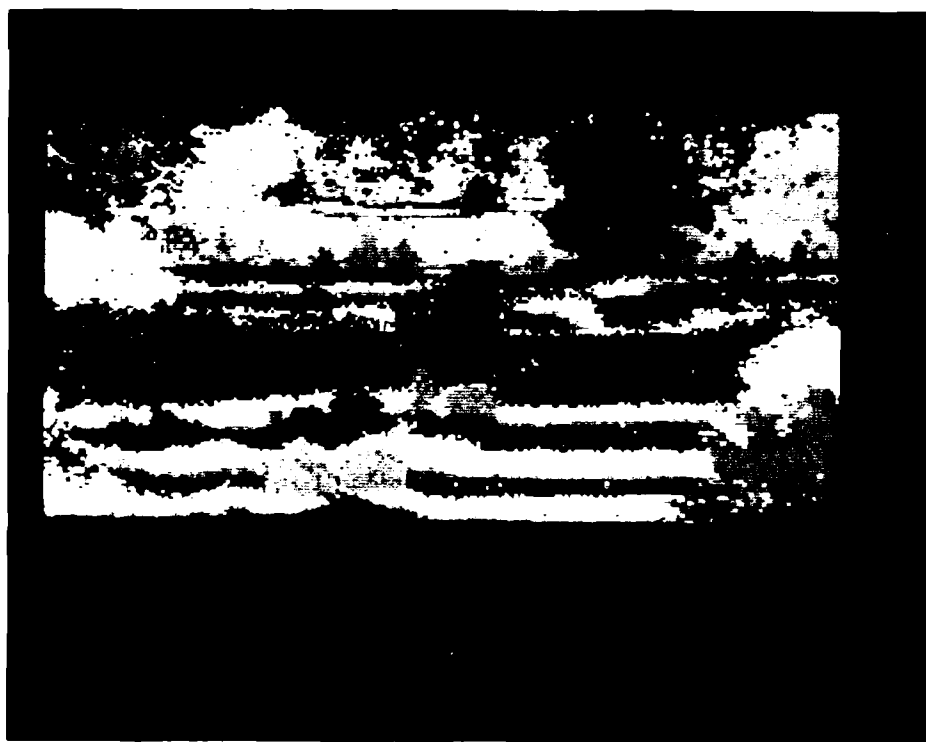


Fig. 6-19: Original Scene Scaled by .0625 Displayed through 255Spec



Fig. 6-20: Original Scene scaled by .0625 Displayed through 255Gray

Another scene geometry where the range values from pixel to pixel varied more slowly would have been less advantageous to the 255Gray scheme. The best that can be done for a gray scale presentation is to have the range values varying rapidly from pixel to pixel or scan line to scan line. Compare the differences between the original scene displayed through the 255Gray look-up-table, and the original scene after scaling by .0625 as displayed through the 255Spec look up table. It could be argued that the viewable quantization level of the original data viewed through the 255Gray look-up-table is not the original quantization level of .33 meters in range. The quantization level of the scene which has been scaled by .0625 and displayed through the 255Spec look-up-table has the same quantization viewable as unscaled scene viewed through 255Gray. The difference is the HVS limited the number of differentiable range values in the 255Gray look-up-table, whereas the 255Spec look-up-table controlled the number of differentiable range values. Actually, the range quantization of the original data at a value of .33 meters is accurately displayed by 255Spec in the original unscaled scene. Clearly, displaying the full dynamic range of the low byte may not be desirable under most circumstances. The power of a color presentation lies in the extended contrast range it provides over gray scale presentations. Additional complexities arise when the human may be required to do

different functions with the ladar data. Target recognition and target detection are two such functions that require different presentation schemes.(recall discussion earlier in this section). More research has to be conducted on the presentation of image data to humans via color versus gray scale; the objective of the presentation should be well structured into the display format. No single display scheme will provide the necessary information in the most effective manner under all circumstances. It is possible that multiple display schemes that can be manipulated by the operator will provide the necessary flexibilty to display the information in an effective manner.

## Chapter 7

### Recommendations and Conclusions

This thesis had three objectives:

- 1) Verification of synthetic ladar data.
- 2) Design of a display format for representing the full dynamic range of 16 bit range imagery.
- 3) Investigate the advantages or possible benefit of color coding ladar data.

It is clear that the use of synthetically created ladar data for the purposes of display to humans is acceptable when the target signatures are considered. Training humans to recognize target signatures generated by a simulation should pose no problems. Use of the synthetic data to simulate target signatures is confined by sensor noise only. Limitations arise due to the difficulty in predicting noise and clutter content of the scenes. Using simulated data for complete training of humans to recognize targets in realistic scenes has not been investigated. The simulation used in this effort could be modified to provide background clutter, but it is unlikely that such scenes would look much like data collected by a real sensor. The recommended approach to modelling a full complex scene involving both targets and clutter would be to deterministically create target information and stochastically model the background clutter. More analyses of actual CO<sub>2</sub> ladar data is necessary in order to compile

the necessary statistics for the stochastic noise and background generator. Any display schemes for the presentation of the data should, however, consider using the deterministic target signatures that are created by the current simulation, and then display real data through any scheme developed by using the synthetic data. Throughout the course of this thesis, it was found that the target signatures derived from the simulation were, with the exception of noise, compatible with the target signatures in the real sensor data. From a design standpoint, changes in the display scheme appeared as imagined, even before the display scheme was created and implemented on synthetic data. This was most helpful in determining what would work and what would fail with respect to the target signatures. The limitations of the synthetic data approach broke down when the background clutter was considered. Often a change in the look-up-table structure would produce the expected change in the target signature, but produced unexpected effects in the background clutter. Use of synthetic data was beneficial when the target signature alone was considered. No display scheme should be wholly based on the effects the display has on synthetic target signatures data alone.

### 7.1. Dynamic Range Presentations

For this thesis, the use of color only was investigated. The full dynamic range display was developed as a starting point only. For static image presentation,

this was about the most that could be done. The high byte displayed on an edge of the screen, with the low byte displayed on the screen provided all the information about the scene geometry in an understandable fashion. The investigation concerning how this display should be configured was most useful in uncovering the limiting factor in displaying range data to humans. This limitation is clearly the human. Color coding the information has the major advantage over gray scale in that more viewably different entities may be portrayed using color. The exact number of different color entities that may be displayed on a CRT should be investigated, or at least modelled. It is unlikely, however than any human would be able to perform reliably with a large number of differentiable colors presented on the CRT. It is more desirable to have a limited number of colors, and have the human operator scale the range values in order to vary the color content of the scene until a desirable effect is found. Many other schemes such as this may be developed and tested against each other if that is found to be necessary.

During the course of this investigation it was found that the context of what the human was expected to perform with the data was of primary importance. Some schemes that had distinct advantages over other schemes with regard to target detail, had severe disadvantages with respect to those same schemes when target detection was concerned. In

pattern recognition systems that attempt to find targets in real scenes a similar phenomena occurs when throughput of the processor is concerned. For example, target detection using sensor data is usually a throughput intensive operation. This means that every pixel that is collected by the sensor must be interrogated by some process in an attempt to limit the number of candidate pixels that might constitute part of the target signature. The other aspect of the problem results when the regions of the scene that have been segmented as possible targets have been extracted from the scene. At this point, most of the pixels in the scene have been discarded and closer inspection of the regions segmented may reveal a target. The operation of processing the regions of interest is a computationally intensive operation. These effects were found with regard to the HVS. Target detection requires a different display scheme than does target recognition. Put another way, an optimal target detection display scheme for a human viewer may not be an optimal or even an acceptable display scheme for a human performing target identification. The trade-offs between these two functional requirements with ladar data, and the impact that this has on any display scheme needs to be investigated.

## 7.2. Possible Plans for Further Studies

- 1) Continuation of low level studies
- 2) Investigation of high-level processes

### **7.2.1 Low Level Studies**

The continuation of low level studies would include an investigation concerning the number of entities that would be displayed to the human in an operational environment. The next issue would involve the creation of an n-dimensional color space that would be modelled as an n-dimensional orthogonal or maximum difference color space. The desired effect would be to create as many single colors that are required for the display, and place each of these single colors as far away from each of the colors in perceptual color space. This could then be thought of as an n-dimensional color space which is perceptually orthogonal. This would have several advantages over the color spectrum schemes used in this thesis, providing the colors can be sensibly grouped by the human operator in order. The perceptual differences would be satisfied in that each single color would be as different as possible from each of the remaining colors. This would be another low-level approach to enhancing the display of the ladar data.

### **7.2.2 High Level Process Enhancement**

It has been shown in this thesis that there are some benefits to be found by displaying range data in color as opposed to gray scale. Since the schemes used in this thesis used only low-level approaches to the problem. A high level approach to displaying the ladar data would involve processing of the sensor data by a processor for the

purposes of ordering the data. By ordering the data, the processor would be adding information, and decreasing the entropy of the the image before it is displayed to the human. Due to the metric quality of the ladar data, the high level approach to enhancing ladar data may be of most benefit to a human operator. A proposed high level scheme that would reduce the computations by the human is as follows:

- 1) Segment the incoming sensor data into planar surfaces
- 2) Calculate the mean square range to the planar surfaces
- 3) Color the surfaces according to the mean square range

Such an approach would then allow the human to view the scene and connect the surfaces together to create objects. This would reduce the burden of having the human screen every pixel. The problems with any such scheme is that the processing algorithm will have sensitivities as well as a probability of false alarm and a probability of detection as all pattern recognition algorithms have. It will, in effect, be detecting planar surfaces in ladar data. Schemes of this sort will probably provide the most flexibilty and increase in performance of the man-in-the-loop. The current trend of ever rising complexity in the cockpit, and increased pilot workload, may require such a scheme, as the pilot or weapon systems operator may be performing in a time limited capacity.

### 7.3. Limit of Human Visual Capacity

Ultimately, the target recognition may be totally done by computer, and only confirmation of the target would be required of the pilot or weapon system operator. The time line may then require a quick response from the operator in order to launch a weapon to destroy the target. High level processes of the computer may assist in reducing pilot reaction time by properly displaying the ladar data to the pilot in a concise, quickly recognizable format. The only alternative to displaying the ladar data to the human would be to construct a world model in a cartoon or synthetic display format, and train the pilot on the world model that the computer is using to communicate with him. All this would involve a series of higher and higher level processes. This may lead to the total removal of the man-in-the-loop. When the system has to make progressively more complicated calculations in order to describe the world state to the human than it requires to internally ascertain the world state, then it is necessary to remove the man from the loop.

## 8. BIBLIOGRAPHY

1. Baldemar, Gil; Mitchie, Amar; and Aggarwal, JK, Experiments in Combining Range and Edge Maps, Computer Graphics and Image Processing, 21, 395-414, 1983.
2. Barton, B.K., Radar System Analysis, Artech House, Dedham, Mass., 1976.
3. Burnham, Robert; Clarence, H. Vision and Visual Perception, John Wiley and Sons, Inc., NY, 1965.
4. Committee on Colorimetry of the Optical Society of America, The Science of Color, Optical Society of America, Wash, D.C., 1963.
5. Duda, R., Nitzan, D., Use of Range and Reflectance Data to Find Planar Surface Regions, IEEE Transactions on Pattern Recognition, PAMI-1, No 3, p.259, July 1979.
6. Graham, Clarence, Vision and Visual Perception, John Wiley and Sons, Inc., NY, 1963.
7. Gregory, RL, Eye and Brain, McGraw-Hill, NY, 1966.
8. Hall, Ernest; Computer Image Processing and Recognition Academic Press, NY, 1979.
9. Jelalian, A.V., Laser Radar Theory, IEEE Handbook, 1978.
10. Judd, Deane, Wyszecki, G., Color in Business, Science, and Industry, John Wiley and Sons, Inc, NY, 1963.
11. Kabrisky, M., A Proposed Model for Visual Information Processing in the Human Brain, University of Illinois Press, 1966.

12. Levine, Martin, Vision in Man and Machine, McGraw-Hill, NY, 1985.
13. Pirenne, M.H., Vision and the Human Eye, Chapman and Hall, London, 1967.
14. Skolnik, M.I., Intro to Radar Systems, McGraw-Hill, NY 1976.
15. Watkins, W., Barsalou, N., Range Image Synthetic Scene Simulation Reference Manual, Air Force Armament Laboratory Technical Report No. 83-81, October 1983.
16. Yachida, M., Saburo, T., Application of Color Information to Visual Perception, Pattern Recognition, Pergamon Press, London, 1971.
17. Wolfe, William, The Infra-Red Handbook, Office of Naval Research, Dept of the Navy, Wash, D.C., 1978.

## A. Listings for Target Files

### A.1. Listing for Stair Step Model Target File

All target dimensions are given in inches.  
Dimensions are accurate to .025 inches.  
X,Y,Z are ordinates, LN = Link Code, C=Component

#### Code

X	Y	Z	C	LN
0.00	0.00	39.38	0.00	10.00
0.00	0.00	39.48	0.00	20.00
0.00	0.00	0.00	0.00	30.00
0.00	39.38	39.38	0.00	40.00
0.00	39.38	0.00	0.00	50.00
-91.95	39.38	39.38	0.00	60.00
-91.95	39.38	0.00	0.00	70.00
-91.95	0.00	39.38	0.00	80.00
-91.95	0.00	0.00	0.00	90.00
0.00	0.00	39.38	0.00	100.00
0.00	0.00	0.00	0.00	110.00
0.00	0.00	0.00	0.00	120.00
0.00	0.00	39.38	0.00	10.00
0.00	0.00	39.38	0.00	20.00
0.00	39.38	39.38	0.00	30.00
-39.38	0.00	39.38	0.00	40.00
-39.38	39.38	39.38	0.00	50.00
-39.38	39.38	39.38	0.00	60.00
0.00	0.00	0.00	0.00	10.00
0.00	0.00	0.00	0.00	20.00
0.00	39.38	0.00	0.00	30.00
-91.95	0.00	0.00	0.00	40.00
-91.95	39.38	0.00	0.00	50.00
-91.95	39.38	0.00	0.00	60.00
-39.38	0.00	78.76	0.00	10.00
-39.38	0.00	78.76	0.00	20.00
-39.38	0.00	39.38	0.00	30.00
-39.38	39.38	78.76	0.00	40.00
-39.38	39.38	39.38	0.00	50.00
-91.95	39.38	78.76	0.00	60.00
-91.95	39.38	39.38	0.00	70.00
-91.95	0.00	78.76	0.00	80.00
-91.95	0.00	39.38	0.00	90.00

X	Y	Z	LN	C
-39.38	0.00	78.76	0.00	100.00
-39.38	0.00	39.38	0.00	110.00
-39.38	0.00	39.38	0.00	120.00
-39.38	0.00	78.76	0.00	10.00
-39.38	0.00	78.76	0.00	20.00
-39.38	39.38	78.76	0.00	30.00
-91.95	0.00	78.76	0.00	40.00
-91.95	39.38	78.76	0.00	50.00
-91.95	39.38	78.76	0.00	60.00
-59.07	0.00	98.45	0.00	10.00
-59.07	0.00	98.45	0.00	20.00
-59.07	0.00	78.76	0.00	30.00
-59.07	39.38	98.45	0.00	40.00
-59.07	39.38	78.76	0.00	50.00
-91.95	39.38	98.45	0.00	60.00
-91.95	39.38	78.76	0.00	70.00
-91.95	0.00	98.45	0.00	80.00
-91.95	0.00	78.76	0.00	90.00
-59.07	0.00	98.45	0.00	100.00
-59.07	0.00	78.76	0.00	110.00
-59.07	0.00	78.76	0.00	120.00
-59.07	0.00	98.45	0.00	10.00
-59.07	0.00	98.45	0.00	20.00
-59.07	39.38	98.45	0.00	30.00
-91.95	0.00	98.45	0.00	40.00
-91.95	39.38	98.45	0.00	50.00
-91.95	39.38	98.45	0.00	60.00
-72.26	0.00	111.64	0.00	10.00
-72.26	0.00	111.64	0.00	20.00
-72.26	0.00	98.45	0.00	30.00
-72.26	39.38	111.64	0.00	40.00
-72.26	39.38	98.45	0.00	50.00
-91.95	39.38	111.64	0.00	60.00
-91.95	39.38	98.45	0.00	70.00
-91.95	0.00	111.64	0.00	80.00
-91.95	0.00	98.45	0.00	90.00
-72.26	0.00	111.64	0.00	100.00
-72.26	0.00	98.45	0.00	110.00
-72.26	0.00	98.45	0.00	120.00
-72.26	0.00	98.45	0.00	10.00
-72.26	0.00	98.45	0.00	20.00
-72.26	39.38	111.64	0.00	30.00
-91.95	0.00	111.64	0.00	40.00
-91.95	39.38	111.64	0.00	50.00
-91.95	39.38	111.64	0.00	60.00
0.00	0.00	0.00	0.00	0.00
0.00	0.00	0.00	0.00	0.00

0.00 0.00 0.00 0.00 0.00  
0.00 0.00 0.00 0.00 0.00

Continue entry of zero values until a total of  
200 data points are entered into the target file.

A.2. Listing of Target File for Cone

TARGET FILE FOR CONE

All target dimensions are given in inches.

Dimensions are accurate to .025 inches.

X	Y	Z	C	LN
240.00	0.00	0.00	0.00	1.00
240.00	0.00	0.00	0.00	20.00
0.00	0.00	720.00	0.00	30.00
231.82	62.12	0.00	0.00	40.00
0.00	0.00	720.00	0.00	50.00
207.85	120.00	0.00	0.00	60.00
0.00	0.00	720.00	0.00	70.00
169.71	169.71	0.00	0.00	80.00
0.00	0.00	720.00	0.00	90.00
120.00	207.85	0.00	0.00	100.00
0.00	0.00	720.00	0.00	110.00
62.12	231.82	0.00	0.00	120.00
0.00	0.00	720.00	0.00	130.00
0.00	240.00	0.00	0.00	140.00
0.00	0.00	720.00	0.00	150.00
-62.12	231.82	0.00	0.00	160.00
0.00	0.00	720.00	0.00	170.00
-120.00	207.85	0.00	0.00	180.00
0.00	0.00	720.00	0.00	190.00
-169.71	169.71	0.00	0.00	200.00
0.00	0.00	720.00	0.00	210.00
-207.85	120.00	0.00	0.00	220.00
0.00	0.00	720.00	0.00	230.00
-231.82	62.12	0.00	0.00	240.00
0.00	0.00	720.00	0.00	250.00
-240.00	0.00	0.00	0.00	260.00
0.00	0.00	720.00	0.00	270.00
-231.82	-62.12	0.00	0.00	280.00
0.00	0.00	720.00	0.00	290.00
-207.85	-120.00	0.00	0.00	300.00
0.00	0.00	720.00	0.00	310.00

X	Y	Z	C	LN
-169.71	-169.71	0.00	0.00	320.00
0.00	0.00	720.00	0.00	330.00
-120.00	-207.85	0.00	0.00	340.00
0.00	0.00	720.00	0.00	350.00
-62.12	-231.82	0.00	0.00	360.00
0.00	0.00	720.00	0.00	370.00
0.00	-240.00	0.00	0.00	380.00
0.00	0.00	720.00	0.00	390.00
62.12	-231.82	0.00	0.00	400.00
0.00	0.00	720.00	0.00	410.00
120.00	-207.85	0.00	0.00	420.00
0.00	0.00	720.00	0.00	430.00
169.71	-169.71	0.00	0.00	440.00
0.00	0.00	720.00	0.00	450.00
207.85	-120.00	0.00	0.00	460.00
0.00	0.00	720.00	0.00	470.00
231.82	-62.12	0.00	0.00	480.00
0.00	0.00	720.00	0.00	490.00
240.00	0.00	0.00	0.00	500.00
0.00	0.00	720.00	0.00	510.00
0.00	0.00	720.00	0.00	52.00
240.00	0.00	0.00	0.00	1.00
240.00	0.00	0.00	0.00	20.00
0.00	0.00	0.00	0.00	30.00
231.82	62.12	0.00	0.00	40.00
0.00	0.00	0.00	0.00	50.00
207.85	120.00	0.00	0.00	60.00
0.00	0.00	0.00	0.00	70.00
169.71	169.71	0.00	0.00	80.00
0.00	0.00	0.00	0.00	90.00
120.00	207.85	0.00	0.00	100.00
0.00	0.00	0.00	0.00	110.00
62.12	231.82	0.00	0.00	120.00
0.00	0.00	0.00	0.00	130.00
0.00	240.00	0.00	0.00	140.00
0.00	0.00	0.00	0.00	150.00
-62.12	231.82	0.00	0.00	160.00
0.00	0.00	0.00	0.00	170.00
-120.00	207.85	0.00	0.00	180.00
0.00	0.00	0.00	0.00	190.00
-169.71	169.71	0.00	0.00	200.00
0.00	0.00	0.00	0.00	210.00
-207.85	120.00	0.00	0.00	220.00
0.00	0.00	0.00	0.00	230.00
-231.82	62.12	0.00	0.00	240.00
0.00	0.00	0.00	0.00	250.00
-240.00	0.00	0.00	0.00	260.00



0.00	0.00	0.00	0.00	0.00
0.00	0.00	0.00	0.00	0.00
0.00	0.00	0.00	0.00	0.00
0.00	0.00	0.00	0.00	0.00
0.00	0.00	0.00	0.00	0.00
0.00	0.00	0.00	0.00	0.00

Continue entry of zero values until a total of  
200 data points are entered into the target file.

**B. Target Signature Verification**

**B.1. 500 Meter Range**

**B.1.1. Target Aspect 0 Degrees**

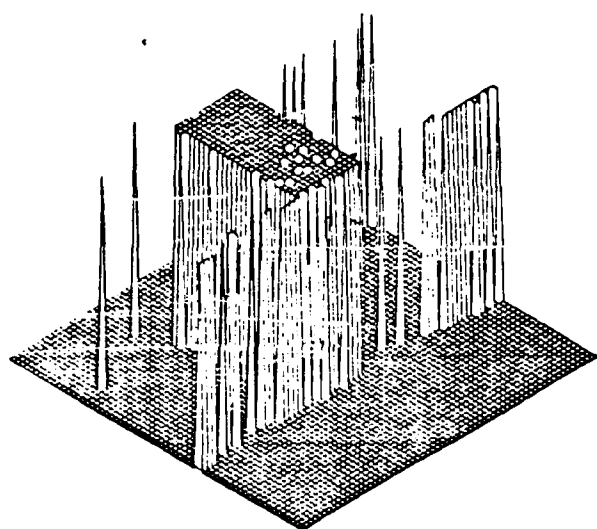


**Fig. B-1: Real Signature**

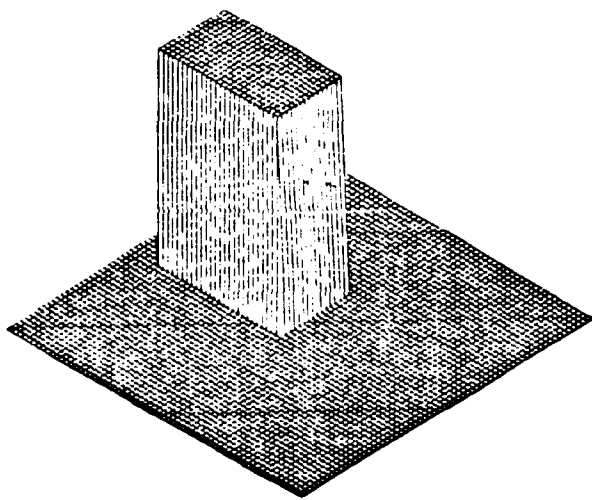


**Fig. B-2: Synthetic Signature**

B.1.2. Target Aspect 45 Degrees

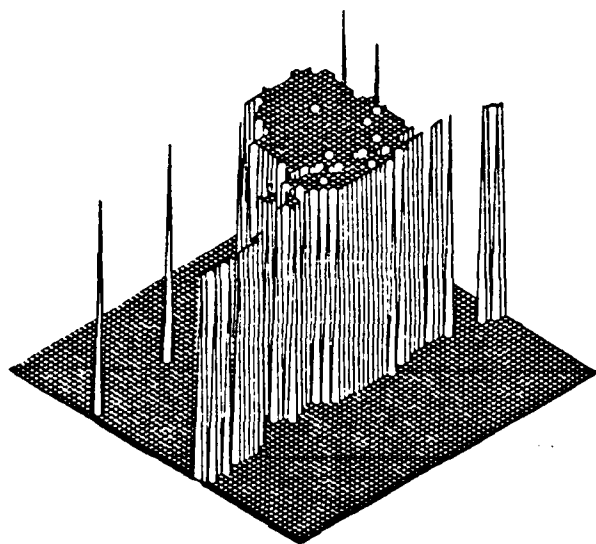


Fig. B-3: Real Signature

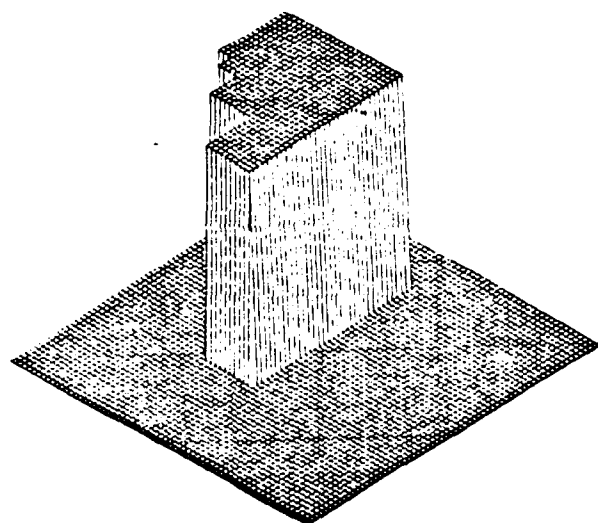
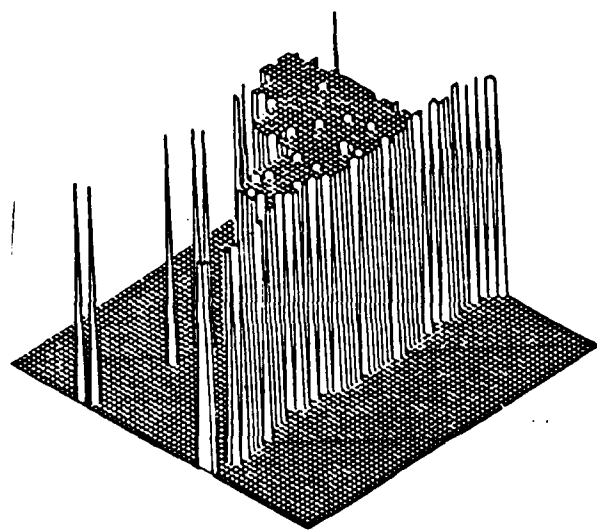
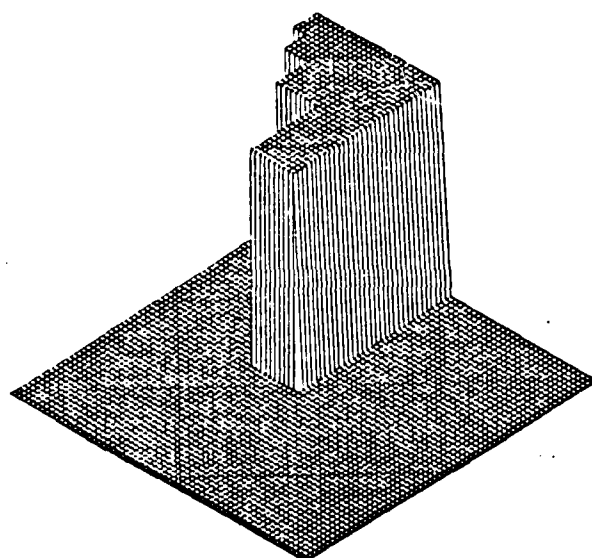


Fig. B-4: Synthetic Signature

**B.2. Target Aspect 90 Degrees**



**Fig. B-5: Real Signature**



**Fig. B-6: Synthetic Signature**

B.3. Range 800 Meters  
B.3.1. Aspect 0 Degrees

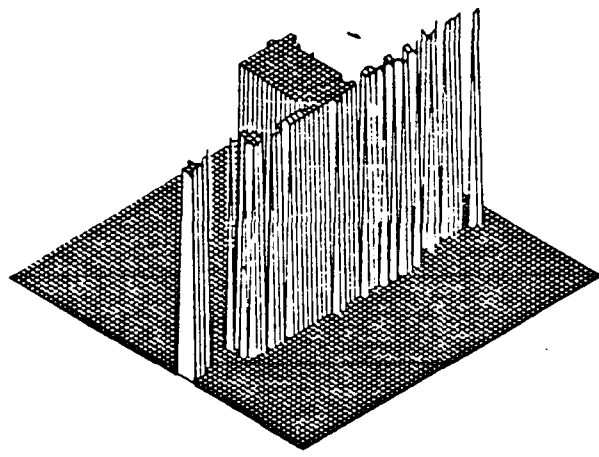


Fig. B-7: Real Signature

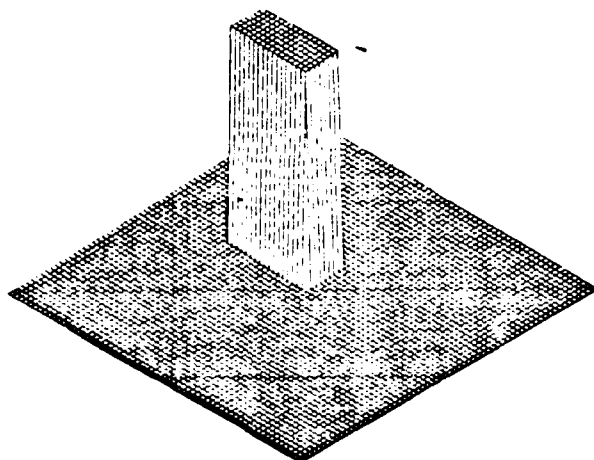
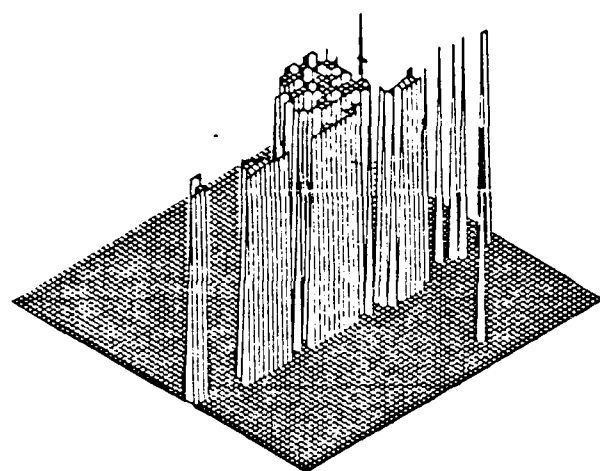
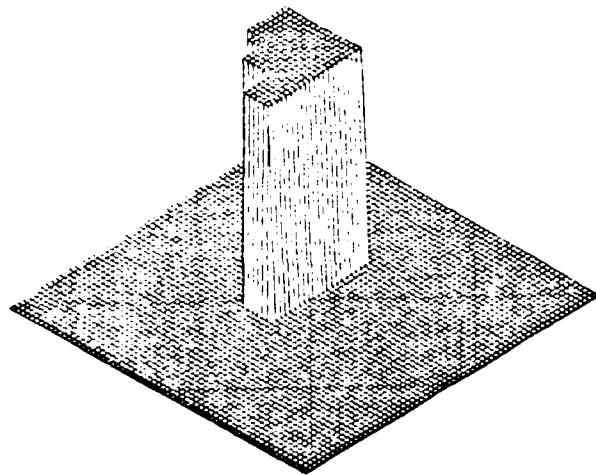


Fig. B-8: Synthetic Signature

**B.3.2. Target Aspect 45 Degrees**



**Fig. B-9: Real Signature**



**Fig. B-10: Synthetic Signature**

**B.3.3. Target Aspect 90 Degrees**

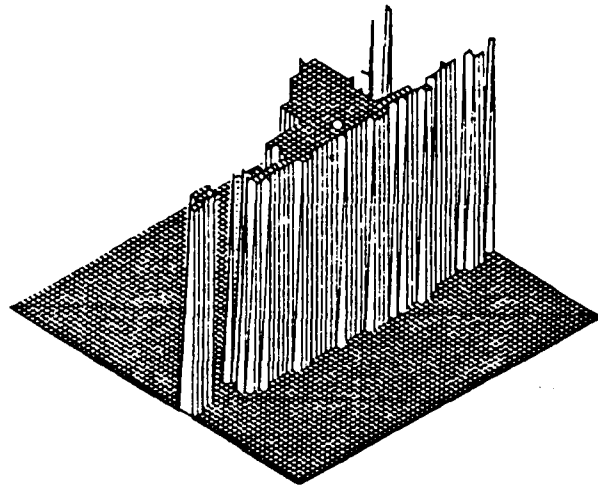


**Fig. B-11: Real Signature**

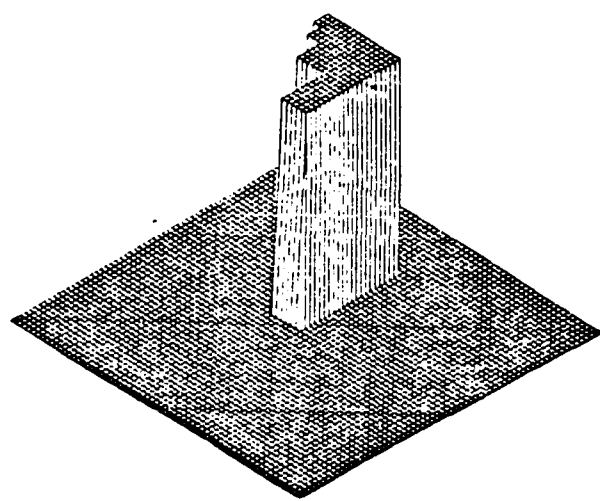


**Fig. B-12: Synthetic Signature**

Processed Ladar Imagery  
B.4. Range 500 Meters  
B.4.1. Target Aspect 0 Degrees

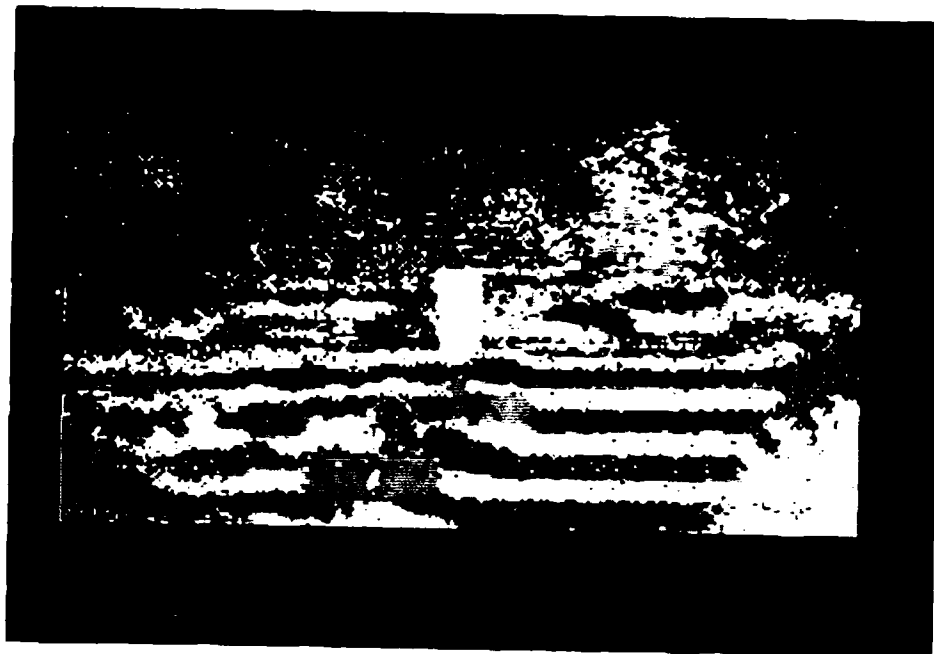


Fig. B-13: Original Scene - 255Gray Look-Up-Table



Fig. B-14: Original Scene -255Spec Look-Up-Table

B.4.1.1. Scene Scaled by .0625



Fig. B-15: 255Gray Look-Up-Table

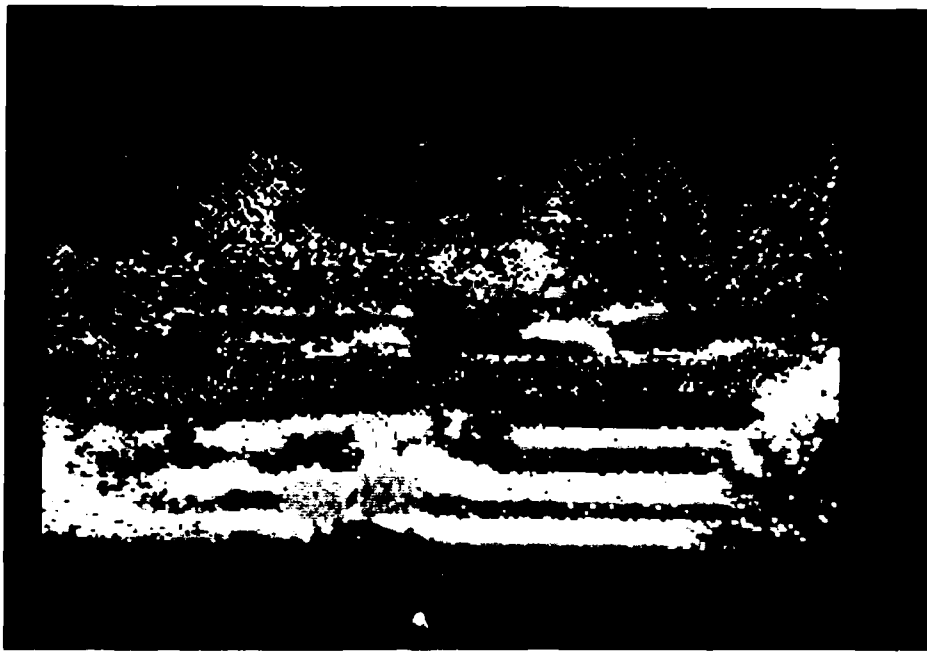


Fig. B-16: 255Spec Look-Up-Table

B.4.1.2. Synthetic Scenes

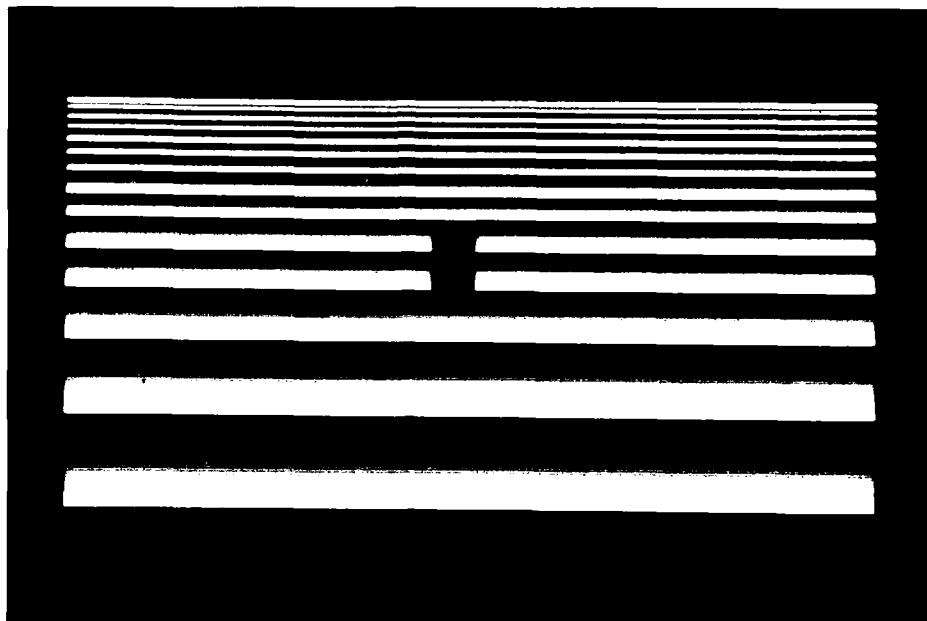


Fig. B-17: 255Gray Look-Up-Table

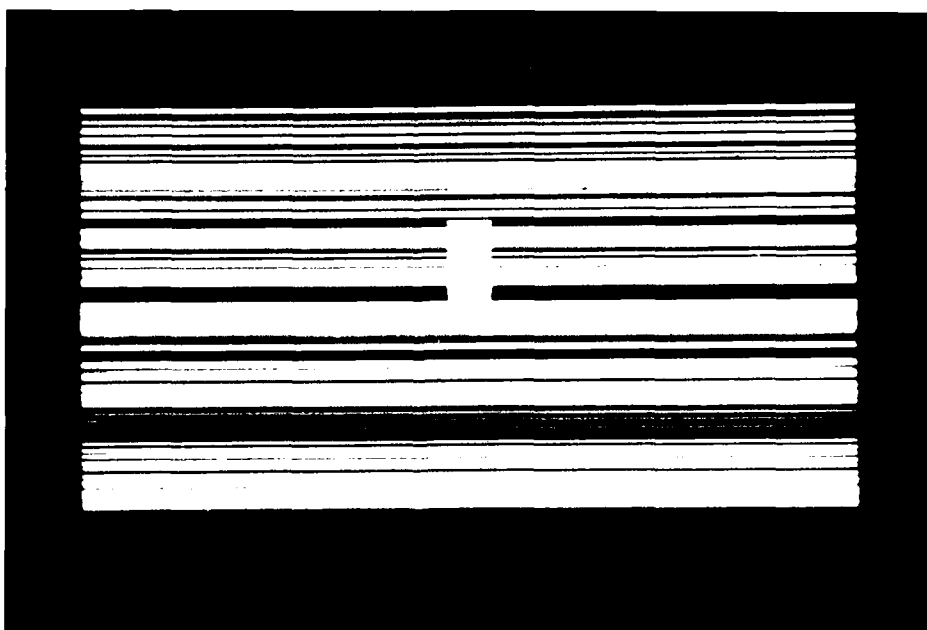


Fig. B-18: 255Spec Look-Up-Table

**B.4.2. Aspect Angle 45 Degrees**

**B.4.2.1. Original Scene**



**Fig. B-19: Original Scene - 255Gray**



**Fig. B-20: Original Scene - 255Spec**

B.4.2.2. Scene Scaled by .0625



Fig. B-21: 255Gray



Fig. B-22: 255Spec

B.4.2.3. Synthetic Scenes

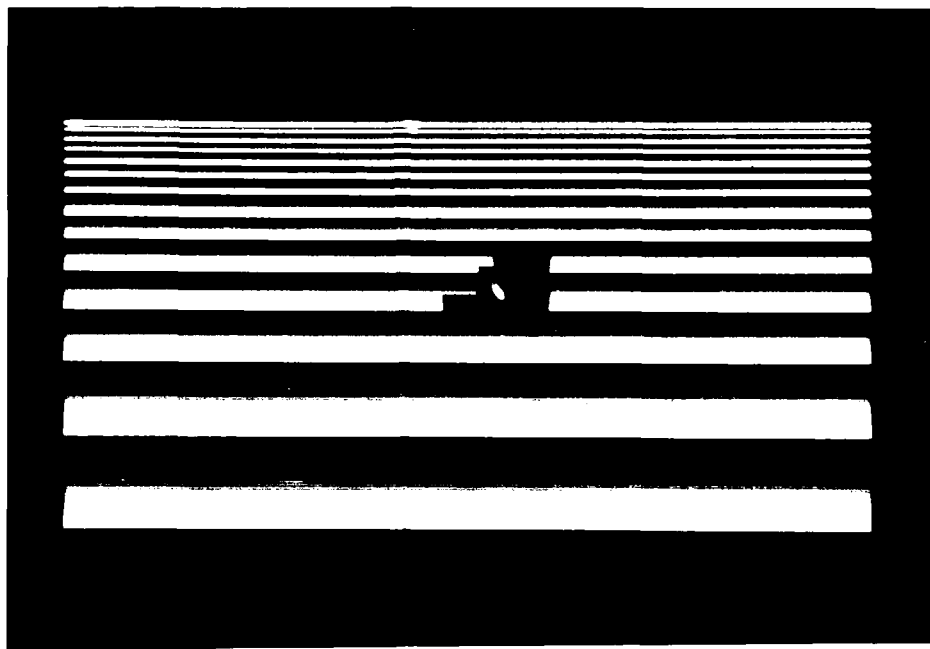


Fig. B-23: 255Gray

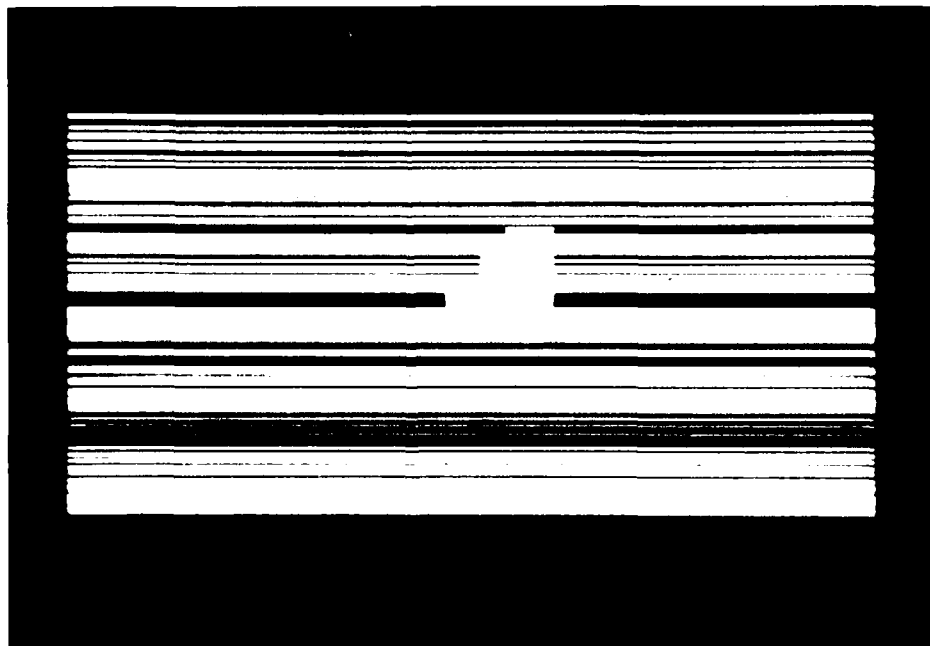


Fig. B-24: 255Spec

#### B.4.3. Aspect 90 Degrees

Chapter 6 presented the original sensor data of the 500 meter data with 90 degrees target aspect in a comparison between a gray scale display format, and a color display format. This section presents the same data, but of synthetic source.

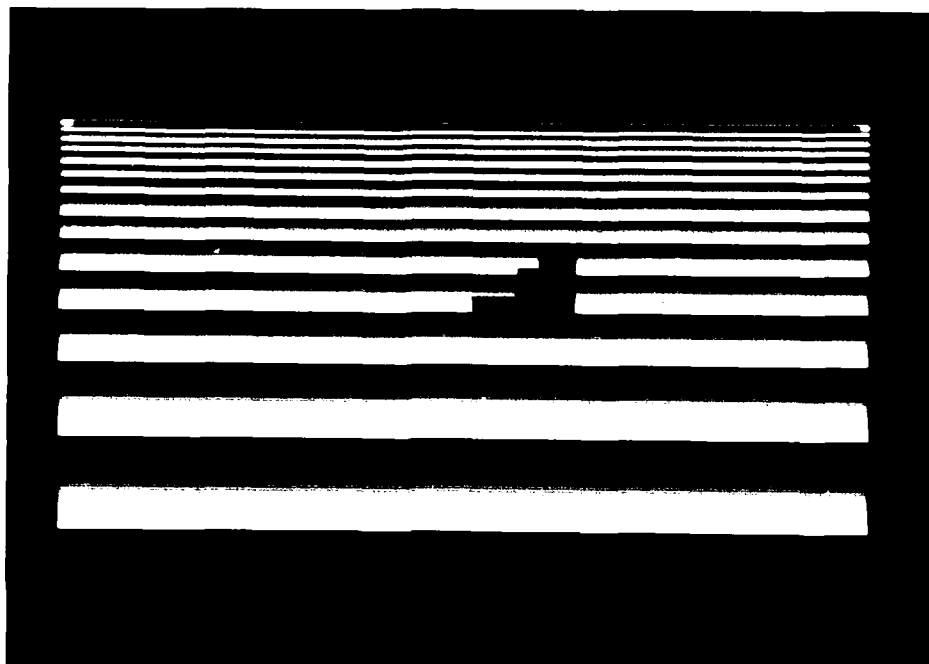
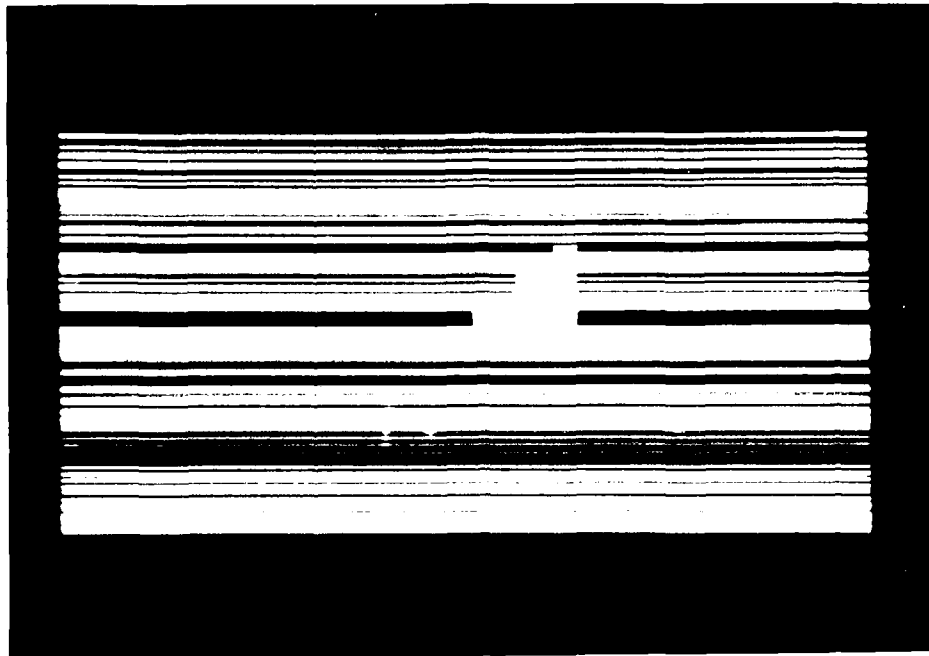


Fig. B-25: Full Resolution Data - 255Gray



**Fig. B-26: Full Resolution - 255Spec**

B.4.3.1. Synthetic Data Scaled by .5



Fig. B-27: 255Gray

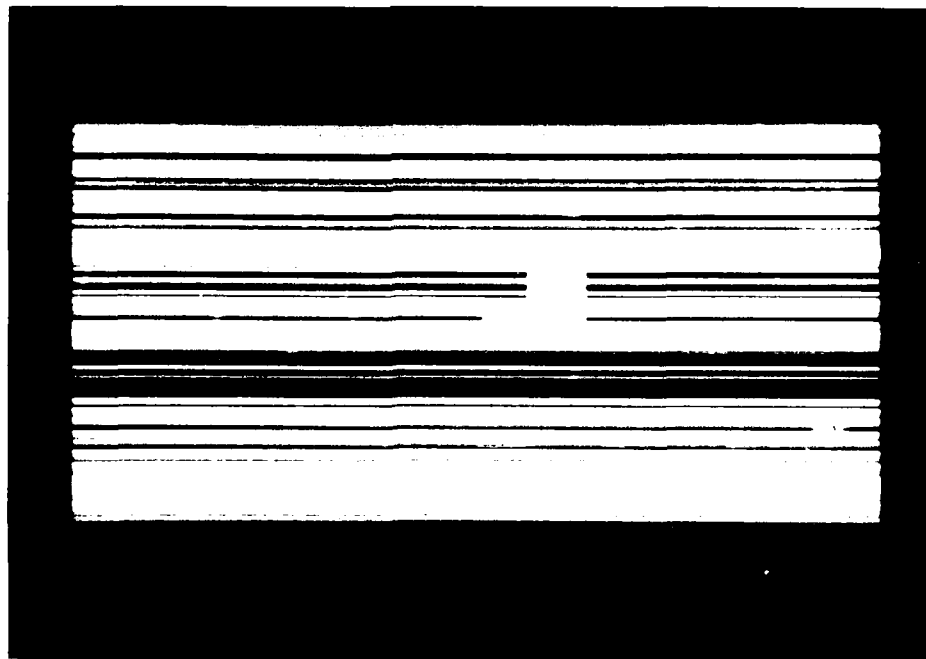


Fig. B-28: 255Spec

B.4.3.2. Synthetic Data Scaled by .25

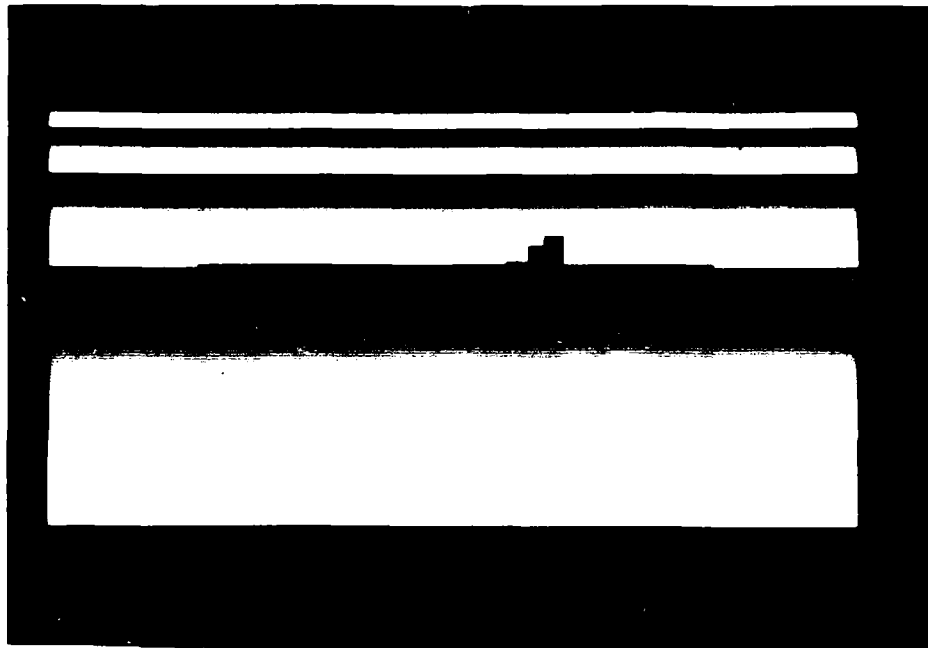


Fig. B-29: 255Gray

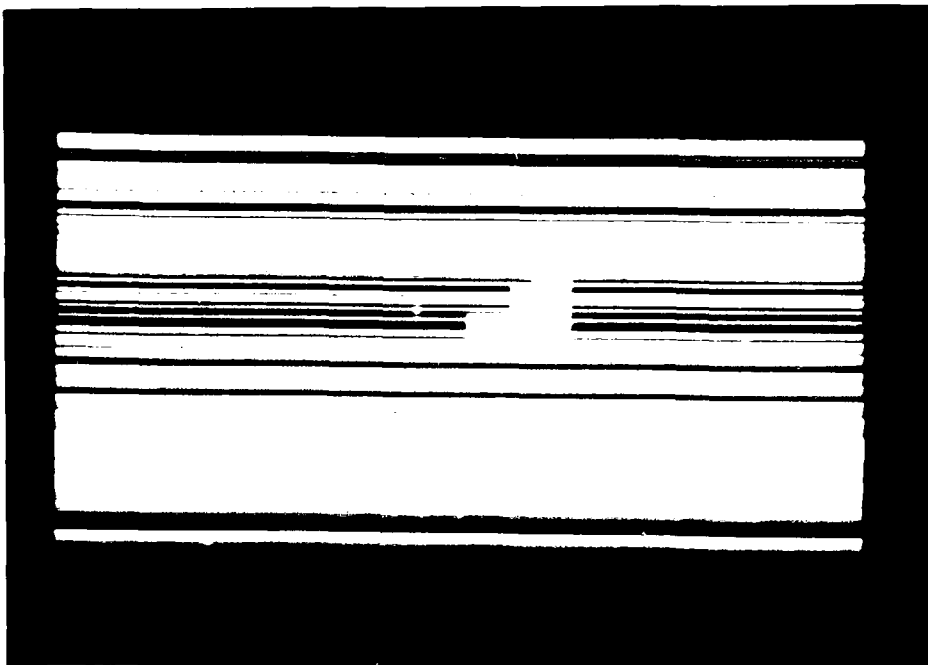


Fig. B-30: 255Spec

B.4.3.3. Synthetic Data Scaled by .125

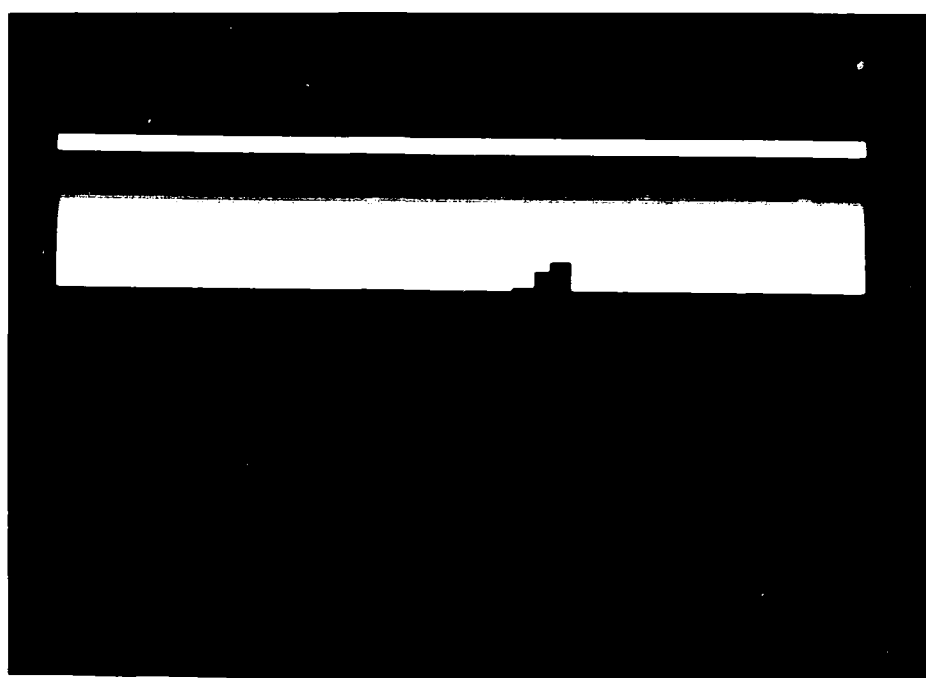


Fig. B-31: 255Gray

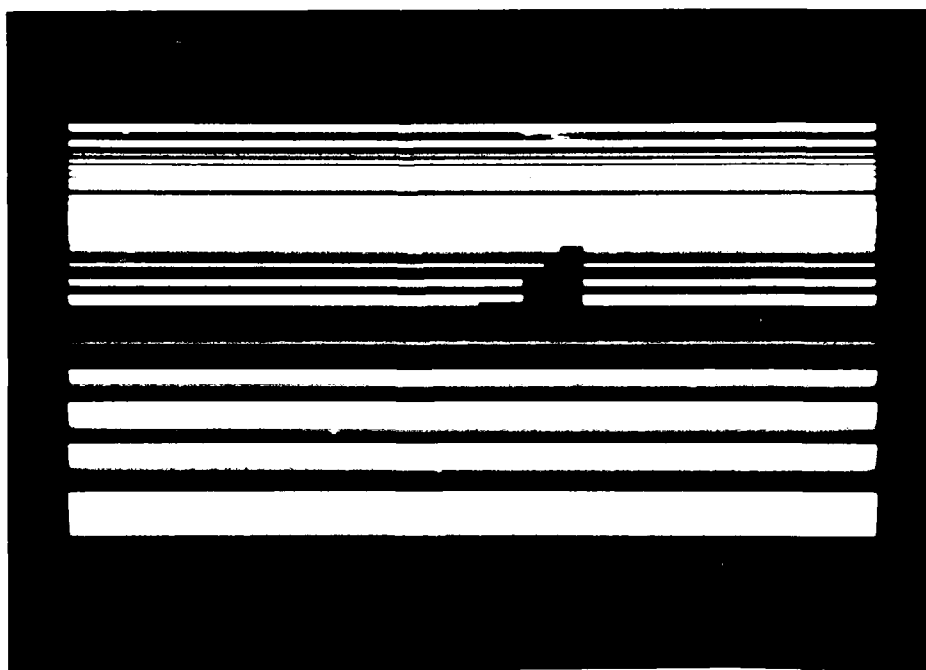


Fig. B-32: 255Spec

B.5. 800 Meter Range  
B.5.1. Aspect 0 Degrees  
B.5.1.1. Original Scene

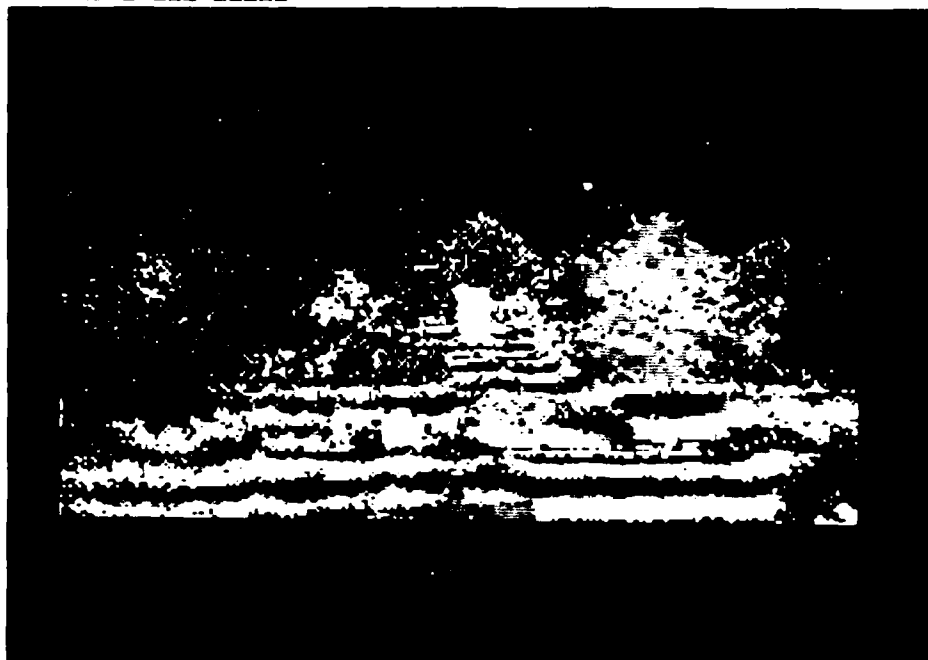


Fig. B-33: 255Gray



Fig. B-34: 255Spec

B.5.1.2. Scene Scaled by .0625



Fig. B-35: 255Gray



Fig. B-36: 255Spec

B.5.1.3. Synthetic Scene



Fig. B-37: 255Gray

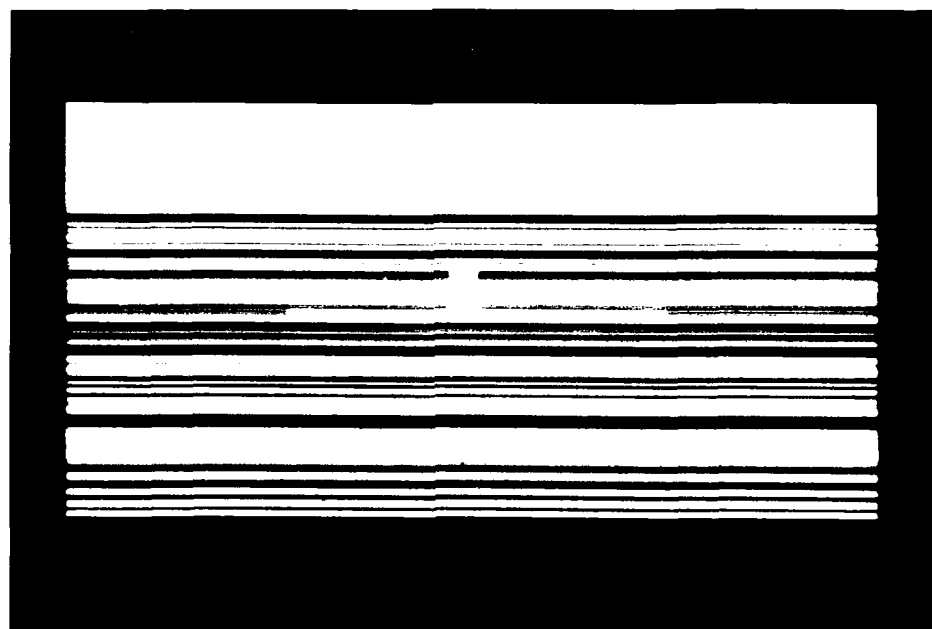


Fig. B-38: 255Spec

B.5.2. Aspect 45 Degrees  
B.5.2.1. Original Scene

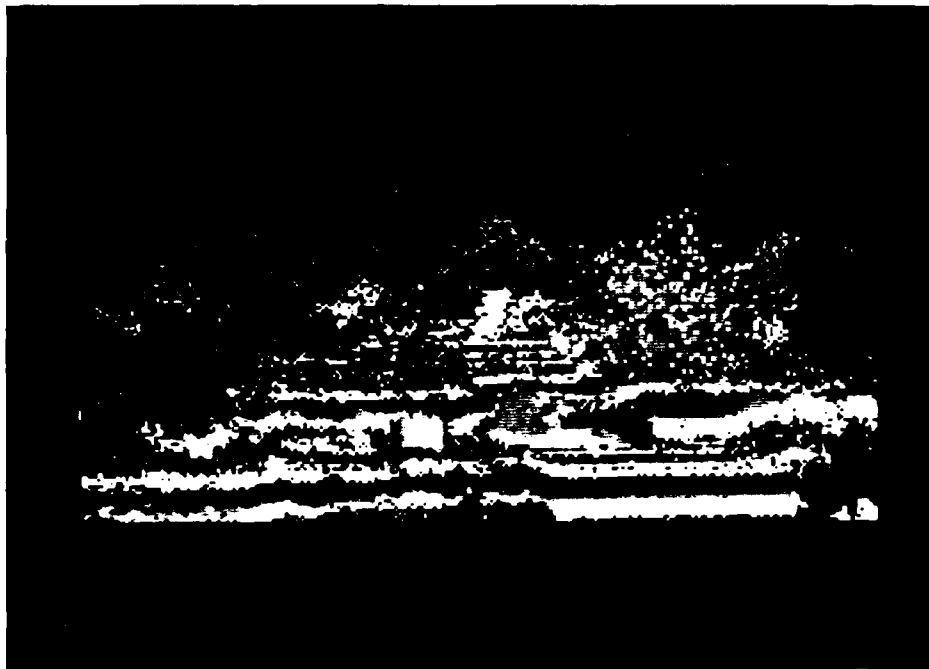


Fig. B-39: 255Gray

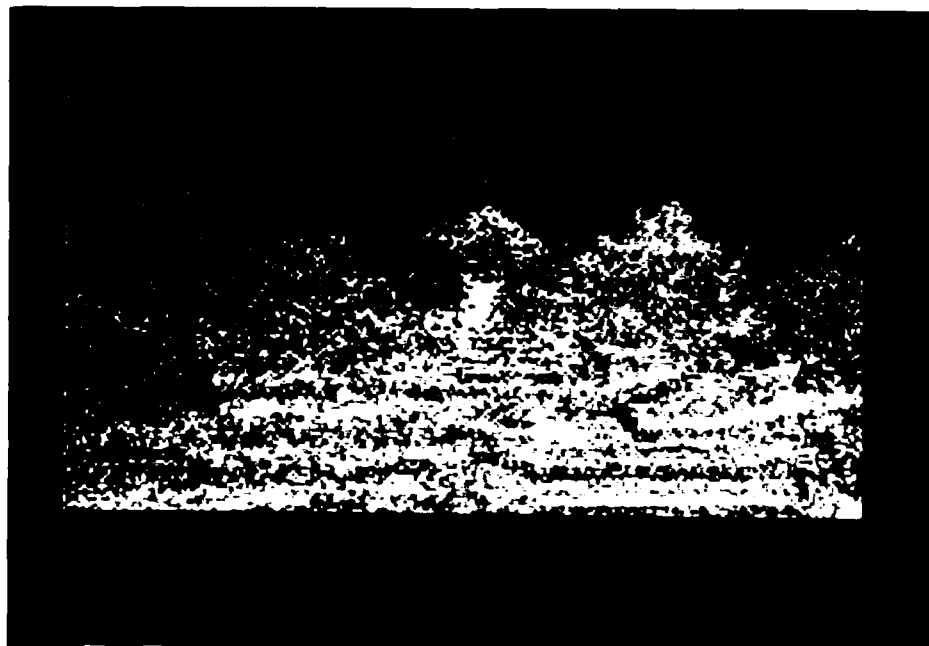


Fig. B-40: 255Spec

B.5.2.2. Scene Scaled by .0625



Fig. B-41: 255Gray



Fig. B-42: 255Spec

B.5.2.3. Synthetic Scene



Fig. B-43: 255Gray

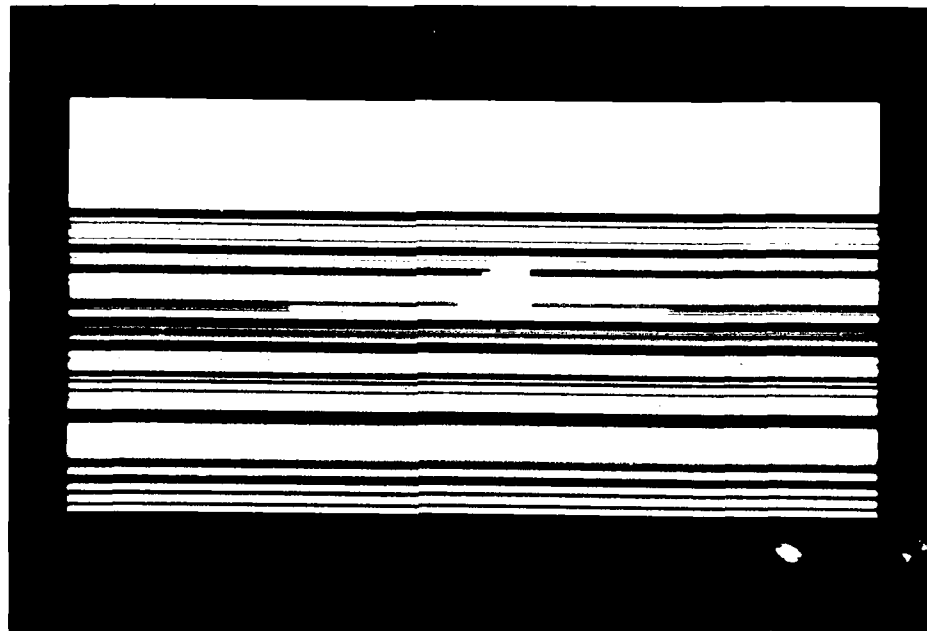


Fig. B-44: 255Spec

B.5.3. Aspect 90 Degrees  
B.5.3.1. Original Scene

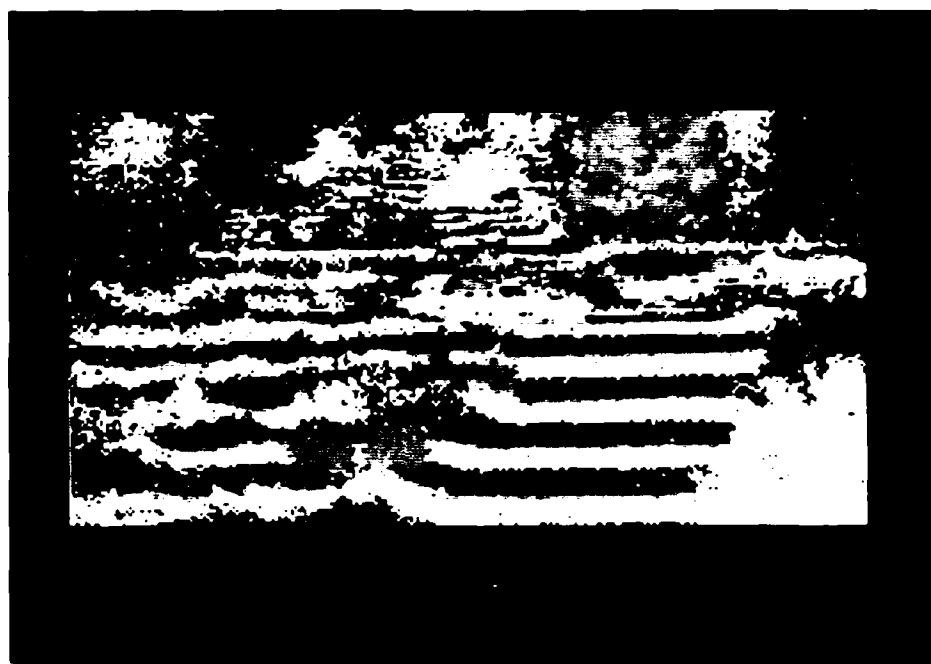


Fig. B-45: 255Gray



Fig. B-46: 255Spec

B.5.3.2. Scene Scaled by .0625



Fig. B-47: 255Gray



Fig. B-48: 255Spec

B.5.3.3. Synthetic Scene



Fig. B-49: 255Gray

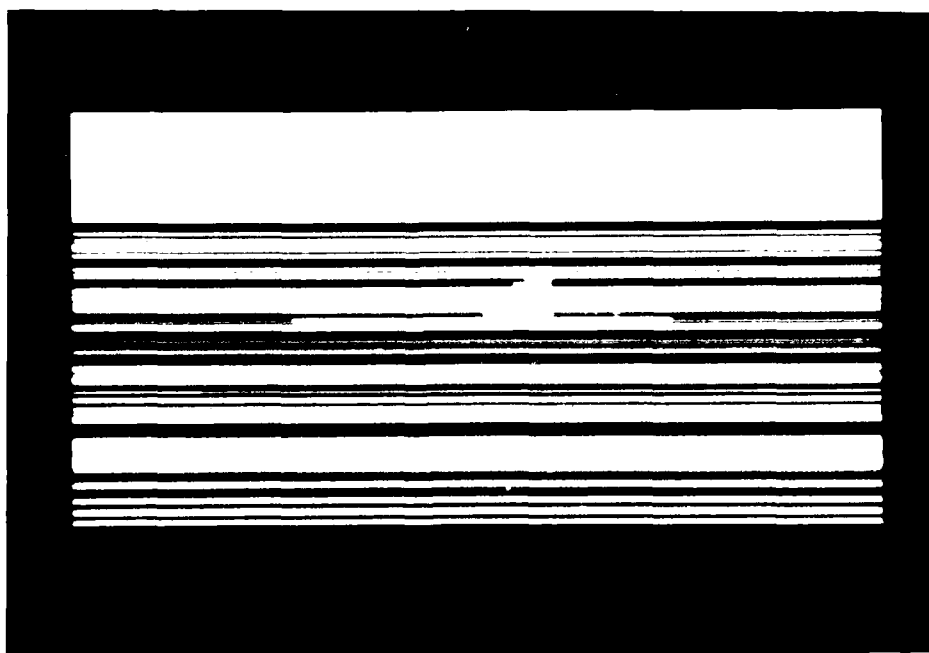


Fig. B-50: 255Spec

**BLANK PAGE**

## C. Source Listing for Synthetic Scene Generator

### C.1. Main Program Listing

THIS IS THE FORTRAN SOURCE FOR THE SYNTHETIC SCENE GENERATOR  
USED TO CREATE THE SYNTHETIC IMAGERY FOR THIS PROJECT  
FULL DETAILS OF ALL ROUTINES CAN BE FOUND IN THE AIR FORCE  
ARMAMENT LABORATORY (AFATL) TECHNICAL REPORT TR-83-37.  
THIS VERSION LISTED IN THIS APPENDIX WILL RUN ON A DEC VAX  
FAMILY COMPUTER

#### PROGRAM SSS

```
*****  
C  
C 3-D SYNTHETIC SCENE SIMULATOR  
C PROGRAMMER/ANALYST-- BILL WATKINS, GENERAL RESEARCH CORP.  
C AIRFORCE ENGINEER--LT. NORM BARSALOU, AFATL/DLM  
C  
*****  
COMMON AZ,XTC,YTC,BETAT,FOV(2),HT,RMIN,THETAT,COSA,COSB  
+,COSC,IT,JT,RG,NI,NJ,THETAC,X(5,30002),TANP(3),KTAPE,NUM,BIAS(3)  
+,GAM(3),COSI,VEL(3),DISP(3),IPIX(512,512,2),  
+PASS(10),THETA,BETA,IS,JS,IE,JE,XBOX(3,16),  
+JPASS(10),LTAPE,NUMB,QUANT,IDL,DGAM(3),DDISP(3),  
+NHIT,IHIT,IP,JP,TEMP,MGRD,XC,IDS,KOUNT,DTR  
INCLUDE 'DOUBLE.FOR'  
COMMON /SIGMA/ SIGMA(5),AM(5),SEED(5)  
COMMON /NOISE/ XNLAST(5),XNOISE(5),XNK1(5),XNK2(5)  
CHARACTER*30 CONTROL  
INTEGER*2 ITEMP(365)  
CHARACTER*30 TARGET  
INTEGER*2 IARRAY(512)  
LOGICAL*2 INAME(10)  
CHARACTER*30 INAME2  
TYPE *, ' ENTER INPUT TARGET FILE NAME ENCLOSED IN SINGLE  
+QUOTES'  
READ(5,*) TARGET  
TYPE *, ' ENTER CONTROL FILE NAME ENCLOSED IN SINGLE  
+QUOTES'  
READ(5,*) CONTROL  
TYPE*, 'OUTPUT FILE NAME? '  
READ(5,*)INAME2  
OPEN (UNIT=7,FILE=CONTROL,STATUS='OLD')  
OPEN (UNIT=10,FILE=TARGET,FORM='UNFORMATTED',STATUS='OLD')  
OPEN (UNIT=22,STATUS='SCRATCH')  
OPEN (UNIT=23,STATUS='SCRATCH')  
OPEN (UNIT=24,STATUS='SCRATCH')  
OPEN (UNIT=25,STATUS='SCRATCH')  
REWIND 7  
REWIND 10
```

```
REWIND 20
KTAPE=10
CALL INPUT
CALL SETUP
C SET BOUNDARY FOR A NEIGHBORHOOD AROUND TARGET CENTER
JS=JT-40
JE=JT+39
IS=IT-39
IE=IT+40
IF(JS.LT.1) JS=1
IF(JE.GT.NJ) JE=NJ
IF(IS.LT.1) IS=1
IF(IE.GT.NI) IE=NI
20 CONTINUE
C BEGIN SUBROUTINE CALLS
IF(IDS.EQ.1) CALL FIXED2
IF(IDS.EQ.2) CALL PUSH2
OPEN (UNIT=21,FILE=INAME2,RECL=128,STATUS='NEW'
+,FORM='UNFORMATTED'
+,ORGANIZATION='SEQUENTIAL',RECORDTYPE='FIXED')
ILEN=NI
DO 110 K=1,512
IARRAY(K)=0
110 CONTINUE
K=1
DO 100 J=1,NJ
DO 999 I=1,NI
ITEMP(I)=IPIX(I,J,K)
IARRAY(I)=ITEMP(I)
999 CONTINUE
WRITE(21) (IARRAY(JK),JK=1,256)
IF(NI.GT.256)WRITE(21)(IARRAY(JK),JK=257,512)
100 CONTINUE
IHDR=0
CLOSE(21)
STOP
END
```

## C.2. Source for Subroutine TRANSF

```
SUBROUTINE TRANSF
C*****
C
C THIS SUBROUTINE ROTATES AND TRANSLATES TARGET DATA FILE
C
C
C*****
COMMON AZ,XTC,YTC,BETAT,FOV(2),HT,RMIN,THETAT,COSA,COSB,
+COSC,IT,JT,RG,NI,NJ,THETAC,X(5,30002),TANP(3),KTAPE,NUM,BIAS(3)
+,GAM(3),COSI,VEL(3),DISP(3),IPIX(512,512,2),
+PASS(10),THETA,BETA,IS,JS,IE,JE,XBOX(3,16),
+JPASS(10),LTAPE,NUMB,QUANT,IDL,DGAM(3),DDISP(3),
+NHIT,IHIT,IP,JP,TEMP,MGRD,XC,IDS,KOUNT,DTR
INCLUDE 'DOUBLE.FOR'
DIMENSION XX(2),YY(2),ZZ(2)
REAL*8 SINA,XR,YR,XX,YY,ZZ,DUM
C INITIALIZE MAX AND MIN TARGET DATA POINTS
XX(2)=-1000000.
XX(1)=1000000.
YY(2)=-1000000.
ZZ(2)=-1000000.
ZZ(1)=1000000.
YY(1)=1000000.
C COMPUTE TRIG FUNCTIONS
IF(AZ.NE.90.) GO TO 4
SINA=1.
COSA=0.
GO TO 9
4 IF(AZ.NE.180.) GO TO 6
SINA=0.
COSA=-1.
GO TO 9
6 IF(AZ.NE.270.) GO TO 8
SINA=-1.
COSA=0.
GO TO 9
8 SINA=SIN(AZ*DTR)
COSA=COS(AZ*DTR)
9 CONTINUE
JMAX=0
C READ NEW BATCH OF TARGET FACETS
10 CONTINUE
J1=JMAX+1
J2=JMAX+NUM
READ(KTAPE,END=15) ((X(I,J),I=1,5),J=J1,J2)
15 JMAX=J-1
C BEGIN TRANSFORMATION LOOP FOR CURRENT BATCH OF DATA POINTS
DO 100 J=J1,JMAX
XX(2)=DMAX1(X(1,J),XX(2))
```

```

XX(1)=DMIN1(X(1,J),XX(1))
YY(2)=DMAX1(X(2,J),YY(2))
YY(1)=DMIN1(X(2,J),YY(1))
ZZ(2)=DMAX1(X(3,J),ZZ(2))
ZZ(1)=DMIN1(X(3,J),ZZ(1))
X(1,J)=X(1,J)+BIAS(1)
X(2,J)=X(2,J)+BIAS(2)
X(3,J)=X(3,J)+BIAS(3)
C  ROTATE TARGET COORDINATES
  XR=X(1,J)*COSA-X(2,J)*SINA
  YR=X(2,J)*COSA+X(1,J)*SINA
C  TRANSLATE TARGET COORDINATES
  X(1,J)=XR+XTC
  X(2,J)=YR+YTC
  X(3,J)=X(3,J)
C  STORE MAX & MIN X,Y,Z
C  END LOOP FOR CURRENT BATCH OF DATA POINTS
100  CONTINUE
C  WRITE TRANSFORMED DATA POINTS ON SCRATCH TAPE
125  FORMAT(3F10.2)
      IF(X(5,JMAX).GT.0.) GO TO 10
      JPASS(3)=JMAX
      CLOSE (KTAPE)
      REWIND KTape
      CALL BOX(XX,YY,ZZ)
      WRITE(6,150)
150  FORMAT(' MIN AND MAX VALUES OF THE TARGET X,Y,Z COORDINATES')
      WRITE(6,200) XX,YY,ZZ
200  FORMAT(6F10.2)
      RETURN
      END

```

### C.3. Source for Subroutine SCANNER

```
SUBROUTINE SCANNER
C*****
C
C THIS SUBROUTINE COMPUTES LOS DIRECTION COSINES AND SLANT RANGE
C TO THE GROUND PLANE
C
C*****
COMMON AZ,XTC,YTC,BETAT,FOV(2),HT,RMIN,THETAT,COSA,COSB,
+COSC,IT,JT,RG,NI,NJ,THETAC,X(5,30002),TANP(3),KTAPE,NUM,BIAS(3)
+,GAM(3),COSI,VEL(3),DISP(3),IPIX(512,512,2),
+PASS(10),THETA,BETA,IS,JS,IE,JE,XBOX(3,16),
+JPASS(10),LTAPE,NUMB,QUANT,IDL,DGAM(3),DDISP(3),
+NHIT,IHIT,IP,JP,TEMP,MGRD,XC,IDS,KOUNT,DTR
INCLUDE 'DOUBLE.FOR'
COMMON /NOISE/ XNLAST(5),XNOISE(5),XNK1(5),XNK2(5)
DIMENSION XCOR(4),YCOR(4)
REAL*8 SINT,COSBET,COST,RX,RY,RZ
SINT=SIN(THETA)
COSBET=COS(BETA)
COST=COS(THETA)
C COMPUTE CURRENT DIRECTION COSINES OF THE LOS
C IN SCANNER COORDINATES
COSA=COST*COSBET
COSB=SIN(BETA)
COSC=SINT*COSBET
C ROTATE SCANNER THROUGH ROLL, PITCH AND YAW ANGLES
IF(JPASS(1).EQ.1) CALL ROTATE
C COMPUTE SLANT RANGE TO GROUND AND THE X,Y,Z COMPONENTS
RG=-DISP(3)/COSC
RMIN=RG*1.000001
IF(RMIN.LT.0.)RMIN=0.
COSI=-COSC
RX=RG*COSA
RY=RG*COSB
RZ=RG*COSC
XCOR(1)=RX+DISP(1)
YCOR(1)=RY+DISP(2)
CALL TEXTUR(1,1,XCOR,YCOR,TEMP)
C COMPUTE TANGENTS OF LOS PROJECTIONS ON THE PRINCIPAL PLANES
TANP(1)=(RX/RZ)
TANP(2)=(RY/RZ)
TANP(3)=(RZ/RX)
RETURN
END
```

#### C.4. Source for Subroutine FACET

```
SUBROUTINE FACET
C*****
C THIS SUBROUTINE COMPUTES PIXEL IMAGE DATA FOR THE TARGET
C*****
COMMON AZ,XTC,YTC,BETAT,FOV(2),HT,RMIN,THETAT,COSA,COSB,
+COSC,IT,JT,RG,NI,NJ,THETAC,X(5,30002),TANP(3),KTAPE,NUM,BIAS(3)
+,GAM(3),COSI,VEL(3),DISP(3),IPIX(512,512,2),
+PASS(10),THETA,BETA,IS,JS,IE,JE,XBOX(3,16),
+JPASS(10),LTAPE,NUMB,QUANT,IDL,DGAM(3),DDISP(3),
+NHIT,IHIT,IP,JP,TEMP,MGRD,XC,IDS,KOUNT,DTR
INCLUDE 'DOUBLE.FOR'
DIMENSION A(3),D(3),P(3),AXD(3),XSIGN(3)
DIMENSION COMP(3)
REAL*8 AXAD,AXDM,COSAN,COSBN,COSCN,DEM,F,G,H,ONE,P,
+RP,TANA,TANB,TANC,TMAX,TMIN,XNUM,A,AXD,COMP,D,XSIGN
JPASS(2)=JPASS(2)+1
WRITE(6,888) JPASS(2)
888 FORMAT(5X,I4)
NFACET=1
RP=1000000.
JXS=2
J1=NUM+2
ONE=1.
AXDM=.001
JHIT=0
IHIT=0
C READ NEW SET OF FACETS
JMAX=JPASS(3)
C START LOOP TO TEST EACH FACET
DO 100 JX=JXS,JMAX
IF(X(5,JX).EQ.0.) GO TO 120
NFACET=NFACET+1
J=JX
K=J+1
L=J+2
IF(X(5,L).LT.X(5,K).OR.X(5,K).LT.X(5,J)) GO TO 100
C CHECK GROUND PLANE PROJECTIONS OF THE LOS
TANA=(X(2,J)-DISP(2))/(X(1,J)-DISP(1))
TANB=(X(2,K)-DISP(2))/(X(1,K)-DISP(1))
TANC=(X(2,L)-DISP(2))/(X(1,L)-DISP(1))
TMAX=DMAX1(TANA,TANB,TANC)
TMIN=DMIN1(TANA,TANB,TANC)
IF(TANP(3).LT.TMIN.OR.TANP(3).GT.TMAX) GO TO 100
C CHECK X-Z AND Y-Z PLANE PROJECTIONS OF THE LOS
DO 30 N=1,2
TANA=(X(N,J)-DISP(N))/(-DISP(3)+X(3,J))
TANB=(X(N,K)-DISP(N))/(-DISP(3)+X(3,K))
```

```

TANC=(X(N,L)-DISP(N))/(-DISP(3)+X(3,L))
TMAX=DMAX1(TANA,TANB,TANC)
TMIN=DMIN1(TANA,TANB,TANC)
IF(TANP(N).LT.TMIN.OR.TANP(N).GT.TMAX) GO TO 100
30 CONTINUE
C COMPUTE LOS INTERSECTION WITH A FACET
F=(X(2,K)-X(2,J))*(X(3,L)-X(3,J))-(X(3,K)-X(3,J))*(X(2,L)-X(2,J))
G=(X(1,K)-X(1,J))*(X(3,L)-X(3,J))-(X(3,K)-X(3,J))*(X(1,L)-X(1,J))
H=(X(1,K)-X(1,J))*(X(2,L)-X(2,J))-(X(1,L)-X(1,J))*(X(2,K)-X(2,J))
DEM=F*X(1,J)-G*X(2,J)+H*X(3,J)-H*DISP(3)-DISP(1)*F+DISP(2)*G
XNUM=F*COSA-G*COSB+H*COSC
IF(XNUM.EQ.0) GO TO 100
RP=DEM/XNUM
RP=ABS(RP)
P(1)=RP*COSA+DISP(1)
P(2)=RP*COSB+DISP(2)
P(3)=RP*COSC+DISP(3)
C DO CROSS PRODUCT LOOPS
M=1
N=2
DO 50 MX=1,3
IF(MX.EQ.3) M=1
AXD(1)=(X(M,K)-X(M,J))*(P(N)-X(N,J))-(P(M)-X(M,J))*(X(N,K)-X(N,J))
AXD(2)=(X(M,L)-X(M,K))*(P(N)-X(N,K))-(P(M)-X(M,K))*(X(N,L)-X(N,K))
AXD(3)=(X(M,J)-X(M,L))*(P(N)-X(N,L))-(P(M)-X(M,L))*(X(N,J)-X(N,L))
COMP(MX)=AXD(1)
IF(ABS(AXD(1)).LT.AXDM.OR.ABS(AXD(2)).LT.AXDM.OR.ABS(AXD(3))
+.LT.AXDM)GOTO40
C TEST FOR LOS HIT WITHIN BOUNDARY OF TARGET FACET
XSIGN(1)=SIGN(ONE,AXD(1))
XSIGN(2)=SIGN(ONE,AXD(2))
IF(XSIGN(1).NE.XSIGN(2)) GO TO 100
XSIGN(3)=SIGN(ONE,AXD(3))
IF(XSIGN(3).NE.XSIGN(1)) GO TO 100
C SET FLAG TO INDICATE A SUCCESSFUL TARGET INTERCEPT
40 CONTINUE
M=2
N=3
50 CONTINUE
IF(IHIT.EQ.0) GO TO 100
JHIT=JHIT+1
NGRD=0
MGRD=4
IF(RP.GT.RMIN) GO TO 100
C STORE RANGE TO FACET AND COSINE OF ANGLE OF INCIDENCE
RMIN=RP
IDFAC=NFACT
AAXD=SQRT(COMP(1)*COMP(1)+COMP(2)*COMP(2)+COMP(3)*COMP(3))
COSAN=COMP(2)/AAXD
COSBN=COMP(3)/AAXD
COSCN=COMP(1)/AAXD
COSI=COSA*COSAN+COSB*COSBN+COSC*COSCN

```

```
COSI=ABS(COSI)
TEMP=50.
999 FORMAT(1X,3I3,7F7.3,I3)
100 CONTINUE
C END LOOP FOR CURRENT BATCH OF TARGET FACETS
C STORE LAST TWO DATA POINTS FOR FIRST TWO OF NEXT BATCH

JXS=1
DO 110 I=1,5
X(I,1)=X(I,K)
110 X(I,2)=X(I,L)
120 CONTINUE
IF(RMIN.GT.RG) GO TO 200
KOUNT=KOUNT+1
IF(RMIN.LT.0.OR.RMIN.GT.1.E6) WRITE(6,*) RMIN,IP,JP
145 FORMAT(1X,8I5,2I8)
150 FORMAT(2I10)
200 CONTINUE
RETURN
END
```

### C.5. Source for Subroutine NOISE

```
SUBROUTINE NOISE (IR)
C*****THIS SUBROUTINE IS A BOX-MULLER GAUSSIAN SEQUENCE GENERATOR*****
C
COMMON /NOISE/ XNLAST(5),XNOISE(5),XNK1(5),XNK2(5)
COMMON /SIGMA/ SIGMA(5),AM(5),SEED(5)
DATA LZ/0/
C
C*****...SEEDS PRESERVED FOR SELECTED VARIABLES
C*****....XNK1 & XNK2 WEIGHTS FOR PRODUCING
C*****....WHITE OR CORRELATED SEQUENCES
C
CALL RANSET (SEED(IR))
RN=RANF()
RA=RANF()
A=((COS(6.2831853*RA))*SQRT(-2.* ALOG(RN)))*SIGMA(IR)
CALL RANGET (SEED(IR))
DNOISE=A+AM(IR)
XNOISE(IR)=XNK1(IR)*XNLAST(IR)+XNK2(IR)*DNOISE
XNLAST(IR)=XNOISE(IR)
RETURN
END
```

#### C.6. Source for Subroutine ROTATE

```
SUBROUTINE ROTATE
C*****
C
C TRANSFORMATION FOR ROLL, PITCH AND YAW
C DIRECTION COSINES IN SCANNER COORDINATES TRANSFORMED TO EARTH COORD
C*****
COMMON AZ,XTC,YTC,BETAT,FOV(2),HT,RMIN,THETAT,COSA,COSB
+ ,COSC,IT,JT,RG,NI,NJ,THETAC,X(5,30002),TANP(3),KTAPE,NUM,BIAS(3)
+ ,GAM(3),COSI,VEL(3),DISP(3),IPIX(512,512,2),
+ PASS(10),THETA,BETA,IS,JS,IE,JE,XBOX(3,16),
+ JPASS(10),LTAPE,NUMB,QUANT,IDL,DGAM(3),DDISP(3),
+ NHIT,IHIT,IP,JP,TEMP,MGRD,XC,IDS,KOUNT,DTR
INCLUDE 'DOUBLE.FOR'
DIMENSION T(3,3),XX(3)
REAL*8 T,XXX,S1,S2,S3,C1,C2,C3
C STORE INITIAL LOS DIRECTION COSINES
XX(1)=COSA
XX(2)=COSB
XX(3)=COSC
C COMPUTE TRIG FUNCTIONS
S1=SIN(GAM(1))
C1=COS(GAM(1))
S2=SIN(GAM(2))
C2=COS(GAM(2))
S3=SIN(GAM(3))
C3=COS(GAM(3))
C COMPUTE TRANSFORMATION MATRIX ELEMENT
T(1,1)=C3*C2
T(1,2)=C3*S2*S1-S3*C1
T(1,3)=C3*C1*S2+S3*S1
T(2,1)=S3*C2
T(2,2)=S3*S2*S1+C3*C1
T(2,3)=S3*S2*C1-C3*S1
T(3,1)=-S2
T(3,2)=C2*S1
T(3,3)=C2*C1
C COMPUTE NEW LOS DIRECTION COSINES
COSA=T(1,1)*XX(1)+T(1,2)*XX(2)+T(1,3)*XX(3)
COSB=T(2,1)*XX(1)+T(2,2)*XX(2)+T(2,3)*XX(3)
COSC=T(3,1)*XX(1)+T(3,2)*XX(2)+T(3,3)*XX(3)
RETURN
END
```

### C.7. Source for Subroutine SHOW

```
SUBROUTINE SHOW(L,JS,IS,JE,IE,NI,NJ,IPIX)
C*****
C
C THIS SUBROUTINE IS THE DRIVER FOR THE QUICK-LOOK IMAGE GENERATOR
C
*****
DIMENSION LOC(512),LCH(24)
DIMENSION IPIX(512,512,2)
INTEGER*2 IPIX
DATA LCH/1HA,1HB,1HC,1HD,1HE,1HF,1HG,1HH,1HI,1HJ,1HK,1HL,
+1HM,1HN,1HO,1HP,1HQ,1HR,1HS,1HT,1HU,1HW,
+1HY,1HZ/
MIN=1000000
MAX=0
IMAX=IE-IS+1

NGRAY=24
MMAX=NGRAY-1
DO 100 J=2,NJ
IF(J.LT.JS) GO TO 100
IF(J.GT.JE) GO TO 200
I=IS-1
DO 30 K=1,IMAX
I=I+1
MAX=MAX0(MAX,IPIX(I,J,L))
MIN=MIN0(MIN,IPIX(I,J,L))
30 CONTINUE
100 CONTINUE
200 CONTINUE
INC=(MAX-MIN)/NGRAY
IF(INC.EQ.0) INC=1
DO 300 J=2,NJ
IF(J.LT.JS) GO TO 300

IF(J.GT.JE) GO TO 400
I=IS-1
DO 250 K=1,IMAX
I=I+1
M=(IPIX(I,J,L)-MIN)/INC
IF(M.GT.MMAX) M=MMAX
LOC(K)=LCH(M+1)
250 CONTINUE
WRITE(6,70) (LOC(I),I=2,IMAX)
70 FORMAT(1X,79A1)
300 CONTINUE

400 CONTINUE
RETURN
END
```

### C.8. Source for Subroutine BOX

```
SUBROUTINE BOX(XX,YY,ZZ)
C*****
C
C THIS SUBROUTINE SETS UP THE BOX TEMPLATE DATA POINTS FROM
C THE MAX AND MIN DIMENSIONS OF THE TARGET DATA
C
*****
COMMON AZ,XTC,YTC,BETAT,FOV(2),HT,RMIN,THETAT,COSA,COSB
+,COSC,IT,JT,RG,NI,NJ,THETAC,X(5,30002),TANP(3),KTAPE,NUM,BIAS(3)
+,GAM(3),COSI,VEL(3),DISP(3),IPIX(512,512,2),
+PASS(10),THETA,BETA,IS,JS,IE,JE,XBOX(3,16),
+JPASS(10),LTAPE,NUMB,QUANT,IDL,DGAM(3),DDISP(3),
+NHIT,IHIT,IP,JP,TEMP,MGRD,XC,IDS,KOUNT,DTR
INCLUDE 'DOUBLE.FOR'
DIMENSION IX(48),XX(2),YY(2),ZZ(2)
REAL*8 SINA,XR,YR,XX,YY,ZZ
DATA IX/5*1,2,1,2,1,2,1,8*2,3*1,4*2,3*1,5*2,1,2,4*1,4*2,1,2,1,1/
SINA=SIN(AZ*DTR)
COSA=COS(AZ*DTR)
DO 100 I=1,16
JX=IX(I)
JY=IX(I+16)
JZ=IX(I+32)
C COMPUTE NEW ORIGIN OF BOX
XBOX(1,I)=XX(JX)+BIAS(1)
XBOX(2,I)=YY(JY)+BIAS(2)
XBOX(3,I)=ZZ(JZ)+BIAS(3)
C ROTATE BOX ABOUT ORIGIN
XR=XBOX(1,I)*COSA-XBOX(2,I)*SINA
YR=XBOX(2,I)*COSA+XBOX(1,I)*SINA
C TRANSLATE BOX
XBOX(1,I)=XR+XTC
XBOX(2,I)=YR+YTC
C WRITE(6,80) XBOX(1,I),XBOX(2,I),XBOX(3,I)
80 FORMAT(5F10.2)
100 CONTINUE
RETURN
END
```

### C.9. Source for Subroutine HITBOX

```

SUBROUTINE HITBOX
C*****
C
C THIS SUBROUTINE DETERMINS IF THE LOS HITS THE BOX TEMPLATE
C
C*****
COMMON AZ,XTC,YTC,BETAT,FOV(2),HT,RMIN,THETAT,COSA,COSB,
+COSC,IT,JT,RG,NI,NJ,THETAC,X(5,30002),TANP(3),KTAPE,NUM,BIAS(3)
+,GAM(3),COSI,VEL(3),DISP(3),IPIX(512,512,2),
+PASS(10),THETA,BETA,IS,JS,IE,JE,Z(3,16),
+JPASS(10),LTAPE,NUMB,QUANT,IDL,DGAM(3),DDISP(3),
+NHIT,IHIT,IP,JP,TEMP,MGRD,XC,IDS,KOUNT,DTR
INCLUDE 'DOUBLE.FOR'
DIMENSION A(3),D(3),P(3),AXD(3),XSIGN(3)
DIMENSION COMP(3)
REAL*8 AXDM,DEM,F,G,H,ONE,RP,TANA,TANB,TANC,TMAX,
+TMIN,XNUM,A,AXD,COMP,D,P,XSIGN,Z
NHIT=0
AXDM=.001
ONE=1.
C START LOOP TO TEST EACH FACET
DO 100 JX=1,14
J=JX
K=J+1
L=J+2
C CHECK GROUND PLANE PROJECTIONS FOR INTERSECTION
TANA=(Z(2,J)-DISP(2))/(Z(1,J)-DISP(1))
TANB=(Z(2,K)-DISP(2))/(Z(1,K)-DISP(1))
TANC=(Z(2,L)-DISP(2))/(Z(1,L)-DISP(1))
TMAX=DMAX1(TANA,TANB,TANC)
TMIN=DMIN1(TANA,TANB,TANC)
IF(TANP(3).LT.TMIN.OR.TANP(3).GT.TMAX) GO TO 100
C CHECK X-Z AND Y-Z PLANE PROJECTIONS FOR INTERSECTION
DO 30 N=1,2
TANA=(Z(N,J)-DISP(N))/(-DISP(3)+Z(3,J))
TANB=(Z(N,K)-DISP(N))/(-DISP(3)+Z(3,K))
TANC=(Z(N,L)-DISP(N))/(-DISP(3)+Z(3,L))
TMAX=DMAX1(TANA,TANB,TANC)
TMIN=DMIN1(TANA,TANB,TANC)
IF(TANP(N).LT.TMIN.OR.TANP(N).GT.TMAX) GO TO 100
30 CONTINUE
NPASS=NPASS+1
C COMPUTE LOS INTERSECTION WITH A FACET
F=(Z(2,K)-Z(2,J))*(Z(3,L)-Z(3,J))-(Z(3,K)-Z(3,J))*(Z(2,L)-Z(2,J))
G=(Z(1,K)-Z(1,J))*(Z(3,L)-Z(3,J))-(Z(3,K)-Z(3,J))*(Z(1,L)-Z(1,J))

H=(Z(1,K)-Z(1,J))*(Z(2,L)-Z(2,J))-(Z(1,L)-Z(1,J))*(Z(2,K)-Z(2,J))
DEM=F*Z(1,J)-G*Z(2,J)+H*Z(3,J)-H*DISP(3)-DISP(1)*F+DISP(2)*G

```

```

XNUM=F*COSA-G*COSB+H*COSC
IF(XNUM.EQ.0) GO TO 100
RP=DEM/XNUM
RP=ABS(RP)
P(1)=RP*COSA+DISP(1)
P(2)=RP*COSB+DISP(2)
P(3)=RP*COSC+DISP(3)
C DO CROSS PRODUCT LOOPS
M=1
N=2
DO 50 MX=1,3
IF(MX.EQ.3) M=1
AXD(1)=(Z(M,K)-Z(M,J))*(P(N)-Z(N,J))-(P(M)-Z(M,J))*(Z(N,K)-Z(N,J))
AXD(2)=(Z(M,L)-Z(M,K))*(P(N)-Z(N,K))-(P(M)-Z(M,K))*(Z(N,L)-Z(N,K))
AXD(3)=(Z(M,J)-Z(M,I))*(P(N)-Z(N,L))-(P(M)-Z(M,L))*(Z(N,J)-Z(N,L))
COMP(MX)=AXD(1)
IF(ABS(AXD(1)).LT.AXDM.OR.ABS(AXD(2)).LT.AXDM.OR.ABS(AXD(3))
+.LT.AXDM)GOTO40
C TEST FOR LOS HIT WITHIN BOUNDARY OF FACET
XSIGN(1)=SIGN(ONE,AXD(1))
XSIGN(2)=SIGN(ONE,AXD(2))
IF(XSIGN(1).NE.XSIGN(2)) GO TO 100
XSIGN(3)=SIGN(ONE,AXD(3))
IF(XSIGN(3).NE.XSIGN(1)) GO TO 100
C SET FLAG TO INDICATE A SUCESSFUL BOX INTERCEPT
NHIT=1
40 CONTINUE
M=2
N=3
50 CONTINUE
100 CONTINUE
200 RETURN
END

```

#### C.10. Source for Subroutine HEADER

```
SUBROUTINE HEADER
C*****
C
C THIS SUBROUTINE PRINTS A HEADER ON THE IPL IMAGE TAPE
C
C*****
COMMON AZ,XTC,YTC,BETAT,FOV(2),HT,RMIN,THETAT,COSA,COSB,
+COSC,IT,JT,RG,NI,NJ,THETAC,X(5,30002),TANP(3),KTAPE,NUM,BIAS(3)
+,GAM(3),COSI,VEL(3),DISP(3),IPIX(512,512,2),
+PASS(10),THETA,BETA,IS,JS,IE,JE,XBOX(3,16),
+JPASS(10),LTAPE,NUMB,QUANT,IDL,DGAM(3),DDISP(3),
+NHIT,IHIT,IP,JP,TEMP,MGRD,XC,IDS,KOUNT,DTR
INCLUDE 'DOUBLE.FOR'
DIMENSION IR(512)
DATA IR/512*0/
C SET-UP TAPE HEADER IN FIRST LINE ON IMAGE TAPES
IR(1)=IDS
IR(2)=THETA*1000. 5
IR(3)=DISP(3)
IR(4)=FOV(1)*1000.
IR(5)=NI
IR(6)=NJ
IR(7)=1
IR(8)=DGAM(1)*1.E09
IR(9)=DGAM(2)*1.E09
IR(10)=DGAM(3)*1.E09
IR(11)=FOV(2)*1000.
IR(21)=IDL
IR(22)=IT
IR(23)=JT
IR(24)=AZ
IR(25)=BIAS(1)
IR(26)=BIAS(2)
IR(27)=BIAS(3)
DO 50 K=1,3
DO
IR(23)=JT
IR(24)=AZ
IR(25)=BIAS(1)
IR(26)=BIAS(2)
IR(27)=BIAS(3)
DO 50 K=1,3
DO
IR(23)=JT
IR(24)=AZ
IR(25)=BIAS(1)
IR(26)=BIAS(2)
IR(27)=BIAS(3)
```

```
DO 50 K=1,3
DO 50 I=1,NI
IF(IR(I).GT.65536) IR(I)=65536
IPIX(K,I,1)=IR(I)
50  CONTINUE
5   FORMAT(10I8)
      WRITE(6,4)
4   FORMAT(' TAPE HEADER INFO:')
      WRITE(6,5) (IR(I),I=1,30)
110 FORMAT(10I8)
      RETURN
      END
```

### C.11. Source for Subroutine PUSH2

```
SUBROUTINE PUSH2
C*****
C
C THIS SUBROUTINE IS THE DRIVER FOR A PUSHBROOM SCANNER
C
C*****
COMMON AZ,XTC,YTC,BETAT,FOV(2),HT,RMIN,THETAT,COSA,COSB
+ ,COSC,IT,JT,RG,NI,NJ,THETAC,X(5,30002),TANP(3),KTAPE,NUM,BIAS(3)
+ ,GAM(3),COSI,VEL(3),DISP(3),IPIX(512,512,2),
+ PASS(10),THETA,BETA,IS,JS,IE,JE,XBOX(3,16),
+ JPASS(10),LTAPE,NUMB,QUANT,IDL,DGAM(3),DDISP(3),
+ NHIT,IHIT,IP,JP,TEMP,MGRD,XC,IDS,KOUNT,DTR
INCLUDE 'DOUBLE.FOR'
DIMENSION ITHERM(512),IR(512),IC(512)
WRITE(6,5)
5 FORMAT(//,' IMAGE DATA FOR A PUSHBROOM SCANNER',//)
KOUNT=0
C COMPUTE RANGE DISPLACEMENT PER SCAN LINE AND PER PIXEL
DISP1=DISP(3)/TAN(THETA+(FOV(1)/2.))
DISP2=DISP(3)/TAN(THETA-(FOV(1)/2.))
DISPO=DISP(3)/TAN(THETA)
DISPS=DISP1-DISP2
DDISP(1)=DISPS/FLOAT(NI)
C COMPUTE SCAN ANGLE AND DISTANCE TO TARGET CENTER
BETAT=((NI/2)-IT)*FOV(2)
XTC=DISPO+(JT)*DISPS+(IT-1)*DDISP(1)
YTC=-DISP(3)*TAN(BETAT)/SIN(THETA)
CALL TRANSF
BETA0=(NI/2)*FOV(2)+FOV(2)
CALL HEADER
C START LOOP FOR DOWN RANGE DISPLACEMENT
DO 200 J=1,NJ
BETA=BETA0
C START LOOP FOR CROSS RANGE SWEEP
DO 100 I=1,NI
BETA=BETA-FOV(2)
DO 50 K=1,3
DISP(K)=DISP(K)+DDISP(K)
GAM(K)=GAM(K)+DGAM(K)
50 CONTINUE
CALL SCANER
IF(IDS.EQ.0) GO TO 70
IF(J.LT.JS.OR.J.GT.JE) GO TO 70
IF(I.LT.IS.OR.I.GT.IE) GO TO 70
CALL HITBOX
IF(NHIT.EQ.1) CALL FACET
70 CONTINUE
PIXEL=RMIN*QUANT
```

```
IF(PIXEL.GT.65536.) PIXEL=65536.  
JX=NJ+1-J  
IPIX(I,JX,1)=PIXEL  
IPIX(I,JX,2)=COSI*255  
IPIX(I,JX,3)=THERM  
100 CONTINUE  
C WRITE DATA TAPES FOR THE IPL  
110 FORMAT(10I8)  
200 CONTINUE  
  
80 FORMAT(' NO OF TARGET FILE SEARCHES= ',I6)  
60 FORMAT(' NO OF PIXELS ON TARGET= ',I5)  
WRITE(6,80) JPASS(2)  
WRITE(6,60) KOUNT  
C CALL SUBROUTINES TO GET QUICK-LOOK IMAGES OF RANGE AND COSI  
WRITE(6,400)  
400 FORMAT(//,' RANGE IMAGE',//)  
CALL SHOW(1,JS,IS,JE,IE,NI,NJ,IPIX)  
WRITE(6,450)  
450 FORMAT(//,' REFLECTANCE IMAGE',//)  
CALL SHOW(2,JS,IS,JE,IE,NI,NJ,IPIX)  
WRITE(6,500)  
500 FORMAT(//,' THERMAL IMAGE',//)  
CALL SHOW(3,JS,IS,JE,IE,NI,NJ,IPIX)  
RETURN  
END
```

### C.12. Source for Subroutine FIXED2

```
SUBROUTINE FIXED2
C*****
C THIS SUBROUTINE IS THE DRIVER FOR A STATIONARY SCANNER
C*****
COMMON AZ,XTC,YTC,BETAT,FOV(2),HT,RMIN,THETAT,COSA,COSB,
+COSC,IT,JT,RG,NI,NJ,THETAC,X(5,30002),TANP(3),KTAPE,NUM,BIAS(3)
+,GAM(3),COSI,VEL(3),DISP(3),IPIX(512,512,2),
+PASS(10),THETA,BETA,IS,JS,IE,JE,XBOX(3,16),
+JPASS(10),LTAPE,NUMB,QUANT,IDL,DGAM(3),DDISP(3),
+NHIT,IHIT,IP,JP,TEMP,MGRD,XC,IDS,KOUNT,DTR
INCLUDE 'DOUBLE.FOR'
DIMENSION ITHERM(512),IR(512),IC(512)
REAL*8 BETA0,RRMIN,RPIXEL
INTEGER IPX3
INTEGER*2 IPX2,IPX5
WRITE(6,2)
2 FORMAT(//,' IMAGE DATA FOR A STATIONARY SCANNER',//)
THETAC=ATAN(-DISP(3)/XC)
THETAT=THETAC+((NJ/2)-JT)*FOV(1)
TYPE*, 'DO YOU WANT A REFLECTANCE IMAGE??'
TYPE*, 'TYPE A NUM BIGGER THAN ZERO IF YOU DO'
READ*, TEST
BETAT=((NI/2)-IT)*FOV(2)
XTCA=-DISP(3)/TAN(THETAT)
YTC=-DISP(3)*TAN(BETAT)/SIN(THETAT)
THETA=THETAC+(NJ/2)*FOV(1)+FOV(1)
BETA0=(NI/2)*FOV(2)+FOV(2)
CALL TRANSF
KOUNT=0
CALL HEADER
C START LOOP FOR DOWN RANGE DISPLACEMENT
DO 200 J=1,NJ
WRITE(6,*) J
THETA=THETA-FOV(1)
BETA=BETA0
C START LOOP FOR CROSS RANGE SWEEP
DO 100 I=1,NI
BETA=BETA-FOV(2)
CALL SCANER
IF(IDS.EQ.0) GO TO 70
IF(J.LT.JS.OR.J.GT.JE) GO TO 70
IF(I.LT.IS.OR.I.GT.IE) GO TO 70
CALL HITBOX
IF(NHIT.EQ.1) CALL FACET
CONTINUE
70 IF(RMIN.LT.0.)RMIN=0.
RPIXEL=0.
RPIXEL=RMIN*QUANT
```

```

        PIXEL=PIXEL**2
        PIXEL=RPIXEL
        IF(PIXEL.GT.65536.) PIXEL=65536.
        IF(PIXEL.LT.0.)PIXEL=0.
        IF(PIXEL.GT.0.AND.PIXEL.LT.65536)IPIX(I,J,1)=PIXEL
        IPX5=IPIX(I,J,1)
        IF(TEST.GT.0)IPIX(I,J,2)=COSI*255
100    CONTINUE
110    FORMAT(10I8)
        IF(RMIN.GT.0.AND.PIXEL.NE.65536)THEN
        TYPE*, 'PIXEL=',PIXEL
        WRITE(*,999)IPX5
999    FORMAT(1X,'EQUIV I2 NUM IS ',I5)
        TYPE*, 'DIFF IS ',PIXEL-IPX5
        ENDIF
        TYPE*, 'SCANNED ROW=',J
200    CONTINUE
        ENDFILE 22
        ENDFILE 23
        ENDFILE 25
80    FORMAT(' NO OF TARGET FILE SEARCHES= ',I6)
60    FORMAT(' NO OF PIXELS ON TARGET= ',I5)
        WRITE(6,80) JPASS(2)
        WRITE(6,60) KOUNT
C CALL SUBROUTINES TO GET QUICK-LOOK IMAGES OF RANGE AND COSI
        WRITE(6,400)
400    FORMAT(//,'          RANGE IMAGE',//)
        CALL SHOW(1,JS,IS,JE,IE,NI,NJ,IPIX)
        IF(TEST.GT.0)WRITE(6,450)
450    FORMAT(//,'          REFLECTANCE IMAGE',//)
        IF(TEST.GT.0)CALL SHOW(2,JS,IS,JE,IE,NI,NJ,IPIX)
        WRITE(6,500)
500    FORMAT(//,'          THERMAL IMAGE',//)
D      CALL SHOW(3,JS,IS,JE,IE,NI,NJ,IPIX)
        RETURN
        END

```

### C.13. Source for Subroutine INPUT

```

SUBROUTINE INPUT
C*****
C THIS SUBROUTINE READS AND SCALES INPUT PARAMETERS
C*****
COMMON AZ,XTC,YTC,BETAT,FOV(2),HT,RMIN,THETAT,COSA,COSB
+ ,COSC,IT,JT,RG,NI,NJ,THETAC,X(5,30002),TANP(3),KTAPE,NUM,BIAS(3)
+ ,GAM(3),COSI,VEL(3),DISP(3),IPIX(512,512,2),
+ PASS(10),THETA,BETA,IS,JS,IE,JE,XBOX(3,16),
+ JPASS(10),LTAPE,NUMB,QUANT,IDL,DGAM(3),DDISP(3),
+ NHIT,IHIT,IP,JP,TEMP,MGRD,XC,IDS,KOUNT,DTR
INCLUDE 'DOUBLE.FOR'

COMMON /SIGMA/ SIGMA(5),AM(5),SEED(5)
COMMON /NOISE/ XNLAST(5),XNOISE(5),XNK1(5),XNK2(5)
REAL*8 XXX
DATA XNLAST/5*0./
XXX=1.
DTR=DATAN(XXX)/45.
DO 5 I=1,3
DISP(I)=0.
5 DDISP(I)=0.
DO 6 I=1,10
PASS(I)=0.
6 JPASS(I)=0
C READ AND SCALE SCANNER PARAMETERS
READ(7,*) IDS,DISP(3),XXX,FOV,NI,NJ
WRITE(6,*) IDS,DISP(3),XXX,FOV,NI,NJ
IF(IDS.EQ.1) XC=XXX*12.
IF(IDS.EQ.2) THETA=-XXX*DTR
DISP(3)=DISP(3)*12.
FOV(1)=FOV(1)*DTR
FOV(2)=FOV(2)*DTR
C READ TARGET PARAMETERS
READ(7,*) IDT,IT,JT,AZ,BIAS,NUM
WRITE(6,*) IDT,IT,JT,AZ,BIAS,NUM
C READ AND SCALE MANEUVER PARAMETERS
READ(7,*) GAM,DGAM
WRITE(6,*) GAM,DGAM
DO 10 I=1,3
GAM(I)=GAM(I)*DTR
10 DGAM(I)=DGAM(I)*DTR
C READ STATISTICAL PARAMETERS
READ(7,*) SIGMA,AM,XNK1,XNK2,SEED
WRITE(6,*) SIGMA,AM,XNK1,XNK2,SEED
READ(7,*) QUANT
WRITE(6,*) QUANT
JPASS(1)=1
CLOSE(7)

```

```
    RETURN  
    END
```

#### C.14. Source for Subroutine SETUP

```
      SUBROUTINE SETUP  
C      DIMENSION X(4), Y(4)  
C      COMMON / TXTURE / AMEAN(5) , ASIG(5) , CORX(5) , CORY(5)  
C      .           , INIT(5) , NTERMX(5) , NTERMY(5) , PRIODX(5)  
C      .           , PRIODY(5) , IX,JX  
C      AMEAN(1) = 127.0  
C      ASIG(1) = 40.0  
C      CORX(1) = 100.0*12.  
  
C      CORY(1) = 100.0*12.  
C      PRIODX(1) = 500.0*12.  
C      PRIODY(1) = 500.0*12.  
C      INIT(1) = 0  
C      NTERMX(1) = 0  
C      NTERMY(1) = 0  
C      IX=897  
C      JX=123  
  
C      IOPT=1  
C      ITEXT = 1  
C      DDD = 10.0  
C      X(1) = 0.0  
  
C      X(2) = 50.0  
C      X(3) = 50.0  
C      X(4) = 0.0  
C      Y(1) = 0.0  
C      Y(2) = 0.0  
C      Y(3) = 50.0  
C      Y(4) = 50.0  
      RETURN  
      END
```

### C.15. Source for Subroutine TEXTUR

```
C          SUBROUTINE TEXTUR(IOPT, ITEXT, X, Y, VAL)
C
C          SUBROUTINE TEXTUR IMPLEMENTS AN OBJECT-PLANE BACKGROUND/TEXTURE
C MODEL BASED ON TRIGONOMETRIC-SERIES EXPANSIONS. EACH TEXTURE IS
C DESCRIBED BY VALUES FOR THE MEAN, STANDAGROUND/TEXTURE
C MODEL BASED ON TRIGONOMETRIC-SERIES EXPANSIONS. EACH TEXTURE IS
C DESCRIBED BY VALUES FOR THE MEAN, STANDARD DEVIATION, AND CORRELATION
C LENGTHS IN TWO DIMENSIONS. THE NUMBER OF DIFFERENT TEXTURES THAT
C CAN BE SIMULATED DEPENDS ON THE DIMENSIONS OF THE ARRAYS PROVIDED
C THROUGH COMMON BLOCK / TXTUR /. DEPENDING ON THE INPUT VALUE OF
C VARIABLE IOPT, THIS SUBROUTINE CAN PROVIDE A VALUE FOR A TEXTURE
C AT A GIVEN POINT OR CAN AVERAGE THE TEXTURE OVER AN AREA DEFINED
C BY A 4-SIDED POLYGON.
C
C          THE ARGUMENT VARIABLES FOR THIS SUBROUTINE ARE AS DESCRIBED BELOW:
C
C
C          IOPT      OPTION FLAG TO CHOOSE BETWEEN EVALUATING THE TEXTURE AT
C                     A POINT ( X(1),Y(1) ) OR TO AVERAGE THE TEXTURE OVER AN
C                     AREA DEFINED BY 4 POINTS.
C
C                  IF IOPT = 0      AREA AVERAGE
C                  IF IOPT <>0    POINT EVALUATION
C
C
C          ITEXT     INDEX NUMBER OF TEXTURE THAT IS BEING REQUESTED.
C
C
C          X,Y      ARRAYS OF SIZE 4. X AND Y COORDINATES OF THE VERTICES OF
C                     THE 4-SIDED AREA FOR AVERAGING THE TEXTURE. ONLY X(1) AND
C                     Y(1) ARE USED FOR POINT EVALUATION.
C
C
C          VAL      OUTPUT TEXTURE VALUE.
C
C
C
C
C          DIMENSION COEFX(15,5) , COEFY(15,5) , SLOPE(4)      , THETAX(15,5)
C          .           ,THETAY(15,5), X(4)           , Y(4)
C
C          COMMON / TXTURE / AMEAN(5)   , ASIG(5)   , CORX(5)   , CORY(5)
C          .           ,INIT(5)    , NTERMX(5) , NTERMY(5) , PRIODX(5)
C          .           ,PRIODY(5),IX,JX
C
C          DATA FCOEFX , FCOEFY / 0.15 , 0.15 /
C          DATA PI      , PISQRD / 3.141593654 , 9.869604404 /
```

```

C
C
C
C
C EACH TEXTURE MUST BE INITIALIZED ONLY ONCE
C
C IF( INIT(IEXT) .NE. 0) GO TO 50
C
C
C### INITIALIZATION #####0#####0#####0#####0#####0#####0#####0#####
C
C
C RATIOX = PRIODX(IEXT) / CORX(IEXT)
C RATIOY = PRIODY(IEXT) / CORY(IEXT)
C
C IF THE NUMBER OF X TERMS IN THE SERIES IS NOT SPECIFIED, THEN
C CHOOSE A NUMBER BASED ON VARIABLES RATIOX AND FCOEFX
C
C IF( NTERMX(IEXT) .LE. 0) THEN
C
C XXX      = PISQRD/RATIOX + RATIOX
C NTERMX(IEXT) = SQRT((XXX/FCOEFX - RATIOX)*RATIOX) / PI + 0.6
C
C
C WRITE(*,1000) NTERMX(IEXT), IEXT
C 1000 FORMAT(//,1X,I3,' X TERMS WILL BE USED IN TEXTURE # ',I2)
C
C END IF
C
C IF THE NUMBER OF Y TERMS IN THE SERIES IS NOT SPECIFIED, THEN
C CHOOSE A NUMBER BASED ON VARIABLES RATIOY AND FCOEY
C
C
C IF( NTERMY(IEXT) .LE. 0) THEN
C
C XXX      = PISQRD/RATIOY + RATIOY
C NTERMY(IEXT) = SQRT((XXX/FCOEY - RATIOY)*RATIOY) / PI + 0.6
C
C
C WRITE(*,1100) NTERMY(IEXT), IEXT
C 1100 FORMAT(//,1X,I3,' Y TERMS WILL BE USED IN TEXTURE # ',I2)
C
C END IF
C
C
C ONE-HALF THE SUM OF THE SQUARES OF THE COEFFICIENTS IS THE
C VARIANCE OF THE TEXTURE.
C
C SUMCOE = 0.0
C
C CALCULATE THE COEFFICIENTS FOR THE X TERMS IN THE SERIES AND CHOOSE
C RANDOM PHASE ANGLES FOR EACH TERM.
C

```

```

      KSIGN = 1
C
      DO 10 I = 1,NTERMX(ITEXT)
C
      KSIGN = -KSIGN
      AX    = 2.0*(1.0 - KSIGN*EXP(-RATIOX))
      AX    = AX / (RATIOX + (FLOAT(I*I)*PISQRD)/RATIOX)
C
      SUMCOE = SUMCOE + AX
      COEFX(I,ITEXT) = SQRT(2.0*AX)
C
      CALL RANDU(IX,JX,PQR)
      THETAX(I,ITEXT) = PQR * 2. * PI
C
      10 CONTINUE
C
C CALCULATE THE COEFFICIENTS FOR THE Y TERMS IN THE SERIES AND CHOOSE
C RANDOM PHASE ANGLES FOR EACH TERM.
C
      KSIGN = 1
C
      DO 20 J = 1,NTERMY(ITEXT)
C
      KSIGN = -KSIGN
      AY    = 2.0*(1.0 - KSIGN*EXP(-RATIOY))
      AY    = AY / (RATIOY + (FLOAT(J*J)*PISQRD)/RATIOY)
C
      SUMCOE = SUMCOE + AY
      COEFY(J,ITEXT) = SQRT(2.0*AY)
C
      CALL RANDU(IX,JX,PQR)
      THETAY(J,ITEXT) = PQR * 2. * PI
C
      20 CONTINUE
C
C ADJUST THE COEFFICIENTS TO ACHIEVE THE DESIRED STANDARD DEVIATION
C
      XXX = ASIG(ITEXT) / SQRT(SUMCOE)
C
      DO 30 I = 1,NTERMX(ITEXT)
      COEFX(I,ITEXT) = COEFX(I,ITEXT) * XXX
      30 CONTINUE
C
      DO 40 J = 1,NTERMY(ITEXT)
      COEFY(J,ITEXT) = COEFY(J,ITEXT) * XXX
      40 CONTINUE
C
C SET FLAG INDICATING THAT TEXTURE # ITEXT HAS BEEN INITIALIZED.
C
      INIT(ITEXT) = 1
C

```

```

C
C### END INITIALIZATION #####
C
C
C      50 CONTINUE
C
C      IF(IOPT .EQ. 0) GO TO 80
C
C
C### COMPUTE TEXTURE VALUE AT A SPECIFIED POINT #####
C
C
C      VAL = AMEAN(ITEXT)
C
C      XXX = PI*X(1)/PRIODX(ITEXT)
C
C      DO 60 I = 1,NTERMX(ITEXT)
C          VAL = VAL + COEFX(I,ITEXT)*COS(FLOAT(I)*XXX + THETAX(I,ITEXT))
C 60 CONTINUE
C
C      XXX = PI*Y(1)/PRIODY(ITEXT)
C      DO 70 J = 1,NTERMY(ITEXT)
C          VAL = VAL + COEFY(J,ITEXT)*COS(FLOAT(J)*XXX + THETAY(J,ITEXT))
C 70 CONTINUE
C
C      RETURN
C
C
C### COMPUTE AVERAGE OF TEXTURE OVER A SPECIFIED AREA #####
C
C
C      CHECK COORDINATES OF VERTICES TO PREVENT DIVISION BY ZERO IN THE
C      EXPRESSIONS BELOW.  TO PREVENT DIVISION BY ZERO, EITHER EXCHANGE
C      VERTEX NUMBERS OR ADD SMALL INCREMENTS TO THE VERTEX COORDINATES.
C
C      80 CONTINUE
C          IF(X(1) .EQ. X(3) .OR. Y(1) .EQ. Y(3)) THEN
C              IF(X(2) .EQ. X(4) .OR. Y(2) .EQ. Y(4)) THEN
C
C                  IF( X(1) .EQ. X(3) ) X(3) = X(3) + 0.000001*CORX(ITEXT)
C                  IF( Y(1) .EQ. Y(3) ) Y(3) = Y(3) + 0.000001*CORY(ITEXT)
C
C              ELSE
C
C      EXCHANGE VERTEX NUMBERS
C
C          X1 = X(1)
C          Y1 = Y(1)
C          DO 90 I=1,3
C              X(I) = X(I+1)
C 90          Y(I) = Y(I+1)

```

```

      X(4) = X1
      Y(4) = Y1
C
      END IF
C
      END IF
C
      DO 100 KK = 2,4,2
C
      IF(X(KK) .EQ. X(1)) X(KK) = X(KK) + .000001*CORX(ITEXT)
      IF(X(KK) .EQ. X(3)) X(KK) = X(KK) + .000001*CORX(ITEXT)
      IF(X(KK) .EQ. X(1)) X(KK) = X(KK) + .000001*CORX(ITEXT)
C
      IF(Y(KK) .EQ. Y(1)) Y(KK) = Y(KK) + .000001*CORY(ITEXT)
      IF(Y(KK) .EQ. Y(3)) Y(KK) = Y(KK) + .000001*CORY(ITEXT)
      IF(Y(KK) .EQ. Y(1)) Y(KK) = Y(KK) + .000001*CORY(ITEXT)
C
      100 CONTINUE
C
C      CALCULATE THE AREA OF THE 4-SIDED POLYGON
C
      BASE = SQRT( (X(3)-X(1))**2 + (Y(3)-Y(1))**2 )
C
      COSANG = (Y(3) - Y(1)) / BASE
      SINANG = (X(1) - X(3)) / BASE
      COS2   = COSANG*COSANG
      SIN2   = SINANG*SINANG
      SINCOS = SINANG*COSANG
C
      AREA = (BASE/2.) * (ABS( COSANG*(X(4)-X(1)) + SINANG*(Y(4)-Y(1)))
      .           + ABS( COSANG*(X(2)-X(1)) + SINANG*(Y(2)-Y(1))))
C
      COMPUTE SLOPE OF EACH SIDE OF THE POLYGON
C
      DO 110 I=1,4
      I1 = I + 1
      IF(I .EQ. 4) I1 = 1
      SLOPE(I) = (-SINANG*(X(I1)-X(I)) + COSANG*(Y(I1)-Y(I))) /
      .           ( COSANG*(X(I1)-X(I)) + SINANG*(Y(I1)-Y(I)) )
C
      110 CONTINUE
C
C      MULTIPLY MEAN BY AREA TO CANCEL THE DIVISION BY AREA DONE BELOW
C
      VAL = AMEAN(ITEXT) * AREA
C
C      CALCULATE X CONTRIBUTION TO THE AVERAGE. FOR EACH TERM IN THE
C      SERIES, THERE ARE 4 TERMS IN THE AVERAGE.
C

```

```

C
DO 130 I = 1,NTERMX(I TEXT)
C
CONST = FLOAT(I)*PI/PRIODX(I TEXT)
XXX = 0.0
III = 4
C
DO 120 II = 1,4
C
XXX = XXX + COS(CONST*X(II) + THETAX(I,I TEXT)) *
. ( 1. / (SIN2*SLOPE(III) - SINCOS) - 1. / (SIN2*SLOPE(II) - SINCOS))
C
III = II
C
120 CONTINUE
C
VAL = VAL + XXX*COEFX(I,I TEXT) / (CONST*CONST)
C
130 CONTINUE
C
C
C CALCULATE Y CONTRIBUTION TO THE AVERAGE. FOR EACH TERM IN THE
C SERIES, THERE ARE 4 TERMS IN THE AVERAGE.
C
C
DO 150 J = 1,NTERMY(I TEXT)
C
CONST = FLOAT(J)*PI/PRIODY(I TEXT)
XXX = 0.0
JJ1 = 4
C
DO 140 JJ = 1,4
C
XXX = XXX + COS(CONST*Y(JJ) + THETAY(J,I TEXT)) *
. ( 1. / (COS2*SLOPE(JJ1) + SINCOS) - 1. / (COS2*SLOPE(JJ) + SINCOS))
C
JJ1 = JJ
C
140 CONTINUE
C
VAL = VAL + XXX*COEFY(J,I TEXT) / (CONST*CONST)
C
150 CONTINUE
C
VAL = VAL / AREA
C
RETURN
END

```

**D. RGB Listing for 255 Spec Color Look-Up-Table**

This is the 255Spec color look-up-table values.

This appendix contains the RGB values corresponding to the indicated pixel value.

Pixel Value	RED	GREEN	BLUE
1	255	0	0
2	255	12	12
3	255	25	25
4	255	38	38
5	255	51	51
6	255	64	64
7	255	76	76
8	255	89	89
9	255	102	102
10	255	115	115
11	255	128	128
12	255	140	140
13	255	153	153
14	255	166	166
15	255	179	179
16	255	192	192
17	255	64	0
18	255	70	8
19	255	76	17

Pixel Value	RED	GREEN	BLUE
20	255	83	25
21	255	89	34
22	255	96	42
23	255	102	51
24	255	108	59
25	255	115	68
26	255	121	76
27	255	128	85
28	255	134	93
29	255	140	102
30	255	147	110
31	255	153	119
32	255	160	128
33	255	128	0
34	255	134	8
35	255	140	17
36	255	147	25
37	255	153	34
38	255	160	42
39	255	166	51
40	255	172	59
41	255	179	68
42	255	185	76

Pixel Value	RED	GREEN	BLUE
43	255	192	85
44	255	198	93
45	255	204	102
46	255	211	110
47	255	217	119
48	255	224	128
49	224	160	0
50	226	164	8
51	228	168	17
52	230	172	25
53	232	177	34
54	234	181	42
55	236	185	51
56	238	189	59
57	240	194	68
58	242	198	76
59	244	202	85
60	246	206	93
61	248	211	102
62	250	215	110
63	252	219	119
64	255	224	128
65	255	255	0

Pixel Value	RED	GREEN	BLUE
66	255	255	14
67	255	255	29
68	255	255	44
69	255	255	59
70	255	255	74
71	255	255	89
72	255	255	104
73	255	255	119
74	255	255	134
75	255	255	149
76	255	255	164
77	255	255	179
78	255	255	194
79	255	255	209
80	255	255	224
81	128	128	32
82	136	136	38
83	144	144	44
84	153	153	51
85	161	161	57
86	170	170	64
87	178	178	70
88	187	187	76
89	195	195	83

Pixel Value	RED	GREEN	BLUE
90	204	204	89
91	212	212	96
92	221	221	102
93	229	229	108
94	238	238	115
95	246	246	121
96	255	255	128
97	128	96	32
98	136	104	38
99	144	113	44
100	153	121	51
101	161	130	57
102	170	138	64
103	178	147	70
104	187	155	76
105	195	164	83
106	204	172	89
107	212	181	96
108	221	189	102
109	229	198	108
110	238	206	115
111	246	215	121
112	255	224	128
113	128	64	32

Pixel Value	RED	GREEN	BLUE
114	136	72	38
115	144	81	44
116	153	89	51
117	161	98	57
118	170	106	64
119	178	115	70
120	187	123	76
121	195	132	83
122	204	140	89
123	212	149	96
124	221	157	102
125	229	166	108
126	238	174	115
127	246	183	121
128	255	192	128
129	96	128	0
130	102	136	8
131	108	144	17
132	115	153	25
133	121	161	34
134	128	170	42
135	134	178	51
136	140	187	59
137	147	195	68

Pixel Value	RED	GREEN	BLUE
138	153	204	76
139	160	212	85
140	166	221	93
141	172	229	102
142	179	238	110
143	185	246	119
144	192	255	128
145	0	128	0
146	12	136	12
147	25	144	25
148	38	153	38
149	51	161	51
150	64	170	64
151	76	178	76
152	89	187	89
153	102	195	102
154	115	204	115
155	128	212	128
156	140	221	140
157	153	229	153
158	166	238	166
159	179	246	179
160	192	255	192
161	0	128	224

Pixel Value	RED	GREEN	BLUE
162	14	136	226
163	29	144	228
164	44	153	230
165	59	161	232
166	74	170	234
167	89	178	236
168	104	187	238
169	119	195	240
170	134	204	242
171	149	212	244
172	164	221	246
173	179	229	248
174	194	238	250
175	209	246	252
176	224	255	255
177	64	0	255
178	74	14	255
179	85	29	255
180	96	44	255
181	106	59	255
182	117	74	255
183	128	89	255
184	138	104	255
185	149	119	255

Pixel Value	RED	GREEN	BLUE
186	160	134	255
187	170	149	255
188	181	164	255
189	192	179	255
190	202	194	255
191	213	209	255
192	224	224	255
193	64	0	192
194	72	8	196
195	81	17	200
196	89	25	204
197	98	34	208
198	106	42	213
199	115	51	217
200	123	59	221
201	132	68	225
202	140	76	229
203	149	85	234
204	157	93	238
205	166	102	242
206	174	110	246
207	183	119	250
208	192	128	255
209	64	0	128

Pixel Value	RED	GREEN	BLUE
210	74	8	136
211	85	17	144
212	96	25	153
213	106	34	161
214	117	42	170
215	128	51	178
216	138	59	187
217	149	68	195
218	160	76	204
219	170	85	212
220	181	93	221
221	192	102	229
222	202	110	238
223	213	119	246
224	224	128	255
225	0	0	0
226	17	17	17
227	34	34	34
228	51	51	51
229	68	68	68
230	85	85	85
231	102	102	102
232	119	119	119
233	136	136	136

Pixel Value	RED	GREEN	BLUE
234	153	153	153
235	170	170	170
236	187	187	187
237	204	204	204
238	221	221	221
239	238	238	238
240	255	255	255
241	255	0	255
242	255	14	255
243	255	29	255
244	255	44	255
245	255	59	255
246	255	74	255
247	255	89	255
248	255	104	255
249	255	119	255
250	255	134	255
251	255	149	255
252	255	164	255
253	255	179	255
254	255	194	255
255	255	209	255
256	255	224	255

#### E. RGB Listing for 32Spec Color Look-Up-Table

32SPEC OR 32 COLOR SCHEME THAT TRAVERSES THE VISIBLE SPECTRUM

This appendix contains the RGB values corresponding to the indicated pixel value.

Pixel Value	RED	GREEN	BLUE
1	255	0	0
2	255	26	0
3	255	51	0
4	255	76	0
5	255	101	0
6	255	126	0
7	255	152	0
8	255	177	0
9	255	202	0
10	255	227	0
11	255	252	0
12	222	255	0
13	179	255	0
14	135	255	0
15	92	255	0
16	48	255	0
17	5	255	0
18	0	255	32
19	0	255	73
20	0	255	115

Pixel Value	RED	GREEN	BLUE
21	0	255	157
22	0	255	198
23	0	255	240
24	0	241	248
25	0	214	235
26	0	187	221
27	0	161	208
28	0	134	195
29	0	107	181
30	0	80	168
31	0	53	154
32	0	26	141

From this point on all values of RGB are 0 for  
all values of data through 255.

**F. RGB Listing for 32Gray Look-Up-Table**

**32 GRAY SCALE LOOK UP TABLE- THIS LOOK UP TABLE COVERS  
THE TOTAL DYNAMIC RANGE OF THE DISPLAY IN MONOCHROME**

**This appendix contains the RGB values corresponding  
to the indicated pixel value.**

<b>Pixel Value</b>	<b>RED</b>	<b>GREEN</b>	<b>BLUE</b>
1	255	255	255
2	247	247	247
3	239	239	239
4	231	231	231
5	223	223	223
6	215	215	215
7	207	207	207
8	199	199	199
9	191	191	191
10	183	183	183
11	175	175	175
12	167	167	167
13	159	159	159
14	151	151	151
15	143	143	143
16	135	135	135
17	127	127	127
18	119	119	119
19	111	111	111

Pixel Value	RED	GREEN	BLUE
20	103	103	103
21	95	95	95
22	87	87	87
23	79	79	79
24	71	71	71
25	63	63	63
26	55	55	55
27	47	47	47
28	39	39	39
29	31	31	31
30	23	23	23
31	15	15	15
32	7	7	7

From this point through the value of 255, the RGB values are all identically 0.

**G. RGB Listing for 255Gray Look-Up-Table**

**255GRAY LOOK UP TABLE**

This appendix contains the RGB values corresponding to the indicated pixel value.

Pixel Value	RED	GREEN	BLUE
1	255	255	255
2	254	254	254
3	253	253	253
4	252	252	252
5	251	251	251
6	250	250	250
7	249	249	249
8	248	248	248
9	247	247	247
10	246	246	246
11	245	245	245
12	244	244	244
13	243	243	243
14	242	242	242
15	241	241	241
16	240	240	240
17	239	239	239
18	238	238	238
19	237	237	237

Pixel Value	RED	GREEN	BLUE
20	236	236	236
21	235	235	235
22	234	234	234
23	233	233	233
24	232	232	232
25	231	231	231
26	230	230	230
27	229	229	229
28	228	228	228
29	227	227	227
30	226	226	226
31	225	225	225
32	224	224	224
33	223	223	223
34	222	222	222
35	221	221	221
36	220	220	220
37	219	219	219
38	218	218	218
39	217	217	217
40	216	216	216
41	215	215	215
42	214	214	214
43	213	213	213

Pixel Value	RED	GREEN	BLUE
44	212	212	212
45	211	211	211
46	210	210	210
47	209	209	209
48	208	208	208
49	207	207	207
50	206	206	206
51	205	205	205
52	204	204	204
53	203	203	203
54	202	202	202
55	201	201	201
56	200	200	200
57	199	199	199
58	198	198	198
59	197	197	197
60	196	196	196
61	195	195	195
62	194	194	194
63	193	193	193
64	192	192	192
65	191	191	191
66	190	190	190
67	189	189	189

Pixel Value	RED	GREEN	BLUE
68	188	188	188
69	187	187	187
70	186	186	186
71	185	185	185
72	184	184	184
73	183	183	183
74	182	182	182
75	181	181	181
76	180	180	180
77	179	179	179
78	178	178	178
79	177	177	177
80	176	176	176
81	175	175	175
82	174	174	174
83	173	173	173
84	172	172	172
85	171	171	171
86	170	170	170
87	169	169	169
88	168	168	168
89	167	167	167
90	166	166	166
91	165	165	165

Pixel Value	RED	GREEN	BLUE
92	164	164	164
93	163	163	163
94	162	162	162
95	161	161	161
96	160	160	160
97	159	159	159
98	158	158	158
99	157	157	157
100	156	156	156
101	155	155	155
102	154	154	154
103	153	153	153
104	152	152	152
105	151	151	151
106	150	150	150
107	149	149	149
108	148	148	148
109	147	147	147
110	146	146	146
111	145	145	145
112	144	144	144
113	143	143	143
114	142	142	142
115	141	141	141

AD-A164 213

PSEUDO-COLOR DISPLAY OF LASER RADAR IMAGERY(U) AIR  
FORCE INST OF TECH WRIGHT-PATTERSON AFB OH SCHOOL OF  
ENGINEERING N BARSALOU 82 DEC 85 AFIT/GE/ENG/85D-3

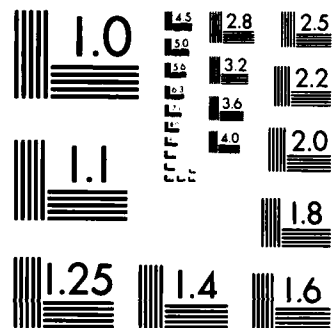
3/3

UNCLASSIFIED

F/G 14/5

ML





MICROCOPY RESOLUTION TEST CHART  
STANDARDS 1963-A

Pixel Value	RED	GREEN	BLUE
116	140	140	140
117	139	139	139
118	138	138	138
119	137	137	137
120	136	136	136
121	135	135	135
122	134	134	134
123	133	133	133
124	132	132	132
125	131	131	131
126	130	130	130
127	129	129	129
128	128	128	128
129	127	127	127
130	126	126	126
131	125	125	125
132	124	124	124
133	123	123	123
134	122	122	122
135	121	121	121
136	120	120	120
137	119	119	119
138	118	118	118
139	117	117	117

Pixel Value	RED	GREEN	BLUE
140	116	116	116
141	115	115	115
142	114	114	114
143	113	113	113
144	112	112	112
145	111	111	111
146	110	110	110
147	109	109	109
148	108	108	108
149	107	107	107
150	106	106	106
151	105	105	105
152	104	104	104
153	103	103	103
154	102	102	102
155	101	101	101
156	100	100	100
157	99	99	99
158	98	98	98
159	97	97	97
160	96	96	96
161	95	95	95
162	94	94	94
163	93	93	93

Pixel Value	RED	GREEN	BLUE
164	92	92	92
165	91	91	91
166	90	90	90
167	89	89	89
168	88	88	88
169	87	87	87
170	86	86	86
171	85	85	85
172	84	84	84
173	83	83	83
174	82	82	82
175	81	81	81
176	80	80	80
177	79	79	79
178	78	78	78
179	77	77	77
180	76	76	76
181	75	75	75
182	74	74	74
183	73	73	73
184	72	72	72
185	71	71	71
186	70	70	70
187	69	69	69

Pixel Value	RED	GREEN	BLUE
188	68	68	68
189	67	67	67
190	66	66	66
191	65	65	65
192	64	64	64
193	63	63	63
194	62	62	62
195	61	61	61
196	60	60	60
197	59	59	59
198	58	58	58
199	57	57	57
200	56	56	56
201	55	55	55
202	54	54	54
203	53	53	53
204	52	52	52
205	51	51	51
206	50	50	50
207	49	49	49
208	48	48	48
209	47	47	47
210	46	46	46
211	45	45	45

Pixel Value	RED	GREEN	BLUE
212	44	44	44
213	43	43	43
214	42	42	42
215	41	41	41
216	40	40	40
217	39	39	39
218	38	38	38
219	37	37	37
220	36	36	36
221	35	35	35
222	34	34	34
223	33	33	33
224	32	32	32
225	31	31	31
226	30	30	30
227	29	29	29
228	28	28	28
229	27	27	27
230	26	26	26
231	25	25	25
232	24	24	24
233	23	23	23
234	22	22	22
235	21	21	21

Pixel Value	RED	GREEN	BLUE
236	20	20	20
237	19	19	19
238	18	18	18
239	17	17	17
240	16	16	16
241	15	15	15
242	14	14	14
243	13	13	13
244	12	12	12
245	11	11	11
246	10	10	10
247	9	9	9
248	8	8	8
249	7	7	7
250	6	6	6
251	5	5	5
252	4	4	4
253	3	3	3
254	2	2	2
255	1	1	1
256	0	0	0

#### H. RGB Listing for 32Ran Color Look-Up-Table

##### 32RAN OR 32 COLOR RANDOM LOOK UP TABLE

This appendix contains the RGB values corresponding to the indicated pixel value.

Pixel Value	RED	GREEN	BLUE
1	207	0	0
2	255	111	0
3	255	207	0
4	255	0	63
5	255	111	63
6	255	207	63
7	255	63	0
8	159	111	255
9	111	207	159
10	111	255	0
11	111	111	0
12	0	0	0
13	63	159	63
14	0	0	255
15	159	255	255
16	0	0	0
17	111	63	0
18	63	255	111
19	159	0	0

Pixel Value	RED	GREEN	BLUE
20	0	63	159
21	207	0	63
22	255	207	111
23	255	111	111
24	0	159	111
25	207	63	207
26	111	0	111
27	63	255	0
28	255	111	111
29	63	255	63
30	255	207	207
31	111	159	111
32	0	0	0

The remainder of the RGB values for pixel values through 255 are all identically 0.

## I. Eglin AFB CO<sub>2</sub> Ladar System Specifications

### Ladar System Specifications

#### TRANSMITTER:

RF pumped, EO modulated, 10.6 um laser  
Pulsed or CW format  
Average power of 10 W (minimum) in CW format  
Average power of 5 W (minimum) in pulsed format  
with 22 ns pulselwidth @ 87 khz PRF (laser output)  
PRF is adjustable from 30 khz to over 100khz

#### RECEIVER:

Heterodyne with local oscillator, 70 mhz offset  
Log video output with 75 dB dynamic range  
50 mhz IF bandwidth  
First Pulse Logic

#### OPTICS/SCANNER:

Common aperture 7.5 cm diameter  
IFOV 0.27 full angle "spatial resolution"  
FOV 2 x 1.75 degree raster  
128 lines per frame

#### PROCESSOR:

16 bit unambiguous range (> 5 km)  
1 ns granularity  
5 bit peak amplitude sample at 2 dB/LSB  
MULTIBUS compatible digital acquisition and  
scan control

VITA

Norman Barsalou was born in Worcester, Massachusetts, on July 3, 1958. He graduated from Niceville High School in Niceville, Florida in 1975, and attended the University of Florida, from which he graduated in June 1978 with a Bachelor of Science in Mathematics. He was commissioned in the Air Force in June, 1979. Upon entering active duty he attended the Air force Institute of Technology to pursue a B.S. degree in Electrical Engineering. After receiving his BSEE from AFIT, he was assigned to the Air Force Armament Laboratory at Eglin AFB, Florida. He remained at the Armament Laboratory from March 1981 until his assignment to AFIT in May 1984.

He is married to the former Patricia Lynn Benson of New Orleans, Louisiana.

Permanent address: 8131 Pioneer Hills  
Converse, Tx 78109

AD A164213

## REPORT DOCUMENTATION PAGE

1a. REPORT SECURITY CLASSIFICATION <b>UNCLASSIFIED</b>		1b. RESTRICTIVE MARKINGS	
1c. SECURITY CLASSIFICATION AUTHORITY		1d. DISTRIBUTION/AVAILABILITY OF REPORT	
2b. DECLASSIFICATION/DOWNGRADING SCHEDULE		Approved for public release; distribution unlimited	
4. PERFORMING ORGANIZATION REPORT NUMBER(S) <b>AFIT/CE/ENG/85D-3</b>		5. MONITORING ORGANIZATION REPORT NUMBER(S)	
6a. NAME OF PERFORMING ORGANIZATION <b>School of Engineering</b>	6b. OFFICE SYMBOL (If applicable)	7a. NAME OF MONITORING ORGANIZATION	
6c. ADDRESS (City, State and ZIP Code) <b>AFIT Wright-Patterson AFB, OH 45424</b>		7b. ADDRESS (City, State and ZIP Code)	
8a. NAME OF FUNDING SPONSORING ORGANIZATION <b>AF Armament Laboratory</b>	8b. OFFICE SYMBOL (If applicable) <b>AFATL/DLM1</b>	9. PROCUREMENT INSTRUMENT IDENTIFICATION NUMBER	
10. ADDRESS (City, State and ZIP Code) <b>Eglin AFB, FLA 32542</b>		11. SOURCE OF FUNDING NOS.	
		12a. PROGRAM ELEMENT NO.	PROJECT NO.
		12b. TASK NO.	WORK UNIT NO.
11. TITLE (Include security classification) <b>See block 19</b>		13. DATE OF REPORT (Yr., Mo., Day) <b>85-Dec-2</b>	
12. PERSONAL AUTHOR(S) <b>Norman Barsalou, Capt, USAF</b>		15. PAGE COUNT <b>197</b>	
13a. TYPE OF REPORT <b>Thesis</b>	13b. TIME COVERED FROM _____ TO _____	14. DATE OF REPORT (Yr., Mo., Day)	
16. SUPPLEMENTARY NOTATION			
17. REF ID: #S	18. SUBJECT TERMS (Continue on reverse if necessary and identify by block number) <b>INFRARED OPTICAL SYSTEMS; Television display Systems; Laser-radar display</b>		
19. ABSTRACT (Provide in one or more paragraphs and identify by block number)			
<p><b>Approved for public release; see AFIT 85D-3.</b></p> <p><b>LYNN E. WOLAYER 15 JAN 86</b></p> <p><b>Dean for Research and Professional Development Air Force Institute of Technology (AFIT) Wright-Patterson AFB OH 45433</b></p> <p><b>Dean for Research and Professional Development Air Force Institute of Technology (AFIT) Wright-Patterson AFB OH 45433</b></p>			
20. DISTRIBUTION/AVAILABILITY OF ABSTRACT		21. ABSTRACT SECURITY CLASSIFICATION	
UNCLASSIFIED		22. ABSTRACT SECURITY CLASSIFICATION	
22a. NAME OF PERSON ASSIGNED TO INDEX AND LIST		22b. TELEPHONE NUMBER (Area Code)	22c. OFFICE SYMBOL
		<b>AFIT/ENG</b>	

UNCLASSIFIED  
SECURITY CLASSIFICATION OF THIS PAGE

**Abstract**

A pseudo-color representation of CO<sub>2</sub> laser radar data is developed. The pseudo-color scheme is based on the dilution of a set of baseline hues by white. The synthetic generation of laser radar scenes is used for display creation, and the results of analysis on synthetic scenes is applied to data collected by a CO<sub>2</sub> pulsed ladar system.

END

FILMED

(3)

-86

DTIC